Electrochemical Society

UNIV. OF MICHIGAN
MAY 3 - 1954
EAST ENGINEERING
LIBRARY

ELECTROCHEMICAL INDUSTRY

TVA Power Area

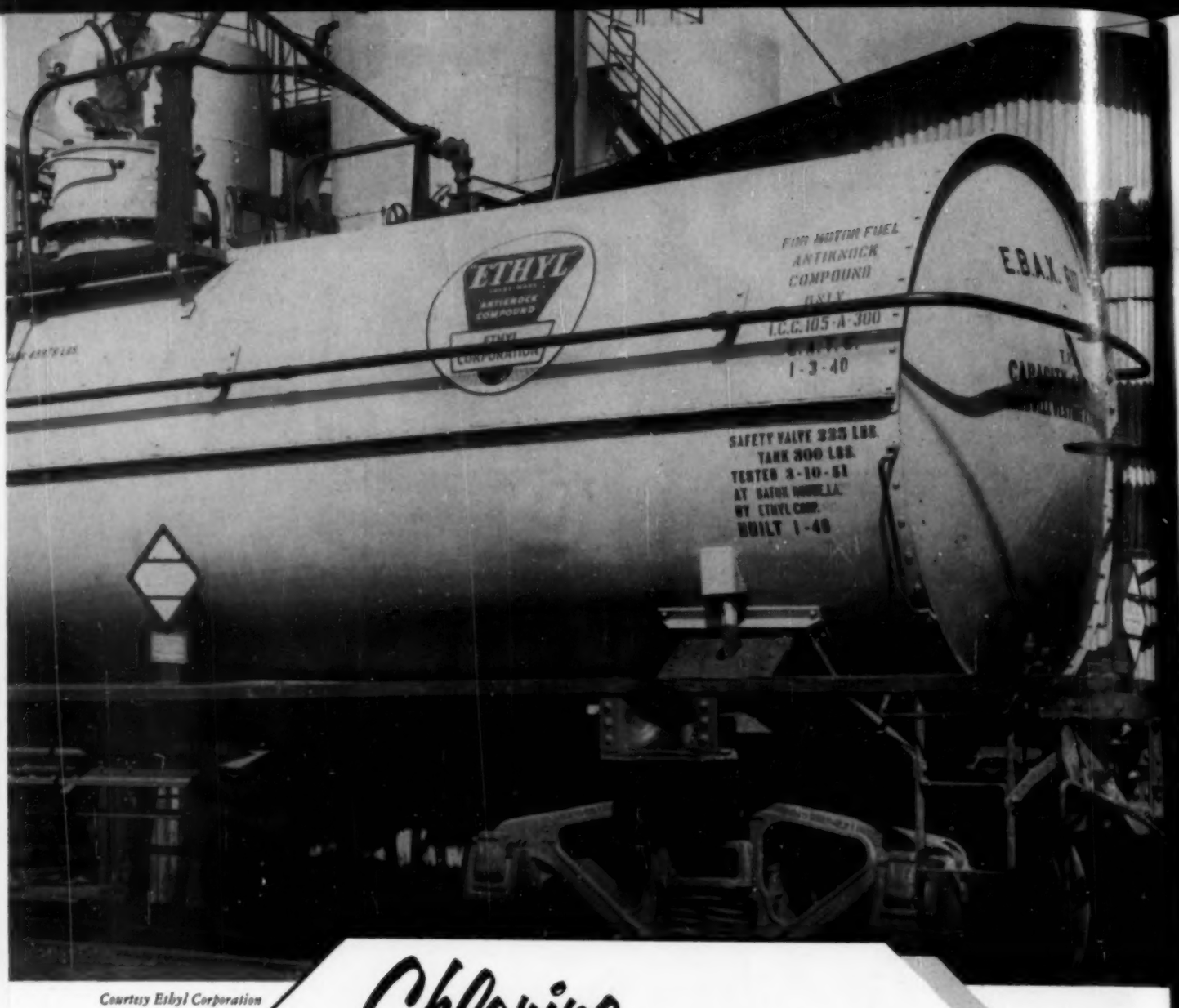

Courtesy Ethyl Corporation

Chlorine...

for antiknock compounds

Ethyl chloride, ethylene dichloride and ethylene dibromide play an important part in the manufacture of antiknock compounds for combustion engine gasolines.

Uniformly high quality GLC Graphite Anodes play an important part too—in helping the electrolytic industry meet the growing civilian and defense needs for chlorine and caustic soda.

ELECTRODE DIVISION

Great Lakes Carbon Corporation

Niagara Falls, N.Y. GLC® Morganton, N. C.

Graphite Electrodes, Anodes, Molds and Specialties

Sales office: Niagara Falls, N.Y. **Other offices:** New York, N.Y., Oak Park, Ill., Pittsburgh, P

Sales Agents: J. B. Hayes, Birmingham, Ala.; George O'Hara, Long Beach, Cal.; Great Northern Carbon & Chemical Co., Ltd., Montreal, Can

Overseas Carbon & Coke Company, Inc., Geneva, Switzerland; Great Eastern Carbon & Chemical Co., Inc., Chiyoda-Ku, Tokyo

Kinetics of the Reaction of Hydrogen with Zirconium[1]

JACK BELLE, B. B. CLELAND, AND M. W. MALLETT

Battelle Memorial Institute, Columbus, Ohio

ABSTRACT

The rate of reaction of hydrogen with high purity zirconium was determined for the temperature range of 250° to 425°C at 1 atm pressure. The reaction was found to follow a parabolic law, and the parabolic rate constant in $(ml/cm^2)^2$ per second was calculated to be $k = 2.3 \times 10^5 e^{-17,200/RT}$ where 17,200 ± 200 cal/mole is the activation energy for the reaction.

INTRODUCTION

Kinetics of surface reactions of zirconium with nitrogen and oxygen have been discussed in previous papers from this laboratory (1, 2). The present paper concerns the kinetics of the zirconium-hydrogen reaction. Very little on this subject was found in the literature. Gulbransen and Andrew (3) investigated the reaction in the temperature range 235° to 300°C at pressures from 0.6 to 2.6 cm, using thin zirconium foil, 0.005 in. thick. Their conclusions can be summarized as follows: (*a*) a surface film is not formed as a product of the reaction; (*b*) the rate of the reaction deviates from a linear law; and (*c*) the rate of the reaction is directly proportional to the square root of the pressure.

The present study was made in the temperature range 250° to 425°C at a hydrogen pressure of 1 atm, using low-hafnium zirconium (0.01 weight % hafnium) in the form of solid cylinders.

EXPERIMENTAL

Method.—The method for measuring the rate of the reaction between zirconium and hydrogen was essentially that previously described for other zirconium-gas reactions (1, 2). A schematic diagram of the apparatus used is shown in Fig. 1. Vacuum-ground stopcocks greased with Apiezon N grease were used throughout except for the air inlets to the McLeod gauge and to the mechanical pumps. The system was evacuated by a 2-stage glass mercury-diffusion pump backed by a mechanical pump. The cold trap between the diffusion pump and the reaction system was cooled with liquid nitrogen. It was found necessary to place an additional trap, cooled with dry ice-acetone, adjacent to the reaction tube to remove contaminating grease and mercury vapors.

A modified White gas buret (4) was used to store the hydrogen and to measure the rate of consumption of gas. The buret consisted of 10 bulbs, each of approximately 25 ml, and of a connected open-end full-length manometer, one arm of which was a graduated 25-ml buret. The entire assembly was maintained at constant temperature (±0.5°C) with running water.

The Vycor reaction tube was sealed to the system with Apiezon W wax, and its dead volume was decreased by a bundle of fused Vycor rods. The reaction tube was heated by a resistance-wound furnace which was controlled by a Brown Pyro-Vane controller with a V20 Variac in the input line. Temperature was controlled to ±5°C.

Prior to specimen preparation, machined zirconium cylinders about 2 cm long and 0.6 cm in diameter were degassed to about 1 to 2 ppm hydrogen by heating in vacuum at 900°C for 24 hr. Specimens were abraded with kerosene-soaked 240-, 400-, and 600-grit silicon carbide papers and washed in successive baths of naphtha, ether, and acetone. Care was taken to keep specimens under acetone until they were placed in the reaction tube.

The reaction tube was sealed to the system which, then, was evacuated to about 10^{-5} mm Hg as measured by the ion gauge. The specimen was annealed under vacuum for 1 hr at 800°C, after which the furnace was removed and its temperature adjusted to that of the rate run. The furnace was again placed around the reaction tube. The temperature was permitted to stabilize while hydrogen was being generated and stored.

With the specimen at the desired temperature, hydrogen was admitted from the buret and maintained at atmospheric pressure in the reaction tube by manual manipulations of the buret leveling bulb, except when the gas was expanded into the buret from storage bulbs. Short-time pressure fluctuations did not affect reaction rates. Readings, taken as the buret manometer arms were precisely leveled, were made as often as possible for rapid reaction rates and every 2 to 10 min for slower rates. The quantity of gas consumed by the specimen was the volume

[1] Manuscript received October 15, 1953. Work performed under AEC Contract W-7405-eng-92.

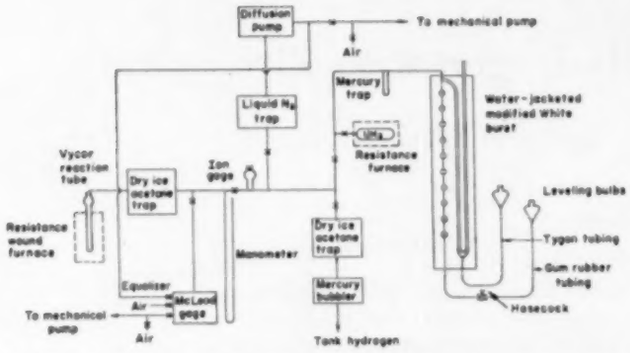

FIG. 1. Schematic diagram of modified hydrogen Sieverts apparatus.

added from the buret minus that remaining in the gas phase in the calibrated dead space. Geometric dimensions of specimens were used in calculating the quantity of hydrogen reacted per unit area.

Materials.—The pure zirconium used in these experiments was iodide crystal bar produced by the de Boer process, arc-melted, forged to 1⅛ in.² at 1450°F, hot rolled at 1450°F, and cold drawn to ⅜-in. diameter rod. Test specimens were machined from this rod. Impurities in zirconium were determined by spectrographic, chemical, and vacuum-fusion analyses. Weight percentages of principal impurities detected were: silicon, 0.03; iron, 0.02; hafnium, 0.01; oxygen, 0.04; nitrogen, 0.002; and hydrogen, 0.003 (before degassing).

Pure hydrogen was obtained from the thermal decomposition of uranium hydride. The hydride was prepared by reacting tank hydrogen, dried in a dry ice-acetone cold trap, with degreased high purity uranium chips.

Results and Discussion

Initial deviations are often observed for gas-metal reactions which follow the parabolic law, $w^2 = kt$. Gulbransen (5) has enumerated a number of complex factors which contribute to the breakdown of the law during early stages of the reaction. In addition to these phenomena, there may be interface effects. As was discussed by Jost (6) and Kubaschewski and Hopkins (7), these interface reactions may become rate-determining in initial stages of the reaction. The empirical equation which combines both reaction at an interface and diffusion through the film can be written in the form, $w^2 + \frac{k_p}{k_1} w = k_p t$. Here, k_1 represents the contribution of any linear interface reaction and k_p is the parabolic rate constant determined by diffusion through the growing film. If w is plotted as a function of t/w, the slope of the straight line is the parabolic rate constant, k_p. Such a plot is often more convenient to use than the quadratic plot, particularly for those reactions where an induction period is present or initial stages of the reaction are uncertain.

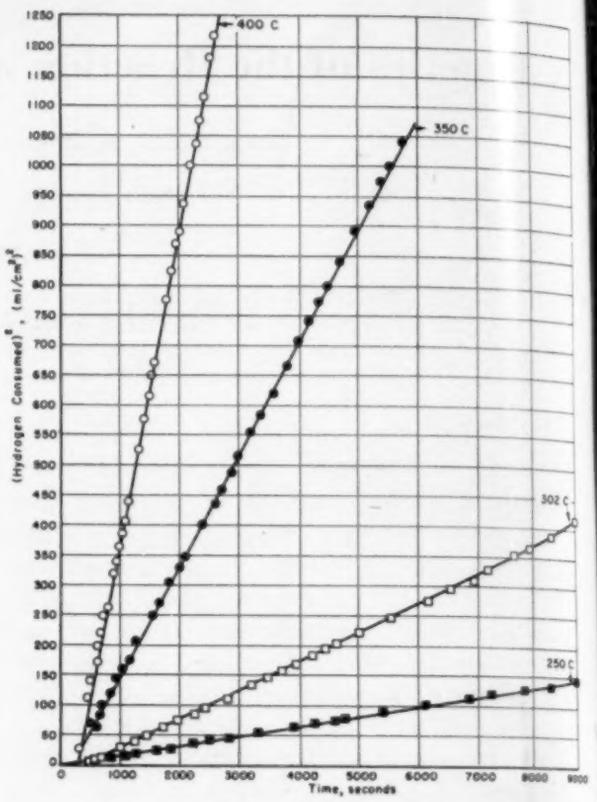

FIG. 2. Reaction of zirconium with hydrogen (ml H_2, STP, consumed per cm² metal surface)² vs. time.

The rate of the surface reaction of zirconium with hydrogen was measured in the range 250° to 425°C at 1 atm pressure. Results of several measurements are shown in Fig. 2 and 3. In Fig. 2, the square of the quantity (ml STP) of hydrogen consumed per unit surface area of the metal is plotted against time for four temperatures. Fig. 3 is a plot of w vs. t/w for two temperatures. It was found that, in all cases, the reaction conformed to the parabolic rate law with initial deviations in the direction of a slower initial rate. The duration of the induction period was usually less than five minutes and was independent of the annealing time, provided the system was evacuated to about 10^{-4} to 10^{-5} mm Hg.

In addition to the short induction period, there were also some deviations from the parabolic law after considerable hydrogen had been reacted. (The film thickness produced by the parabolic reaction ranged from 150μ at 300°C to 300μ at 425°C.) Deviations, which were always in the direction of a faster rate, did not occur below 300°C, and were not always present above that temperature. It is suspected that this breakdown of the parabolic nature of the reaction may be due to cracking of the film. It is not known why this effect was not reproducible.

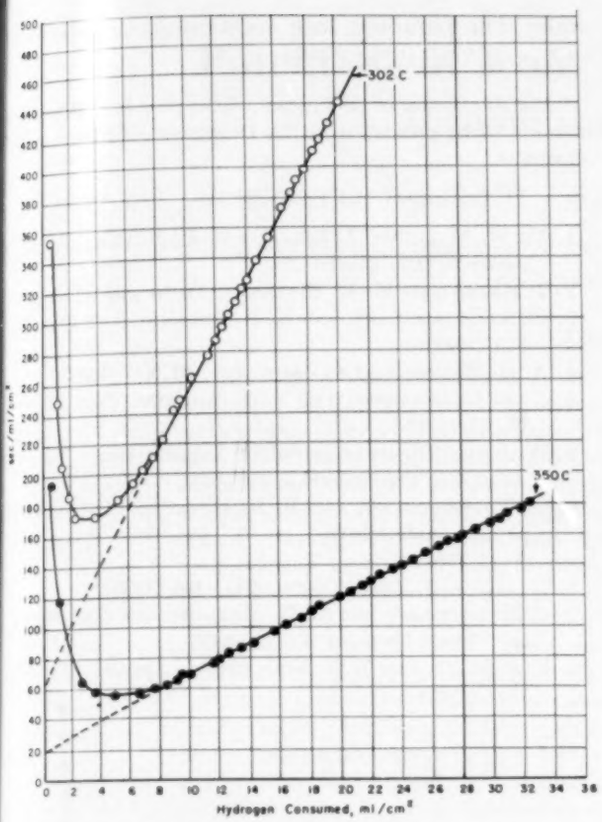

FIG. 3. Reaction of zirconium with hydrogen

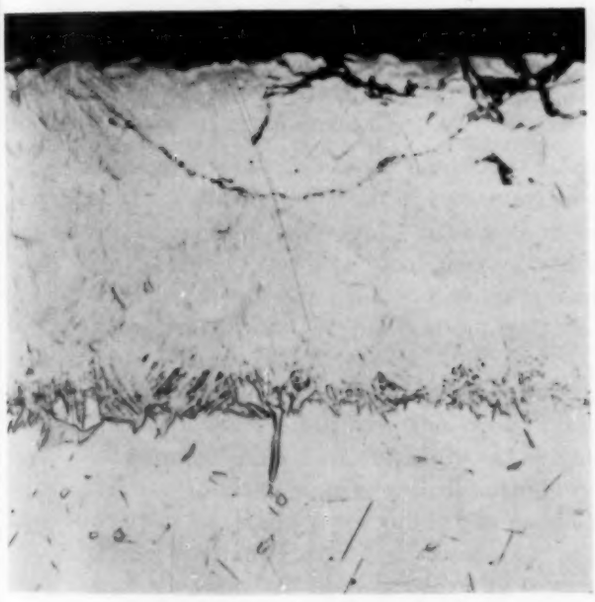

FIG. 4. Hydrogen reacted with iodide zirconium at 302°C for 2½ hr at 743 mm Hg absolute pressure. 250×

A reaction product was formed on the surface of all specimens, in contrast with the findings of Gulbransen and Andrew (3) who reported the absence of a surface film. Metallographic examination of the surface film indicated it to be an apparently single-phase layer, as can be seen from the photomicrograph shown in Fig. 4. On the other hand, x-ray diffraction examination of the surfaces of several specimens revealed the presence of three phases: (*a*) an outer layer of tetragonal ZrH_2; (*b*) an intermediate layer of Hägg's (8) ZrH; and (*c*) an inner layer of a second tetragonal hydride phase. When the outer ZrH_2 was removed by light abrasion of the surface, the pattern of ZrH was obtained. Upon further abrasion, another hydride phase

TABLE I. *Parabolic rate constants for the reaction of zirconium with hydrogen*

Temp., C ± 5°	Rate constant, k_p, $(ml/cm^2)^2/sec$	Slope of log-log plot
249	0.015	0.47
250	0.017	0.50
276	0.032	0.47
277	0.035	0.49
302	0.056	0.56
304	0.074	0.52
323	0.12	0.53
323	0.11	0.50
350	0.20	0.57
351	0.19	0.57
353	0.22	0.49
373	0.33	0.57
378	0.38	0.49
397	0.61	0.61
400	0.70	0.64
421	0.88	0.47
424	0.88	0.57
424	1.05	0.58

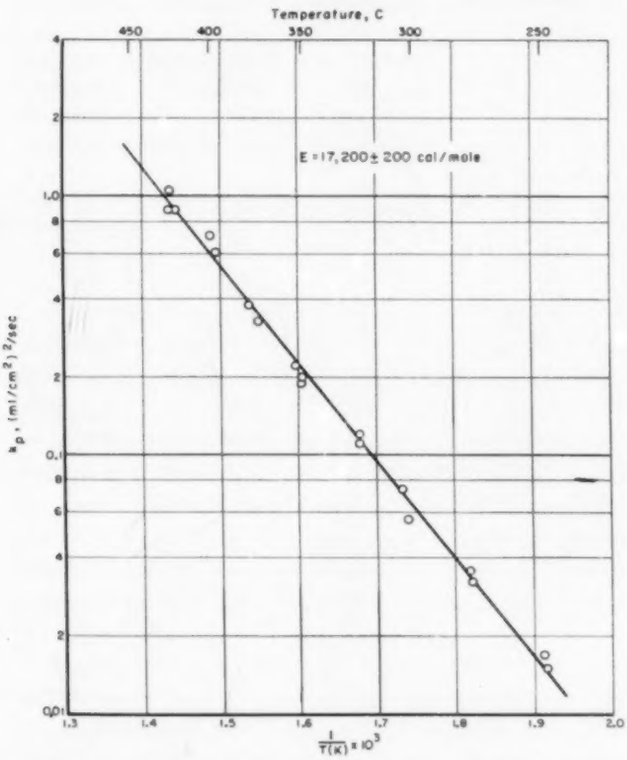

FIG. 5. Zirconium-hydrogen reaction, variation of reaction-rate constant with temperature.

appeared, adjacent to the metal. As discussed by Schwartz and Mallett (9), this latter hydride phase may be similar to the tetragonal phase of lowest hydrogen content reported for the hafnium-hydrogen system by Sidhu and McGuire (10). What effect these multiple hydride phases have on the kinetics of the zirconium-hydrogen reaction is not known.

If the parabolic law is obeyed, a plot of the logarithm of the amount of hydrogen consumed per unit surface area vs. the logarithm of time should give a straight line with a slope equal to 0.5. This was observed, as can be seen from Table I, where the parabolic rate constants, k_p's, calculated from the w vs. t/w plots are also given.

Fig. 5 is a plot of log k_p vs. $1/T$. The equation of the best straight line through the points from 250° to 425°C was determined by the method of least squares. The experimental energy of activation and the frequency factor were calculated from the Arrhenius-type equation, $k = Ae^{-Q/RT}$. Energy of activation was calculated to be 17,200 ± 200 cal/mole. The parabolic rate constant in (ml/cm²)²/sec is $k = 2.3 \times 10^5\ e^{-17,200/RT}$.

Any discussion of this paper will appear in a Discussion Section to be published in the December 1954 issue of the JOURNAL.

REFERENCES

1. M. W. MALLETT, J. BELLE, AND B. B. CLELAND, *This Journal*, **101**, 1 (1954).
2. J. BELLE AND M. W. MALLETT, To be published.
3. E. A. GULBRANSEN AND K. F. ANDREW, *J. Metals*, **185**, 515 (1949).
4. A. H. WHITE, *J. Am. Chem. Soc.*, **22**, 343 (1900).
5. E. A. GULBRANSEN AND K. F. ANDREW, *This Journal*, **98**, 241 (1951).
6. W. JOST, "Diffusion in Solids, Liquids, Gases," p. 353, Academic Press, New York (1952).
7. O. KUBASCHEWSKI AND B. E. HOPKINS, "Oxidation of Metals and Alloys," p. 41, Academic Press, New York (1953).
8. G. HÄGG, *Z. Phys. Chem.*, **B11**, 433 (1930).
9. C. M. SCHWARTZ AND M. W. MALLETT, American Society for Metals Preprint No. 14 (1953).
10. S. S. SIDHU AND J. C. MCGUIRE, *J. Applied Phys.*, **23**, 1257 (1952).

Potentials of Iron, 18-8, and Titanium in Passivating Solutions[1]

HERBERT H. UHLIG AND ARTHUR GEARY

Corrosion Laboratory, Department of Metallurgy, Massachusetts Institute of Technology, Cambridge, Massachusetts

ABSTRACT

Potentials of iron in chromates show a linear relation for $C/\Delta E$ vs. C, where C is concentration and ΔE is change of potential, suggesting that they follow the Langmuir adsorption isotherm. Maximum potential change corresponding to an adsorbed monolayer of chromate ions occurs at 0.0025 molar K_2CrO_4, which approximates the minimum concentration for passivity reported by Robertson. The evidence agrees with a primary mechanism of passivity based on adsorption rather than on oxide film formation. For example, potentials of iron exposed to several organic inhibitors, where the mechanism is undoubtedly one of adsorption, also follow the adsorption isotherm as shown by Hackerman and coworkers. Passivity of 18–8 stainless steel and titanium in sulfuric acid containing cupric or ferric salts appears similarly to be accompanied by adsorption of Cu^{++} or Fe^{+++}. The irreversible nature of the potentials is in accord with the view that the adsorbate, in part, is chemisorbed.

Hydroxyl ions in 4% NaCl produce more active potentials in passive 18–8 or titanium presumably by displacing adsorbed oxygen. Potentials of 18–8 in alkaline NaCl as a function of partial pressure of oxygen follow the adsorption isotherm, which adds confirming evidence that an adsorbed oxygen film is responsible for passivity. The decreased potentials between active and passive areas plus precipitation of passivity-destroying metal chlorides as hydrous oxides at incipient anodes accounts for inhibition of pitting in chloride solutions by alkalies.

Calculated Langmuir isotherm constants, taking into account competitive chemisorption processes, agree qualitatively with expected relative values based on chemical properties of metals and adsorbates.

INTRODUCTION

Chromates are in the class of inhibitors called passivators because the potential of iron immersed in a chromate solution is several tenths volt more noble than in water, and iron no longer corrodes visibly. Two points of view have been proposed regarding the mechanism of passivation by these and similar compounds. Hoar and Evans (1) proposed that chromates react with soluble ferrous salts throwing down a protective film of hydrated ferric and chromic oxides. Accordingly, a film of ferric oxide on air-exposed iron will, if introduced into chromates, be made more protective because the chromate "repairs" the film discontinuities. Since then, this view has been restated by several investigators (2–4). Mayne and Pryor (3) modified the picture somewhat, based on their electron diffraction studies, proposing initial adsorption of chromates followed by direct reaction with iron to form an unhydrated γ Fe_2O_3 film which they suggested was a better diffusion barrier layer than a film of hydrated oxides.

[1] Manuscript received September 1, 1953. This paper was prepared for delivery before the Wrightsville Beach Meeting, September 12 to 16, 1953.

A second view attributes passivity to adsorption of chromate ions on the metal surface (5–8). Formation of an oxide film is considered unnecessary, although such a film may form eventually and aid in the over-all protection. The primary protection, however, is considered to result from satisfaction of valence forces of the surface metal atoms by chemical bonding with chromate ions, and without the metal atoms leaving their respective lattices. A similar mechanism has been proposed for specific organic inhibitors (9).

Passivators, in accord with this view, are substances having high affinity for the metal and accompanying high activation energy for any reaction which results in a new lattice belonging to a surface stoichiometric compound. These are the essential conditions for chemisorption. Consequently, an iron-chromium oxide or iron oxide, whichever forms ultimately when iron is exposed to chromate solutions, accumulates only slowly. Chlorine, for example, is not a passivator because, despite high affinity for the metal, its activation energy for reaction is low, resulting in rapid production of iron chlorides rather than a chemisorbed film of chlorine atoms. Oxygen, by way of contrast, readily

chemisorbs on many metals and is a good passivator. Halide ions break down passivity by competing with oxygen or other passivators for a place on the metal surface; but once they succeed, metal corrodes at such areas until additional passivator adsorbs.

Evans (10) and others (1, 3, 11) isolated oxide films on iron exposed to chromates and supposed these to be the primary source of protection. Circumstantial evidence of this kind is not conclusive, however, in view of the primary process of adsorption which, if it occurs at all, always precedes the formation of oxides or other compounds, and continues in effect even after the usually permeable, although relatively thick, oxide films are formed. In specific instances, some chemical reagents used for stripping of surface films may actually produce an oxide reaction product (12, 13). When this is the case, the stripping reagent may hasten reaction of adsorbed films, if not of other substances, with the metal, resulting in a surface compound where none existed before.

McKinney and Warner (14) in discussing a paper by Evans expressed doubt that chromates could act merely by precipitation of ferric-chromic oxides on the metal surface, in view of the fact that chromic salts are relatively poor inhibitors compared with chromates. Evans (15) replied that, when chromic salts precipitate a film of hydrated chromic oxide on cathodic areas, attack is not hindered; whereas with chromates, mixed hydroxides are precipitated locally at places where anodic attack would otherwise set in and prevents it from developing. This explanation, however, is less convincing in light of Robertson's (8) subsequent data which showed that molybdates and tungstates, analogous to chromates structurally, and inhibiting at the same minimum concentration, fail to oxidize ferrous salts [or do so extremely slowly (4)] and, hence, are quite unlike chromates in their capacity to precipitate a supposed protective anodic coating.[2]

[2] Criticism of Robertson's conclusions has been made on the basis that the otherwise weak oxidizing capacity of molybdate and tungstate in acid solution might be greater in neutral solutions (16) corresponding to actual conditions of *p*H at the surface of iron. However, the oxidizing tendency of these salts is *less* in neutral or alkaline media as compared with acid solutions (as can be demonstrated thermodynamically). This, in fact, was demonstrated for molybdates and tungstates by Pryor and Cohen by titrations in neutral media. They found only 11% of 0.0072*N* ferrous sulfate to be oxidized by 0.1*N* sodium tungstate after as long a period as three days, although they interpret this slow rate as sufficient to form the supposed protective film. Actually, molybdates and tungstates are less effective oxidizers than is dissolved oxygen.

This is not to say that iron does not reduce molybdates and tungstates in solution and become oxidized in the process. However, the minimum concentration of these substances for passivity or inhibition, identical with the minimum concentration of chromates, despite differing oxidizing tendencies, suggests that the mechanism of protection does not depend on an oxidation-reduction reaction.

Rozenfel'd and Akimov leaned to the possibility that anodic polarization of iron by chromates was due to adsorption of the chromate ion (17). Indelli (18) also interpreted potential behavior of iron and 18-8 in chromates in terms of adsorption of the inhibiting ion.

Simnad (19), using radioactive chromium, concluded that the view of Hoar and Evans was corroborated by the almost similar pickup of radioactive chromium whether iron was immersed in chromic chloride or in chromates, and by the spotty deposition of radio-chromium salts on an iron surface exposed to chromates, presumably revealing anode areas. However, his conclusions do not take into account reaction of chromic chloride with iron to form hydrated oxides which adhere to the metal surface in the same manner as hydrous FeO, but which are not protective in the same sense as chromates. Similarly, chromates may be reduced at preferential metal areas, particularly if chlorides or sulfates are present in solution which accelerate consumption of the passivator (20). Impurities in the metal may also accelerate reduction of chromates.

Brasher and Stove (21) report that the amount of radioactive chromium picked up by abraded mild steel after three days' immersion as a function of chromate concentration follows the form of a typical adsorption isotherm. They find a maximum of 5.5×10^{15} chromium atoms/cm^2 geometric surface. Considering a probable value of the roughness factor for an abraded surface equal to 3 (22), and a diameter of CrO_4^{--} equal to 5.4 Å (23), their value corresponds to the equivalent of 4.5 layers of close-packed chromate ions. The number of layers would be less if correction were made for any chromate adsorbed on the air-formed surface oxide or reduced to chromic oxide during the three days' exposure.

Powers and Hackerman (24), also using abraded steel, found, in agreement with Brasher and Stove, that after two days' immersion in $10^{-3}M$ radiochromate at *p*H 7.5 there were 5.2×10^{15} chromium atoms remaining per cm^2 of surface, uniformly distributed.

Potential measurements of iron exposed to chromate solutions add to the pertinent evidence concerning the mechanism of passivation. Data of this kind are presented herewith, together with parallel data for 18-8 stainless steel and titanium in other passivating electrolytes.

Procedure

Potentials were measured using a precision potentiometer and vacuum-tube galvanometer in conjunction with a silver chloride reference electrode

in 0.1N KCl. The potential of the latter on the hydrogen scale omitting liquid junction potentials is 0.288 volt at 25°C. All measurements were conducted in an air thermostat maintained within 0.2° of 25°C. Final values are for steady state where the net change within 12 hr was less than 5 mv. This often required successive measurements over several days. The maximum change, however, within a few centivolts was obtained usually during the first 24 hr.

Iron electrodes were prepared from high purity 0.030-in. diameter wire obtained by courtesy of the National Bureau of Standards (C < 0.001%, total impurities about 0.008%). Six-inch lengths were mounted in glass tubing and sealed, using polystyrene cement with about 1 cm of wire projecting. The surface was prepared by pickling in 10% H_2SO_4, followed by washing and immediate transfer to the test solution.

Electrodes of 18-8 were prepared from Type 304 0.028-in. diameter wire. The wire was first annealed by heating electrically to 1000°C and quenching in air, then was pickled in 15 vol % HNO_3, 2 vol % HF at 70°–80°C, and washed. It was immersed directly into the electrolyte to a depth of about 1 cm.

Titanium electrodes were made by cutting thin strips of Bureau of Mines cold rolled titanium, followed by pickling in HNO_3-HF at 70°–80°C. No heat treatment was employed.

Ferric ion concentration in sulfuric acid was determined by reduction first with stannous chloride, the excess of which was eliminated by adding $HgCl_2$, followed by titration with permanganate. Cupric ion concentration was determined by titration using thiocyanate. Dichromate or chromate solutions were made up by weighing out the required amount of salt. Low carbonate NaOH was prepared by cooling hot saturated NaOH and decanting into wax-lined bottles.

The cell used for potential determinations consisted of a 4-oz bottle fitted with a rubber stopper. A salt bridge containing the same solution as the electrolyte made contact with 0.1N KCl in which the silver chloride electrode was immersed. The latter electrode was mounted in a glass tube, the bottom of which was constricted to provide a liquid junction by means of a sealed-in asbestos fiber.

Air, first bubbled through caustic soda and water, was used to aerate and stir most of the solutions. When nitrogen was used, it was purified by passing over 4 ft of copper turnings maintained at 400°C.

In tests for reversibility,[3] the same metal electrode was used throughout, but for measurements of potentials as a function of concentration, different electrodes in separate cells were set up. In view of the considerable time to reach steady state, the latter arrangement was the only practical procedure. This produced a greater scatter of the data, but also made the observed correlation of potential with concentration more convincing.

[3] Reversibility not in the thermodynamic sense, but referring to reproducibility of potentials as approached from either more concentrated or more dilute solutions.

Potential Data

Iron in Chromates

Iron in contact with distilled water attains noble values of potential as K_2CrO_4 is added. At a concentration of 0.0025 molar, the potential change is about 0.5 volt (Fig. 1). Further change at higher concentrations is not pronounced. The maximum potential change agrees with data presented by Burns (25) for iron in 0.01N $K_2Cr_2O_7$ solution.

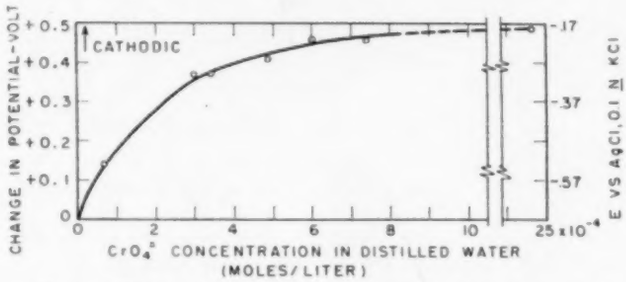

Fig. 1. Effect of $CrO_4^=$ additions on the electrode potential of electrolytic iron in distilled water; (25.0 ± 0.2°C); aerated solutions.

On first immersing the electrodes in a dilute solution of chromate, potentials are relatively active, changing to more noble values within about 2 to 4 hr. The time required is less as the concentration of chromate increases. Steady-state values in all cases were reached in less than 24 hr.

When the electrodes at steady state in 0.0025M chromate are transferred to progressively more dilute solutions, it is found that a maximum of half the ennobling effect of the chromate is lost. This is true even after exposure to distilled water for 41 hr.

18-8 Stainless Steel and Titanium

18-8 stainless steel corrodes in dilute sulfuric acid, but corrosion is effectively inhibited (26) on addition of small amounts of ferric or cupric salts. Similar inhibition is observed to hold for titanium (27, 28), but with the difference that the beneficial effects extend to hydrochloric acid, unlike the situation for 18-8. It is of interest, therefore, to determine the parallel potential behavior of 18-8 and titanium in sulfuric acid as these inhibitors are added. Potentials in 0.2N H_2SO_4 containing up to 0.191M ferric sulfate are summarized in Fig. 2, and for similar additions of cupric sulfate up to 0.70M

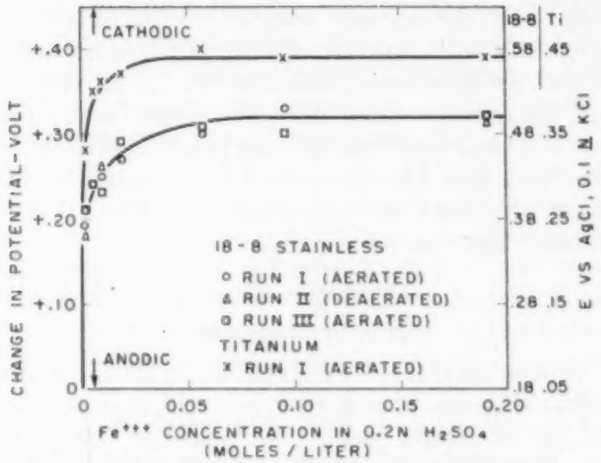

FIG. 2. Effect of Fe^{+++} additions on the electrode potentials of 18-8 stainless steel and titanium in $0.2N$ H_2SO_4; (25.0 ± 0.2°C).

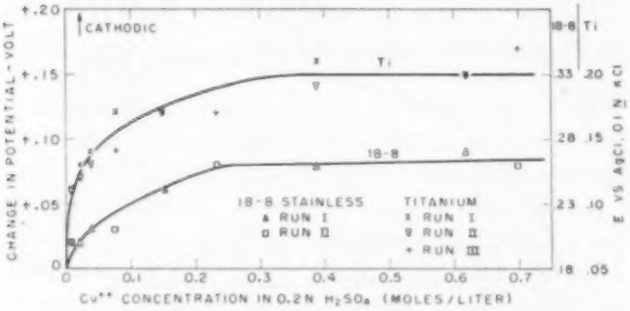

FIG. 3. Effect of Cu^{++} on the electrode potentials of 18-8 stainless steel and titanium in $0.2N$ H_2SO_4; (25.0 ± 0.2°C); aerated solutions.

in Fig. 3. Potentials of 18-8 in ferric sulfate solution, followed for several days, are found to become more noble by a maximum of 0.32 volt, whereas titanium similarly is ennobled to a maximum of 0.39 volt. Since 18-8 is initially more noble than titanium by 0.13 volt, final potentials are not far different. The general reproducibility of measurements can be gauged by a comparison of two separate runs for 18-8 in aerated solutions. In addition, one run in nitrogen-saturated solution showed that oxygen exerts no effect on the potential behavior.

Potentials of 18-8 and titanium are not reversible, as shown by data of Table I. On immersing 18-8, previously at steady state in $0.19M$ Fe^{+++}, into $0.002M$ Fe^{+++} (referring to $0.2N$ H_2SO_4), the second steady-state potential remained more noble by 0.07 volt after 27 hr of exposure than the original steady-state value of 0.18 volt. However, on re-immersing the electrode into $0.19M$ Fe^{+++}, the potential of 0.35 volt at the end of 20 hr was only 0.04 volt more noble than the original value.

With cupric sulfate additions, potential changes are less than for ferric sulfate, even though the final concentration of cupric ion is higher. Maximum ΔE averaged 0.08 volt for 18-8 and 0.15 volt for titanium.

TABLE I. *Test of reversibility*

Electrolyte	Initial ΔE (volt)	Change of concentration in moles/liter	Final ΔE (volt)
		18-8	
$0.19M$ Fe^{+++} in $0.2N$ H_2SO_4	0.31		
	0.26	Decrease to 0.010	0.27 (4 hr)
	0.18	Decrease to 0.002	0.25 (27 hr)
	0.31	Increase to 0.191	0.35 (20 hr)
		Titanium	
$0.70M$ Cu^{++} in $0.2N$ H_2SO_4	0.17		
	0.12	Decrease to 0.23	0.16 (1 hr)
	0.09	Decrease to 0.078	0.14 (1 hr)
	0.00	Decrease to 0.0	0.12 (1 hr)
	0.09	Increase to 0.078	0.13 (1 hr)
	0.12	Increase to 0.23	0.17 (1 hr)
	0.17	Increase to 0.70	0.19 (1 hr)
		Iron	
$2.5 \times 10^{-3}M$ K_2CrO_4	0.49	Decrease to 0.0	0.25 (41 hr)
$0.35M$ NaOH in 4% NaCl	0.45		
	0.18	Decrease to 0.04	0.20 (1 hr)
	0.15	Decrease to 0.025	0.17 (1 hr)
	0.00	Decrease to 0.0	0.10 (1 hr)
	0.15	Increase to 0.025	0.17 (1 hr)
	0.18	Increase to 0.04	0.18 (1 hr)
	0.45	Increase to 0.35	0.35 (1 hr)

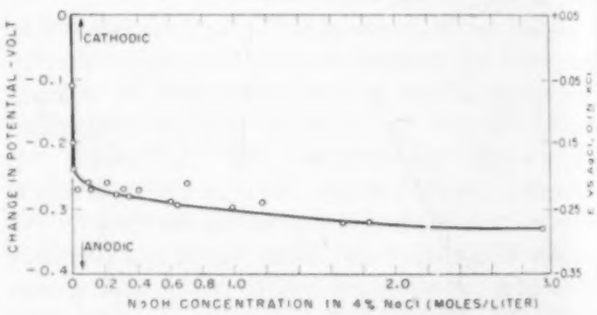

FIG. 4. Effect of NaOH additions on the electrode potential of 18-8 stainless steel in aerated 4% NaCl; (25.0 ± 0.2°C).

In aerated NaCl, 18-8 stainless steels in time corrode by pitting. Addition of alkali inhibits this type of attack (29). Titanium, on the other hand, is relatively resistant to pitting in chloride solutions without alkali additions, including sea water. The potential behavior of 18-8 in 4% NaCl upon addition of NaOH up to 2.9 molar is shown in Fig. 4, and similarly in Fig. 5 for titanium with addition of NaOH up to 0.2 molar. Potentials were followed for a total period of about 120 hr. The remarkable difference in behavior of the metals in this electrolyte compared with previous electrolytes is that NaOH additions produce more *active* potentials, or decrease passivity as measured by potential. Effects are most pronounced with first additions of NaOH below

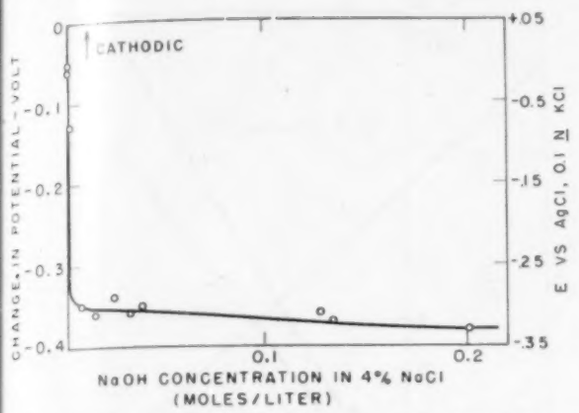

FIG. 5. Effect of NaOH additions on the electrode potential of titanium in aerated 4% NaCl; (25.0 ± 0.2°C).

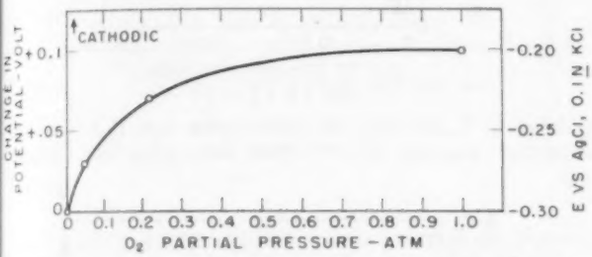

FIG. 6. Effect of varying O_2 partial pressure on the electrode potential of 18-8 stainless steel in 4% NaCl; 0.3*M* NaOH; (25.0 ± 0.2°C).

about 0.01 molar, subsequent additions producing only slight change. The maximum change of potential for 18-8 was −0.33 volt and for titanium −0.38 volt, indicating again similar behavior of both metals.

It was also of interest to learn the effect of oxygen on the potentials of 18-8 in this system, because of the importance oxygen has with respect to passivity of stainless steels exposed to the atmosphere. Potential measurements were carried out in 4% NaCl containing 0.3*M* NaOH through which nitrogen, oxygen, or air was bubbled. Also, one gas mixture was prepared, containing 0.05 atm partial pressure oxygen, by compressing air and nitrogen to appropriate pressures in a single gas cylinder and using this mixture to aerate and stir the electrolyte. Results are given in Fig. 6 showing that oxygen, as expected, ennobles the potential of 18-8 as the partial pressure increases.

Potentials were also determined for iron in 4% NaCl as a function of NaOH additions. Here the potential becomes *more noble*, opposite to the trend for 18-8 or titanium (Fig. 7). About 24 hr or less were required for steady state. The values, on immersing the electrodes in several more dilute NaOH solutions after reaching steady state in 0.35*M* NaOH, were the same as previously determined within 0.02 volt (after one hour) and on returning the electrode to 0.35*M* NaOH, the potential was less noble by 0.1 volt (Table I). It is especially

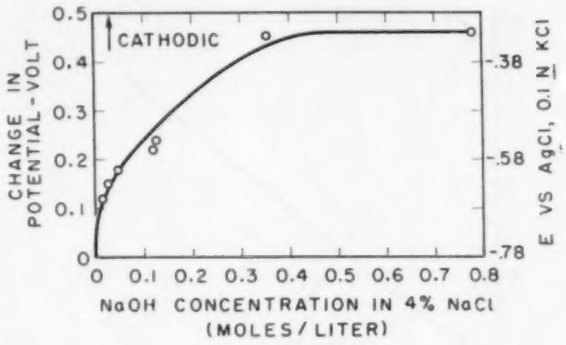

FIG. 7. Effect of NaOH additions on the electrode potential of electrolytic iron in 4% NaCl; (25.0 ± 0.2°C); aerated solutions.

significant that the potential of iron, initially active in 4% NaCl, and the potential of 18-8 initially noble, approach the same value on additions of NaOH. This suggests that the final surface states of iron and 18-8 (which contains 74% iron) in alkaline NaCl are comparable, despite large initial differences in neutral NaCl. Perhaps it is not surprising, therefore, that corrosion rates in alkaline NaCl are comparably low for both metals, but are quite different in neutral or near neutral NaCl solutions.

DISCUSSION

For each metal studied, the potential behavior as a function of passivator or inhibitor concentration resembles a typical adsorption isotherm. This relation is expected if inhibitors function by adsorbing on the metal surface, but would not be predicted, presumably, by any mechanism involving diffusion-barrier oxide or other type reaction-product films. Interpretation of the data, therefore, in terms of an adsorption process appears worthwhile.

Adsorption Isotherm and Potentials

The adsorption isotherm proposed by Langmuir (30) is expressed as follows:

$$x = \frac{abp}{1 + ap}$$

where x is the amount of gas adsorbed per unit area at pressure p, and a and b are constants. The constant b is equal to maximum adsorbate x_m at high values of p, and a is related to heat of adsorption (31). Assuming that Henry's law applies, this can be converted to a similar expression for adsorption from liquids where concentration of solute C substitutes for gas pressure p.

Furthermore, if the ions adsorbing on a metal surface form dipoles each of electric moment μ, electrostatic theory leads to the expression $4\pi n\mu$ for the total change of potential ΔE produced by n

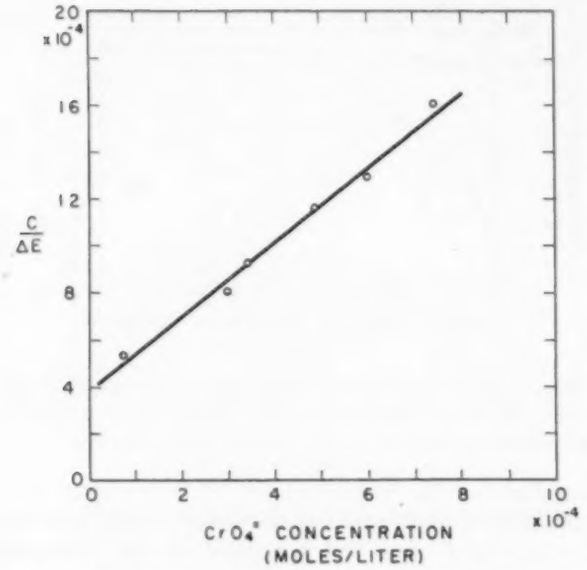

FIG. 8. Langmuir adsorption plot for electrolytic iron in distilled water containing $CrO_4^=$ inhibitor.

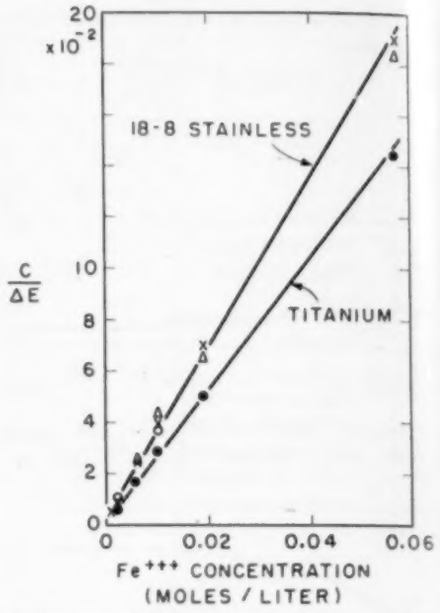

FIG. 9. Langmuir adsorption plot for 18-8 stainless steel and titanium in 0.2*N* H_2SO_4 containing Fe^{+++} inhibitor.

dipoles adsorbing per unit area of metal surface.[4] Therefore, ΔE is proportional to x, and maximum ΔE_m is similarly proportional to x_m.

Therefore, $$\frac{C}{\Delta E} = \frac{C}{\Delta E_m} + \frac{1}{a'\Delta E_m}$$

If the Langmuir isotherm applies, therefore, a linear relation should exist between $C/\Delta E$ plotted with C, the slope of which is equal to $1/\Delta E_m$, and the intercept is equal to $1/a'\Delta E_m$ at $C = 0$. Data for various inhibitor concentrations satisfactorily conform to this relation as shown by Fig. 8 to 13. Potentials for 18-8 and titanium in 0.2*N* H_2SO_4 containing Cu^{++} show a degree of scattering, caused probably by the small measured potential differences in these solutions compared with experimental variations, the maximum ΔE being only 0.08 to 0.15 volt. $C/\Delta E$ vs. C was not reproduced for Ti and 18-8 in 4% NaCl + NaOH, even though linearity is obtained for all but the lowest NaOH concentrations. The test of linearity, however, loses significance when values of ΔE are essentially

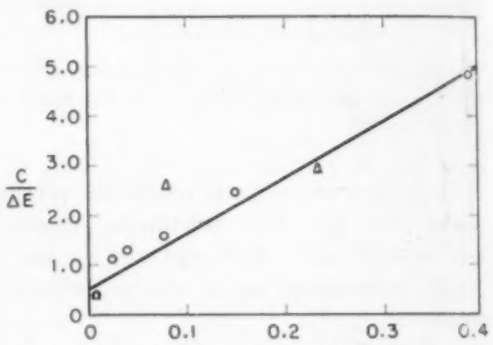

FIG. 10. Langmuir adsorption plot for 18-8 stainless steel in 0.2*N* H_2SO_4 containing Cu^{++} inhibitor.

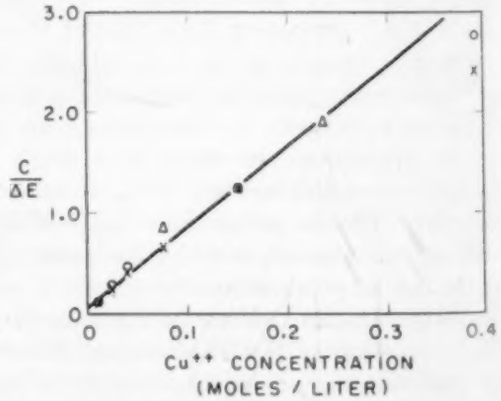

FIG. 11. Langmuir adsorption plot for titanium in 0.2*N* H_2SO_4 containing Cu^{++} inhibitor.

constant with change of inhibitor concentration, as is true in this instance.

Correspondence, by and large, of potential data to the Langmuir type isotherm points strongly to

[4] If one considers a supplementary diffuse double layer in accord with Gouy and Chapman, the additional potential change equals $4\pi\sigma/D\kappa$ (32) where σ is the total electric charge per unit area, D is the dielectric constant, and κ is equal to $(4\pi e^2/DkT\ [\Sigma\ n_i z_i^2])^{\frac{1}{2}}$ having the same significance as in the Debye-Hückel theory of electrolytes. Since κ has the dimensions of reciprocal length and may be identified with the effective separation of charges in the dipole layer, this expression, if $D = 1$, achieves the same form as the expression for a fixed dipole layer.

Adsorption of ions can be looked upon as forming new cathodic areas, the extent of which reaches a maximum at completion of a monolayer. Anodic areas are simultaneously restricted to a minimum corresponding to maximum anodic polarization by corrosion currents and a shift of potential to more noble values.

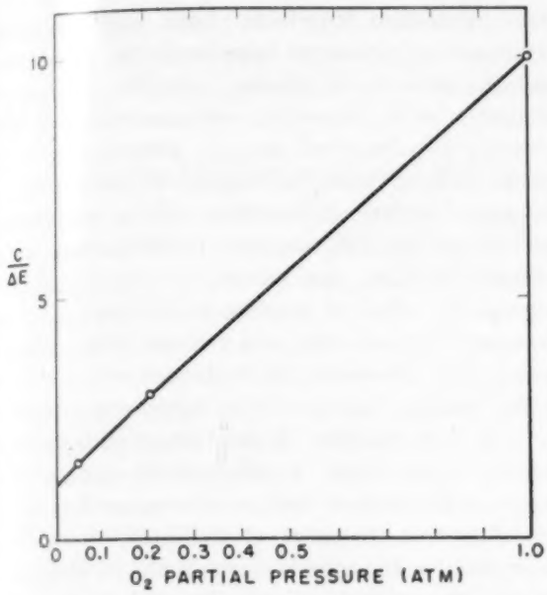

FIG. 12. Langmuir adsorption plot for 18-8 stainless steel in 4% NaCl with 0.3*M* NaOH, varying O_2 partial pressure.

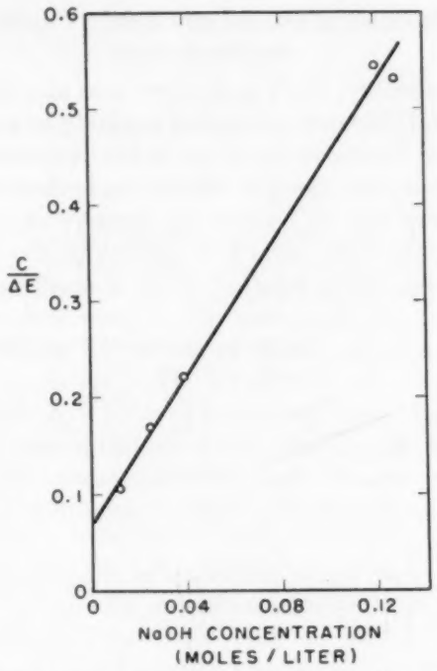

FIG. 13. Langmuir adsorption plot for electrolytic iron in aerated 4% NaCl with NaOH additions.

the view that the inhibitors considered at present function by adsorbing on the metal surface. Furthermore, the observed correspondence suggests adsorption of the monolayer type, as was pointed out by Langmuir in the derivation of his isotherm equation. These conclusions are strengthened by measurements of Hackerman and Sudbury (33), showing that potentials of steel in contact with organic amine inhibitors also follow the Langmuir adsorption isotherm. The linearity of $C/\Delta E$ vs. C reported by them is especially significant, since it is generally conceded that organic inhibitors function by adsorbing on the metal surface (34, 35).

Maximum potential change, in accord with present considerations, occurs with formation of a complete monolayer of chemisorbed ions, any additional adsorption being accompanied by relatively small potential changes and lesser effects on the corrosion rate. It is important to note, therefore, that maximum change of ΔE in Fig. 1 for iron in chromates occurring at 2.5×10^{-3} molar, corresponds approximately to the minimum concentration of chromates (1×10^{-3} molar) found necessary by Robertson (8) for inhibition and passivity. It is probably reasonable to conclude, therefore, that optimum passivity is associated with a monolayer film of adsorbed chromate ions.

Part of the adsorbed chromate is chemisorbed and part is reversibly adsorbed, as is pointed out by the time necessary to achieve steady-state potentials, indicative of the usually longer times required for chemisorption, and by the partially irreversible nature of the potentials. Even after thorough washing in distilled water, iron passivated in radioactive chromates shows residual radioactivity (19, 21, 24), and the potential is more noble than initially. The final irreversible or chemisorbed portion exerts about half the total effect on the potential. This result is in agreement with a similar observation of Gatos (36) who found that, on first immersing iron in chromate solutions, the amount of metal reacting initially when iron is made passive in concentrated nitric acid is less than in absence of chromate exposure, and that half this effect of chromate, but no more, could be removed by washing in water.

Powers and Hackerman (24) suggested adsorption of chromate ions on a surface oxide rather than on the metal. Although such adsorption presumably may occur, any mechanism of corrosion protection accompanying a film of this kind is not yet clear. An air-formed film, at least, is not necessary to adsorption. Preliminary measurements in this laboratory using radiochromate showed that the usual radioactivity is picked up by oxide-free Armco iron sheet (0.024% C). Iron specimens were heated in dried pure H_2 at 1000°C, cooled in this gas, transferred to deaerated $10^{-3}M$ $Cr^{51}O_4$, *p*H 1.9, out of contact with air, and after 2 to 17.5 hr, washed successively in three 200-ml portions of distilled water. Somewhat greater residual chromium (3×10^{16} atoms/cm²) was found than that reported by Brasher and Stove and by Hackerman and Powers for abraded iron. No residual radioactivity was found on similar specimens immersed directly into deaerated radioactive chromic perchlorate of *p*H 1.9.

Adsorption of Oxygen and Ferric, Cupric, and Hydroxyl Ions

Presumably, ferric and cupric ions also adsorb on 18-8 and titanium, producing passivity as gauged by reduced corrosion rates or noble potentials. Ions have a certain electron affinity and when adsorbed receive a certain amount of negative charge from the metal. The net effect, including the effect of negative ions in solution, is an over-all negatively charged ion layer near the surface and an equal positive image charge in the metal, similar to the situation for chromates. This accounts for increasingly noble potentials as more ferric and cupric ions adsorb, trivalent ferric ion being more effective in this respect than divalent cupric ion, corresponding also to the order of inhibition in dilute sulfuric acid (27).

The more active potentials of titanium and 18-8 in sodium chloride solution on addition of sodium hydroxide can be interpreted as competition between hydroxyl ion and oxygen for a place on the metal surface, the adsorbed hydroxyl ion producing a lower order dipole moment than adsorbed oxygen. Chemisorbed oxygen, according to one viewpoint, is primarily responsible for passivity (5, 37, 38) in these metals. If the partial pressure of oxygen is increased, the potential becomes more noble (Fig. 6) in agreement with this view. The potential change from 0 to 1 atmosphere oxygen amounts to only 0.1 volt, suggesting that the fundamental passive layer of chemisorbed oxygen in alkaline NaCl is only slightly disturbed by hydroxyl ions. This concurs with the observation that apparent equilibrium in this instance is effected between dissolved gas and molecularly adsorbed oxygen and not atomically adsorbed oxygen, as shown by the linearity of $p/\Delta E$ plotted with p but lack of linearity plotting $\sqrt{p}/\Delta E$ vs. $\sqrt{p}$, where p refers to partial pressure of oxygen. Previous quantitative adsorption data obtained for oxygen on 18-8 (39) provided evidence, in fact, that the alloy exposed two days to aerated water is covered by a close packed atomic oxygen layer over which a molecular oxygen layer is adsorbed. Were the chemisorbed atomic oxygen on 18-8 entirely displaced by OH^-, the potential change would be in the order of 0.5 volt, corresponding to complete breakdown of passivity, but a potential change of 0.4 volt occurs only in concentrated alkalies, e.g., 20% NaOH (40).

When iron, on the other hand, is immersed in alkaline NaCl, competition includes not only adsorbed OH^- and oxygen, but also adsorbed H. Iron exposed to an aqueous solution has a definite tendency to react, liberating hydrogen and hydrous ferrous oxide, the free energy for the reaction being negative (41) and independent of pH, so long as these corrosion products form and ..o other. Hydrogen so produced adsorbs on the iron surface and, in neutral or alkaline solutions, escapes reluctantly as H_2 impeding corrosion reaction. With presence of dissolved oxygen, adsorbed hydrogen reacts to form water as rapidly as oxygen reaches the metal surface. If, however, rate of consumption falls below the diffusion rate to the surface, excess oxygen, in turn, can adsorb on the metal. This adsorption, when it occurs, is accompanied by a lowered corrosion rate and a more noble potential (passivity). Therefore, as hydroxyl ions are added to the solution, adsorbed H is increasingly displaced by OH^- and reaction of the former with dissolved oxygen slows down. Consequently, oxygen is in excess at the surface, and conditions are favored for its adsorption. Support of this state of affairs is provided by the observation that, in absence of oxygen, the potential of iron in water is more active when alkalies (42, 43) are added, as is expected from the reduced solubility of $Fe(OH)_2$ under these conditions. Only in presence of oxygen does the potential become more noble, the measured potential being a compromise between the iron and oxygen electrode values. In acid media, on the other hand, the iron electrode covered with adsorbed hydrogen behaves approximately as a reversible hydrogen electrode (44, 45). Since iron and 18-8 have about the same potential in aerated alkaline NaCl, the inference is that if oxygen is chemisorbed on 18-8, it is also, under these conditions, chemisorbed on iron and is responsible for observed passivity in both metals. The energy of bonding of oxygen to the metal need not be the same in both cases, however, and, therefore, the degree of passivity may differ.

Powers and Hackerman showed that competitive adsorption of CrO_4^{--} and OH^- takes place on Cr (46) and iron (24) surfaces, similar to competitive adsorption of H, O_2, and OH^- described above.

Pitting Tendencies of 18-8 and Titanium

Inhibition of pitting in 18-8 by hydroxyl ion can be accounted for by the reduced difference of potential between active and passive areas in the galvanic cells that account for pitting (47), since the passive areas are no longer so noble as before. In addition, metal chlorides at incipient pits react with hydroxyl ions which migrate rapidly to anodic areas to form metal hydroxides. Hydroxides, unlike soluble chlorides, do not continuously destroy passivity or, what is the same, do not maintain activity at the site of chemical disturbance; hence, the pit never gets started. With titanium, pitting tendency is decreased by the pronounced tendency of titanium chloride to hydrolyze to hydroxide or hydrous oxide even in absence of hydroxyl ions.

Hence, titanium, better than 18-8, resists pitting in sea water, and potential data indicate that in alkaline salt solutions, the tendency would be still less.

Separation of Charge in Dipole Layer

Values of ΔE in combination with the equation $\Delta E = 4\pi n\mu$ make it possible to calculate the average separation of negative charge in the adsorbed chromate layer from the iron surface. Assuming a diameter of chromate ion equal to 5.4 Å, there will be 4.0×10^{14} ions/cm² adsorbed in a close packed monolayer. A layer based on true surface rather than apparent area would still be equivalent in projected dipole moment to this number of ions. Since the change of potential produced by a monolayer is 0.5 volt (Fig. 1), the calculated value of d, where μ is equal to de (d = separation of negative and positive charge, and e = electronic charge), is $0.5/(300 \times 4\pi \times 4 \times 10^{14} \times 4.8 \times 10^{-10})$ or 0.07×10^{-8} cm. Hence, the excess electrons, according to this calculation, are, on the average, only 0.035×10^{-8} cm from the metal surface, since the positive image charge within the metal is at a similar distance from the surface. In other words, a relatively slight asymmetry of electron density at the metal surface suffices to explain the observed adsorption potentials.

Values of Langmuir Constants

Values of the Langmuir constants ΔE_m and a' are summarized in Table II. In general, ΔE_m calculated from the slope of $C/\Delta E$ vs. C agrees reasonably well with the observed maximum ΔE_m. For iron in alkaline NaCl, the difference in values suggests that potential relations are more complex than the simple adsorption of oxygen alone, in accord with the discussion of iron potentials above.

Values of a' are equal to the reciprocal of the concentration at which half the maximum potential shift is obtained. According to the Langmuir derivation, these values are larger as the heat of adsorption increases. Hence, O_2 on 18-8 and chromates on iron show appreciable affinity of adsorbate for metal. Similarly, ferric ions have greater affinity for 18-8 and titanium than cupric ions. The low value of a' for iron in alkaline NaCl supports the point of view that competitive chemisorption takes place between several species, e.g., H, OH^-, and O_2, heats of adsorption for one species tending to cancel out heats of desorption for the species it displaces. Competition between possible adsorbates very likely accounts for the partial reversibility of potentials involving chemisorbed films. In general, it should be emphasized that values of a' reflect a resultant heat effect of one or more competitive adsorption processes, even if the substance displaced is nothing more than physically adsorbed H_2O. The primary process, of course, has the largest effect. By and large, relative values of a' are in accord with the expected trend based on chemical properties of the metals and adsorbates.

TABLE II. *Values for constants of Langmuir adsorption isotherm*

Electrode	Electrolyte	E vs. AgCl, 0.0N inhib., volt	ΔE_m (volt)		Intercept a'^{-1} ΔE_m^{-1}	a' (liters/mole)
			(calc)	(obs)		
18-8	Fe^{+++} in 0.2N H_2SO_4	0.18	0.30	0.33	0.001	3300
	Cu^{++} in 0.2N H_2SO_4	0.18	0.09	0.08	0.5	22
	O_2 in 0.3N NaOH in 4% NaCl	−0.30	0.11	0.1	0.0011	8400
Ti	Fe^{+++} in 0.2N H_2SO_4	0.05	0.37	0.38	0.001	2700
	Cu^{++} in 0.2N H_2SO_4	0.05	0.13	0.15	0.15	50
Fe	OH^- in aerated 4% $NaClCrO_4^{--}$ in H_2O	−0.78	0.26	0.46	0.065	59
		−0.67	0.63	0.5	0.00039	4000

Acknowledgment

This research was supported by the Office of Naval Research under Contract N5ori-07815 to whom the authors express their appreciation.

Any discussion of this paper will appear in a Discussion Section to be published in the December 1954 issue of the Journal.

REFERENCES

1. T. P. Hoar and U. R. Evans, *J. Chem. Soc.*, **1932**, 2476.
2. T. P. Hoar, *Trans. Faraday Soc.*, **45**, 683 (1949).
3. J. Mayne and M. Pryor, *J. Chem. Soc.*, **1949**, 1831.
4. M. J. Pryor and M. Cohen, *This Journal*, **100**, 203 (1953).
5. H. H. Uhlig, *Chem. Eng. News*, **24**, 3154 (1946).
6. H. H. Uhlig, *Metaux et Corrosion*, **22**, 204 (1947).
7. "Corrosion Handbook," (H. H. Uhlig, Editor) p. 31, John Wiley & Sons, Inc., New York (1948).
8. W. D. Robertson, *This Journal*, **98**, 94 (1951).
9. N. Hackerman and H. Schmidt, *Corrosion*, **5**, 237 (1949).
10. U. R. Evans, *J. Chem. Soc.*, **1927**, 1020.
11. U. R. Evans and J. Stockdale, *ibid.*, **1929**, 2651.
12. W. Vernon, F. Wormwell, and T. Nurse, *J. Iron Steel Inst. (London)*, **150**, 81*P* (1944).
13. M. Fontana, *Trans. Electrochem. Soc.*, **93**, 335 (1948).
14. D. McKinney and J. C. Warner, *Ind. Eng. Chem.*, **37**, 705 (1945).
15. U. R. Evans, *ibid.*, p. 706.
16. M. Pryor and M. Cohen, *This Journal*, **98**, 513 (1951).
17. I. Rozenfel'd and G. Akimov, *Doklady Akad. Nauk. S.S.S.R.*, **67**, 879 (1949); *C. A.*, **44**, 459 (1950).
18. A. Indelli, *Ann. Chim. (Rome)*, **40**, 189 (1950); *C. A.*, **45**, 10177 (1951).
19. M. Simnad, *J. Inst. Metals Monograph No. 13*, p. 23, London (1953).

20. M. Darrin, *Ind. Eng. Chem.*, **38**, 368 (1946).
21. D. Brasher and E. Stove, *Chem. and Ind.*, No. 8, 171 (1952).
22. T. L. O'Connor, Corrosion Lab., M.I.T., Unpublished measurements.
23. B. E. Warren, Private communication.
24. R. Powers and N. Hackerman, *This Journal*, **100**, 314 (1953).
25. R. M. Burns, *J. Applied Phys.*, **8**, 398 (1937).
26. J. Monypenny, "Stainless Iron and Steel," 3rd ed., p. 302, Chapman and Hall, London (1951).
27. J. Cobb and H. H. Uhlig, *This Journal*, **99**, 13 (1952).
28. D. Schlain and J. Smatko, *ibid.*, 417.
29. H. H. Uhlig and J. W. Matthews, *Corrosion*, **7**, 419 (1951).
30. I. Langmuir, *J. Am. Chem. Soc.*, **40**, 1361 (1918).
31. I. Langmuir, *ibid.*, **54**, 2798 (1932).
32. S. Glasstone, "Introduction to Electrochemistry," p. 524, D. Van Nostrand Co., Inc., New York (1942).
33. N. Hackerman and J. Sudbury, *This Journal*, **97**, 109 (1950).
34. U. R. Evans, "Metallic Corrosion, Passivity and Protection," p. 537, Ed. Arnold and Co., London (1946).
35. T. P. Hoar, "Pittsburgh International Conference on Surface Reactions," p. 127, Corrosion Publishing Co., Pittsburgh (1948).
36. H. C. Gatos and H. H. Uhlig, *This Journal*, **99**, 250 (1952).
37. Ref. 7, p. 24
38. H. H. Uhlig, *This Journal*, **97**, 215*C* (1950).
39. H. H. Uhlig and S. S. Lord, Jr., *ibid.*, **100**, 216 (1953).
40. H. H. Uhlig, *Trans. Am. Inst. Mining Met. Engrs.*, **140**, 387 (1940).
41. J. C. Warner, *Trans. Electrochem. Soc.*, **83**, 319 (1943).
42. A. Travers and J. Aubert, *Compt. rend.*, **194**, 2308 (1932).
43. E. Meunier and O. L. Bihet, *Congres. Chem. Ind.*, p. 444 (1933).
44. J. D'Ans and U. Breckheimer, *Z. Elektrochem.*, **58**, 585 (1952).
45. O. Gatty and E. Spooner, "The Electrode Potential Behavior of Corroding Metals in Aqueous Solutions," p. 310, Oxford Press, New York (1938).
46. N. Hackerman and R. Powers, *J. Phys. Chem.*, **57**, 139 (1953).
47. Ref. 7, p. 165.

Contribution to the Theory of Electropolishing[1]

CARL WAGNER

Department of Metallurgy, Massachusetts Institute of Technology, Cambridge, Massachusetts

ABSTRACT

An ideal electropolishing process is characterized by a plateau of the current density-potential curve corresponding to the maximum diffusion rate of an acceptor for metal ions toward the anode. Such a process is amenable to a quantitative theoretical analysis. Formulas are derived for decrease of surface roughness as a function of the recess of the average surface, amount of metal dissolved per unit surface area, and product of current density and time.

INTRODUCTION

Jacquet (1) and others have shown that a plot of current density J vs. cell voltage or anode potential E gives a horizontal plateau for many solutions used in electropolishing processes. Such a curve is found whenever the diffusion of one reactant consumed by an electrode process is the controlling factor, i.e., the concentration of the reactant at the surface of the electrode is much less than its bulk concentration, and the effective thickness of the hydrodynamic boundary layer has a definite value determined by forced or natural convection. In particular, a limiting current density is observed for the electrodeposition of metals at a cathode. Kolthoff and Miller (2) have also observed a limiting current density for the anodic dissolution of mercury if the diffusion of complexing ions such as $S_2O_3^{--}$, SO_3^{--}, CN^-, and SCN^- is the limiting factor.

Elmore (3) has interpreted the occurrence of a limiting current density for the anodic dissolution of a metal by assuming that the solution at the surface of the anode is saturated with respect to a salt of the dissolving metal, and the current density is determined by the diffusion rate of metal ions from the surface of the electrode into the bulk solution. This interpretation, however, is contradictory to the fact that the potential of the anode can be varied within rather wide limits, e.g., between 0.25 and 1.5 volt for copper in 86% H_3PO_4 according to Walton (4), whereas a constant concentration of metal ions at the anode and a constant current density are compatible only with a constant electrode potential.

According to Edwards (5, 6), the plateau of the current density-potential curve is due to diffusion of an "acceptor" for metal ions toward the anode. When silver is electropolished in a cyanide bath (7), cyanide ions are the acceptor forming $Ag(CN)_2^-$. In highly concentrated phosphoric or perchloric acid, the acceptor may be water whose significance has been discussed particularly by Darmois, Epelboin, and Amine (8). Water is needed for the formation of hydrated cations such as $Cu(OH_2)_4^{++}$. A limiting value of the current density corresponds to a maximum concentration gradient when practically all the acceptor approaching the anode readily reacts with metal ions, and thus the acceptor concentration at the anode is much lower than the bulk concentration. This interpretation of the plateau of the current density-potential curve implies that either the standard free energy of nonhydrated cations is much higher than that of hydrated cations, or the activation energy for the formation of nonhydrated cations is considerably greater than the activation energy for the formation of hydrated cations. A process satisfying these conditions will be called an "ideal electropolishing process."

MATHEMATICAL ANALYSIS OF AN IDEAL ELECTROPOLISHING PROCESS

Consider a sine-wave profile surface shown in Fig. 1 with a wave length, a, and an amplitude, b. At the surface of the electrode the concentration, c, of the acceptor determining the dissolution rate is supposed to vanish. Thus

$$c = 0 \text{ at } y = b \sin (2\pi x/a) \qquad \text{(I)}$$

where y is the distance from the "average surface plane" of the anode indicated by the dotted line in Fig. 1, and x is the coordinate parallel to the average surface plane.

If the dimensions a and b are much smaller than the effective thickness of the hydrodynamic boundary layer, only the innermost part of the boundary layer has to be considered, and thus flow of the liquid in the x or y direction may be neglected, since the velocity components at the surface of the electrode vanish. Then Fick's second law applies.

[1] Manuscript received October 15, 1953.

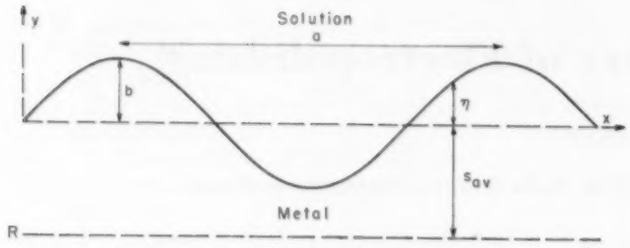

FIG. 1. Sine-wave profile electrode

For steady-state conditions it follows that

$$\frac{\partial c}{\partial t} = D\left(\frac{\partial^2 c}{\partial x^2} + \frac{\partial^2 c}{\partial y^2}\right) = 0 \qquad \text{(II)}$$

where D is the diffusion coefficient of the acceptor.

Edwards (5, 6) has already obtained solutions of equation (II) by determining experimentally the distribution of the electrical potential in a trough, involving a large scale model of the electrode, filled with tap water, and using the similarity between differential equations and boundary conditions for the concentration and the potential field. To arrive at general conclusions, it seems profitable to consider an analytical solution of equation (II). A particular solution reads

$$c(x, y) = B[y - b \exp(-2\pi y/a) \sin(2\pi x/a)] \qquad \text{(III)}$$

where B is a constant. If $b \ll a$, equation (III) virtually satisfies the boundary condition in equation (I) as is verified by substituting $y = b \sin(2\pi x/a)$ in equation (III) and letting the exponential function be unity as a close approximation since the exponent tends to zero for $b/a \to 0$.

Differentiation of equation (III) with respect to y yields

$$\partial c/\partial y = B[1 + (2\pi b/a) \exp(-2\pi y/a) \sin(2\pi x/a)]. \qquad \text{(IV)}$$

From equation (IV) it follows that the concentration gradient becomes virtually independent of x and y at some distance from the electrode, i.e., if $y \gg a$. Furthermore, the constant B is found to be equal to the average value of the concentration gradient at the anode, $(\partial c/\partial y)_{avg}$. A linear dependence of concentration on distance y will be found only in the innermost part of the boundary layer where flow of liquid can be neglected. A schematic concentration distribution for the entire boundary layer is shown schematically in Fig. 2. The effective thickness of the boundary layer, δ, may be defined as the distance of the intersection of the tangent line on the c vs. y curve at $y = 0, x = 0$ and the extrapolated plateau of the bulk concentration c_o. Since equations (III) and (IV) presuppose a virtually constant concentration gradient at $y \gg a$, e.g., $y > 4a$, and thus the region $y < 4a$ must belong to the innermost

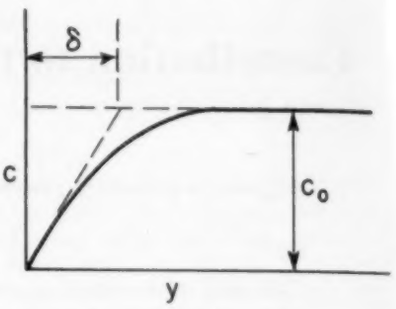

FIG. 2. Schematic graph of acceptor concentration as a function of distance from the electrode.

boundary layer, the effective thickness must be much greater than the wave length of the electrode profile. This is a necessary condition for the validity of equation (III) and subsequent equations derived therefrom.

Upon substituting $y = b \sin(2\pi x/a)$, expanding the exponential function, and neglecting terms involving higher powers of (b/a) except for the first power, the concentration gradient at the surface in the y direction is found to be

$$\left(\frac{\partial c}{\partial y}\right)_{y=b\sin(2\pi x/a)} \cong \left(\frac{\partial c}{\partial y}\right)_{avg}\left[1 + \frac{2\pi b}{a}\sin(2\pi x/a)\right] \qquad \text{(V)}$$

$$\text{if } b \ll a, \qquad a \ll \delta$$

In view of the condition $b \ll a$, we may disregard the difference between the concentration gradient normal to the average surface plane and that normal to the local surface, e.g., at $x = 0$ and $x = \frac{1}{2}a$.

Next, consider the change in the shape of the surface profile as a function of time, t. Let η be the distance of a point at the surface from the average surface plane, and s_{avg} the distance of the average surface plane from the reference plane, R, inside the electrode (see Fig. 1). Then the distance of a point at the surface of the electrode from the reference plane, R, equals

$$s = s_{avg} + \eta \qquad \text{(VI)}$$

where

$$\eta = b \sin(2\pi x/a). \qquad \text{(VII)}$$

Decrease of distances s and s_{avg} per unit time is proportional to the local and to the average dissolution rate, i.e., proportional to the local and the average concentration gradient of the acceptor, respectively. Thus, in view of equation (V)

$$-ds/dt = C[1 + (2\pi b/a) \sin(2\pi x/a)] \qquad \text{(VIII)}$$

$$-ds_{avg}/dt = C \qquad \text{(IX)}$$

where C is a constant, which is equal to the product of the average concentration gradient, the diffusion

coefficient, and the volume of the metal reacting with one mole of the acceptor. Upon substituting equation (VI) in equation (VIII) and subtracting corresponding sides of equations (VIII) and (IX), it follows that

$$-d\eta/dt = C(2\pi b/a) \sin (2\pi x/a). \qquad (X)$$

Decrease of the distance s_{avg} of the average surface plane from the reference plane, R, is equal to the displacement, u, of the average surface plane with respect to its position at time $t = 0$. Thus

$$-ds_{avg} = du. \qquad (XI)$$

Dividing corresponding sides of equations (X) and (IX) and substituting equations (VII) and (XI), one obtains

$$-db/du = 2\pi b/a. \qquad (XII)$$

Upon integration, it follows that

$$b = b_0 e^{-2\pi u/a} \quad \text{if} \quad b \ll a, a \ll \delta \qquad (XIII)$$

where b_0 is the amplitude of the sine-wave surface profile at zero time and b is the amplitude at time, t, corresponding to the displacement, u, of the average surface plane.

From equation (XIII) we readily recognize that percentagewise the amplitude of short sine waves will decrease far more rapidly than the amplitude of long sine waves. In other words, "microroughness" will disappear more rapidly than "macroroughness" in accordance with many observations.

A triangular wave profile or any other periodic profile may be represented by a superposition of sine waves of different wave lengths and amplitudes as a Fourier series. During electropolishing the contributions of the shorter waves disappear more rapidly, and thus the profile approaches a sine wave profile involving the greatest wave length of the original pattern. This is in accord with results reported by Edwards (5, 6).

From equation (XIII) it follows that the displacement, u, for a decrease of the amplitude from b_0 to b is

$$u = a[\ln(b_0/b)]/2\pi. \qquad (XIV)$$

The corresponding loss of metal per unit area, $\Delta m/A$, is found to be

$$\Delta m/A = u\rho = a\rho[\ln(b_0/b)]/2\pi \qquad (XV)$$

where ρ is the density of the metal.

From a copper electrode having a sine-wave profile with a wave length of 0.0134 cm, which was investigated by Edwards (5, 6), one has therefore to remove 0.013 gram/cm² in order to obtain a decrease of the amplitude to half the initial value. This value is in accord with results reported by Edwards for the later stages of experiments when his samples had a nearly sine-wave profile.

The corresponding number of coulombs per unit area, equal to the product of current density, J, and time, t, is found to be

$$J(\text{amp/cm}^2)t(\text{sec}) = \frac{96{,}500}{EqW} \frac{a(\text{cm})\rho(\text{g/cm}^3)}{2\pi} \ln \frac{b_0}{b} \qquad (XVI)$$

where 96,500 is the numerical value of the Faraday constant in coulomb/equivalent and EqW is the equivalent weight of the metal. For copper, e.g., 96 coulombs are required in order to decrease the amplitude by a factor of 10 if the wave length is 0.01 cm.

The foregoing analysis is that of an ideal electropolishing process. The following complications may occur.

1. If the amplitude, b, is not much smaller than the wave length, a, equation (III) does not satisfy equation (I). Qualitatively, the foregoing conclusions remain valid, but a rigorous mathematical analysis would require the replacement of the one-term expression in equation (III) by a Fourier series.

2. If the wave length, a, is not much smaller than the thickness of the boundary layer, the decrease in amplitude will be less than calculated from equation (XIII). This can be readily recognized from a consideration of the extreme case that the thickness of the wave length of the profile is much greater than the effective thickness of the boundary layer. In this case no differences in the local diffusion rate of the acceptor can be expected. Since according to equation (XIII) electropolishing removes microroughness more rapidly than macroroughness if $a \ll \delta$, the case $a \gtrsim \delta$ is not of great interest, especially when the viscosity of the solution is rather high and, therefore, δ is fairly large, e.g., 0.1 cm.

3. In solutions consisting mainly of perchloric or phosphoric acid, enrichment of salt and depletion of water increase viscosity. Accordingly, the diffusion coefficient may not be constant. Under these conditions, equation (II) has to be replaced by a more involved expression and the foregoing analysis has only qualitative significance.

4. Further complications may be caused by the evolution of gas bubbles and, eventually, local variations of the reactivity of the dissolving metal, especially in the case of heterogeneous alloys so that equation (I) is not satisfied at all points of the surface of the electrode.

Interpretation of Etching

For a comparison, consider the behavior of an anode at which polarization is supposed to be negligible. Then the electrical potential φ along the surface is constant and may be set equal to zero as the reference potential. Using the notation introduced in Fig. 1 and equation (I), we have for a sine-wave profile anode

$$\varphi = 0 \text{ at } y = b \sin (2\pi x/a). \qquad \text{(XVII)}$$

Inside the electrolyte, the Laplace equation

$$\partial^2\varphi/\partial x^2 + \partial^2\varphi/\partial y^2 = 0 \qquad \text{(XVIII)}$$

holds. Consequently, we obtain the potential gradient at the surface of the anode in a form analogous to that for the concentration gradient indicated in equation (V),

$$\left(\frac{\partial\varphi}{\partial y}\right)_{y=b\sin(2\pi x/a)} \cong \left(\frac{\partial\varphi}{\partial y}\right)_{\text{avg}} \left[1 + \frac{2\pi b}{a} \sin (2\pi x/a)\right] \qquad \text{(XIX)}$$

$$\text{if } b \ll a, \qquad a \ll \delta.$$

The local current density, J, is proportional to the local potential gradient according to Ohm's law. In view of the similarity between equations (V) and (XIX), equations (XIII) to (XVI) will hold if polarization is negligible. Consequently, the amplitude of a given roughness will decrease in the same manner as in the case of diffusion of an acceptor as the factor determining the local dissolution rate. Actually, however, polarization is not negligible. If the wave length a is small in comparison to the parameter k defined as the product of electrical conductivity and the absolute slope of the potential-current density curve, the current density is far more uniform than according to equation (XVIII) for vanishing polarization (9).

For $a < 0.01$ cm and a current density J lower than the plateau of the J vs. E curve, we have $a \ll k$ and thus we have to expect a practically uniform current density if k is uniform, i.e., the slope of the current density-potential curve is the same at all points of the anode. At different crystallographic faces, however, the magnitude of activation polarization for the anodic dissolution of a metal is different, as is known from investigations involving single crystals (10). This corresponds to local variations of the slope of the current density-potential curve and the parameter k. Thus, different crystallographic faces dissolve at different rates, i.e., we observe electrolytic etching.

Any discussion of this paper will appear in a Discussion Section to be published in the December 1954 issue of the Journal.

REFERENCES

1. P. A. Jacquet, *Bull. soc. chim. France*, (5) **3**, 705 (1936); *Trans. Electrochem. Soc.*, **69**, 629 (1936).
2. I. M. Kolthoff and C. S. Miller, *J. Am. Chem. Soc.*, **63**, 1405 (1941).
3. W. C. Elmore, *J. Appl. Phys.*, **10**, 724 (1939); **11**, 797 (1940).
4. H. F. Walton, *This Journal*, **97**, 219 (1950).
5. J. Edwards, *J. Electrodepositors' Tech. Soc.*, **28**, 137 (1952).
6. J. Edwards, *This Journal*, **100**, 189*C*, 223*C* (1953).
7. L. I. Gilbertson and O. M. Fortner, *Trans. Electrochem. Soc.*, **81**, 199 (1942); D. G. Gray, *Proc. Am. Electroplaters' Soc.*, **35**, 241 (1948); *Metal Finishing*, **47**, 55 (1949); E. Raub and B. Wallhorst, *Die Metalloberflaeche*, **4**, A92 (1949).
8. E. Darmois, I. Epelboin, and D. Amine, *Compt. rend.*, **230**, 386 (1950); **231**, 1222 (1950); I. Epelboin, *J. Chim. Phys.*, **49**, C214 (1952).
9. C. Wagner, *This Journal*, **98**, 116 (1951).
10. A. T. Gwathmey and A. F. Benton, *Trans. Electrochem. Soc.*, **77**, 211 (1940); H. Leidheiser and A. T. Gwathmey, *Trans. Electrochem. Soc.*, **91**, 95 (1947).

Potentiometric Titration of Simple Salts with Potassium in Liquid Ammonia[1,2]

GEORGE W. WATT, GREGORY R. CHOPPIN,[3] AND JAMES L. HALL[4]

Department of Chemistry, The University of Texas, Austin, Texas

ABSTRACT

By means of potentiometric titration of solutions of salts with solutions of potassium in liquid ammonia at −38°, it has been shown that bismuth(III) iodide is reduced to Bi^0, K_3Bi_2, and K_3Bi_3 without intermediation of either the +2 or +1 oxidation state of bismuth. Reduction of iron(II) bromide is very complex and apparently does not involve the intermediate formation of Fe^{+1}. Reduction of potassium nitrate involves only reduction of nitrate ion to nitrite ion, followed by precipitation of potassium hydronitrite. Data relative to reduction of cobalt(II) nitrate have permitted a choice between two possible reduction mechanisms previously proposed. Data presented in this paper clearly demonstrate the usefulness of the potentiometric titration technique in the study of the mechanism of inorganic reduction reactions in ammonia.

INTRODUCTION

In an earlier report (1), equipment and procedures useful in carrying out potentiometric titrations involving solutions of metals in liquid ammonia were described. Subsequently, these techniques have been applied to detection of intermediate oxidation states of Group III nontransitional elements with particular emphasis on aluminum (2–4).

Experiments described in this paper were carried out for the purpose of determining whether the potentiometric titration method might be useful in elucidating the mechanism of reduction of simple inorganic salts with solutions of metals in ammonia. For this purpose, halides and nitrates of two transitional and two nontransitional elements were employed, and the specific cases selected were deliberately ones studied previously by less exacting methods.

EXPERIMENTAL

Materials.—With the exceptions noted below, all materials employed in this work were reagent grade chemicals that were used without further treatment.

Bismuth(III) iodide was prepared in 72% yield by a method described elsewhere (5). Analysis calculated for BiI_3: Bi, 35.4. Found: Bi, 35.4. X-ray diffraction data for this product are listed in Table I.

Iron(II) bromide (as the 6-ammonate) was prepared as described by Watt and Jenkins (7).

Reagent grade potassium nitrate was recrystallized from water and dried to constant weight at 110°C.

Ammonated cobalt(II) nitrate was prepared by displacement of water of hydration with ammonia by recrystallization from liquid ammonia as follows. Cobalt(II) nitrate 6-hydrate was converted to the corresponding 2-hydrate by drying *in vacuo* over concentrated sulfuric acid. A 1-gram sample of the very finely divided 2-hydrate was placed on the fritted glass disk of a filter tube[5] and that end of the tube was sealed about 3 in. from the disk. The tube was cooled, inverted, air in the tube was displaced with ammonia gas, the end of the tube containing the salt was immersed in a dry ice-isopropanol bath at −70°C, and 3 to 4 ml of ammonia was condensed on the salt. The open end of the tube was then sealed, also about 3 in. from the filter disk. The tube was removed from the bath and allowed to warm to and remain at room temperature for three days. The saturated solution was then transferred by inverting the tube and immersing the empty end in a refrigerant bath at −70°C. When the temperature of this solution was allowed to return to *ca.* 25°, a small crop of well-defined pink crystals separated. In this manner, transfer of the solution and removal of crystals was repeated until a major portion of the salt had been crystallized from the ammonia solution. In the final transfer, the ammonated salt was retained on the filter disk and the solution was contained in the end containing the original sample. The tube was opened, the ammonia was allowed to

[1] Manuscript received July 3, 1953.

[2] This work was supported in part by the Office of Naval Research, Contract N6onr-26610.

[3] E. I. du Pont de Nemours and Company Fellow, 1952–53; present address: Radiation Laboratory, University of California, Berkeley, California.

[4] Magnolia Petroleum Company Fellow, 1952–53; present address: Department of Chemistry, Michigan State College, East Lansing, Michigan.

[5] Ace Glass Company filter tube, porosity B, 10 mm ID.

TABLE I. *X-ray diffraction data for bismuth (III) iodide*

This work*		Literature†	
d, A	I/I_1	d, A	I/I_1
7.03	<0.1	3.25	0.7
5.97	<0.1	3.00	1.0
5.17	0.1	2.53	0.7
3.85	0.2	2.27	0.7
3.32	1.0	2.15	1.0
2.57	0.3	2.07	0.9
2.19	0.4	1.96	0.9
1.98	0.1	1.87	1.0
1.83	0.1	1.81	1.0
1.66	<0.1	1.29	0.7
1.40	0.1	1.25	0.7
1.36	0.1	1.10	0.7
1.32	0.1	1.09	0.7
1.07	<0.1	1.03	0.7
		1.02	0.7‡

* Data obtained using Cu K_α radiation, Ni filter, 30-kv tube voltage, 15-ma filament current, and 4-hr exposure.

† These data are taken from the ASTM Index of X-ray Diffraction Patterns and are attributed to Caglioti (6). Lack of agreement between our data and those of Caglioti is obvious and it is concluded that his data are in error since both interplanar spacing and relative intensity data for several different samples prepared in connection with the present work were in excellent agreement. More recently, in entirely independent experiments, these data have been confirmed by Phillip S. Gentile of this laboratory.

‡ Spacings corresponding to relative intensities <0.7 are not included.

evaporate, residual ammonia was displaced with dry, oxygen-free nitrogen, and the tube was transferred to a dry box wherein all subsequent sampling of the ammonated salt was done in an atmosphere of nitrogen. Analysis: calculated for $Co(NO_3)_2 \cdot 6NH_3$: Co, 20.6; NH_3, 35.8; calculated for $Co(NO_3)_2 \cdot 5NH_3$: Co, 22.0; NH_3, 31.7. Found: Co, 20.0; NH_3, 33.0. The composition indicated by these data is $Co(NO_3)_2 \cdot 5.7NH_3$.

Experimental methods.—With but one exception, equipment and methods used in this work were substantially the same as those described earlier (1). In a typical case, the solution to be titrated consisted of the salt in question dissolved in anhydrous liquid ammonia. Into this solution was immersed a platinum reference electrode and a differential electrode comprising a platinum wire immersed in a solution having the same composition as the solution to be titrated, and connected to the main body of this solution by means of a capillary tube. The differential electrode was connected to the positive terminal of the potentiometer.

The exception referred to above was concerned with titrations involving nitrate solutions. For these, a reference electrode comprising the half-cell: Cu; $Cu(NO_3)_2 0.1N$, KNO_3 (satd.), of the type used by Pleskov and Monossohn (8) was employed. This change was incorporated when use of the usual platinum reference electrode gave anomalous results that are currently being further investigated.

The alkali metal used was potassium in all cases, and the titrations were carried out at $-38 \pm 1°C$.

Bismuth(III) iodide.—In a typical experiment, a solution of 0.2298 gram of bismuth(III) iodide in 40 ml of liquid ammonia was titrated with a 0.0975*N* potassium solution. A black precipitate formed upon the first addition of potassium solution, and the reaction mixture assumed a purple color after addition of 17 ml of potassium solution. Total time required for this particular titration was 12 hr; data are shown in Fig. 1. In other titrations that differed only with respect to concentrations of reactants used, somewhat different results were obtained. For example, titration of 0.3485 gram of bismuth(III) iodide in 46 ml of ammonia with 0.0773*N* potassium solution over a period of 7 hr gave the data shown in Fig. 2. Results of the type shown in Fig. 1 and 2 were confirmed both with and without the use of potassium iodide as a supporting electrolyte.

In a related case, 0.0410 gram of potassium dissolved in 50 ml of liquid ammonia was titrated with a saturated solution of bismuth(III) iodide in liquid ammonia (0.2574 gram BiI_3 in 51.0 ml NH_3). Use of these conditions was dictated by limitations imposed by the capacity of available equipment and by solubility relationships; as a consequence, results

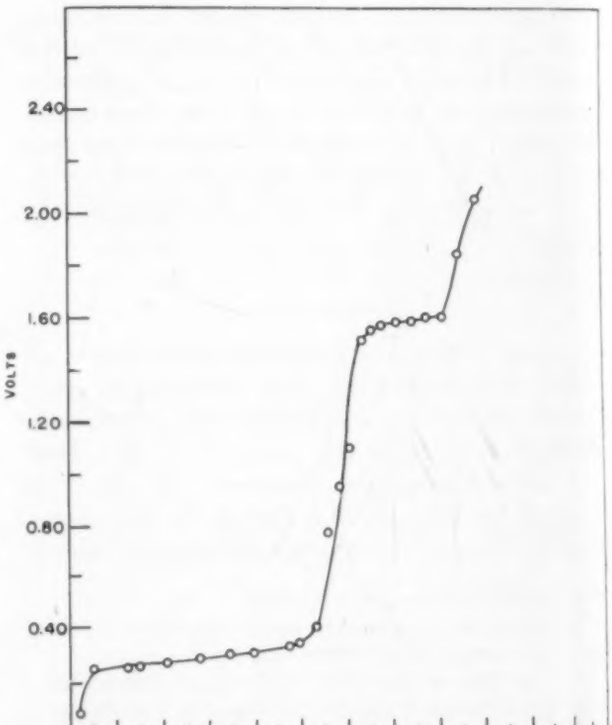

FIG. 1. Potentiometric titration: bismuth(III) iodide with potassium.

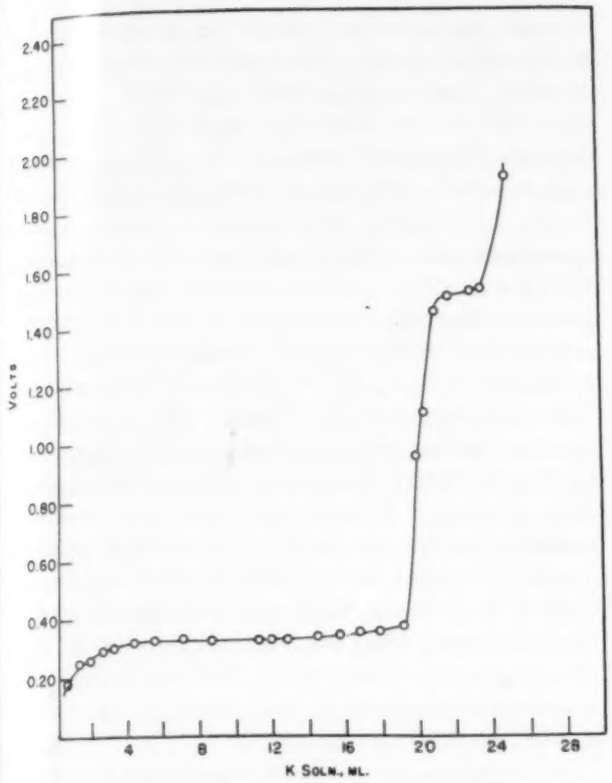

FIG. 2. Potentiometric titration: bismuth(III) iodide with potassium.

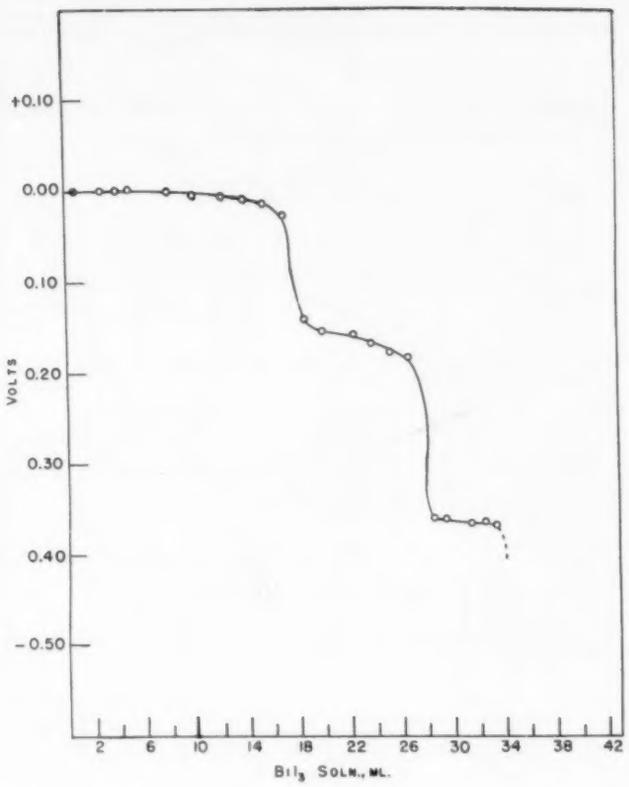

FIG. 3. Potentiometric titration: potassium with bismuth(III) iodide.

must be interpreted on the basis of internal agreement rather than on an absolute basis. Complete titration required 7 hr; data are given in Fig. 3. The characteristic blue color of potassium solution was replaced by a distinct purple color after addition of 18.3 ml of saturated bismuth(III) iodide solution. After 33 ml had been added, the purple color decreased in intensity and the presence of a black precipitate was observed.

Iron(II) bromide.—Iron(II) bromide 6-ammonate (0.0917 gram) in 50 ml of liquid ammonia was titrated with 0.0449*N* potassium solution over a period of 6 hr. Early stages of the titration were characterized by erratic emf values; after 8.3 ml of potassium solution had been added, a progressive, but at no time abrupt, increase in potential began and amounted to a total change of 700 mv by the time 15.9 ml of potassium solution had been added. The characteristic blue color of potassium solution was not observed, even though an excess of almost two gram-atoms of potassium/mole of bromide was added.

Potassium nitrate.—A solution of 0.0332 gram of potassium nitrate in 45 ml of liquid ammonia was titrated with 0.0969*N* potassium solution. As titration proceeded over a period of 29 hr, the solution became yellowish-green in color, then intensely green, and finally a yellow precipitate formed. The titration curve is shown in Fig. 4.

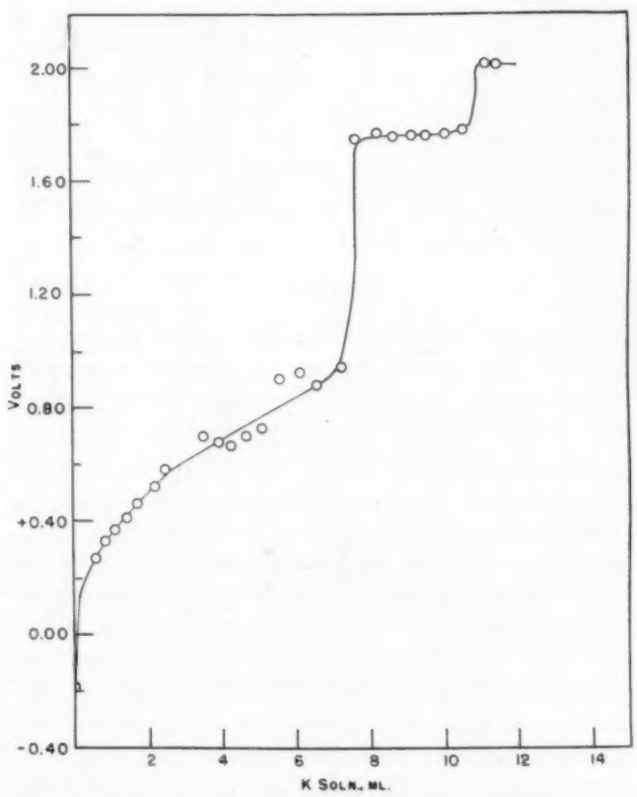

FIG. 4. Potentiometric titration: potassium nitrate with potassium.

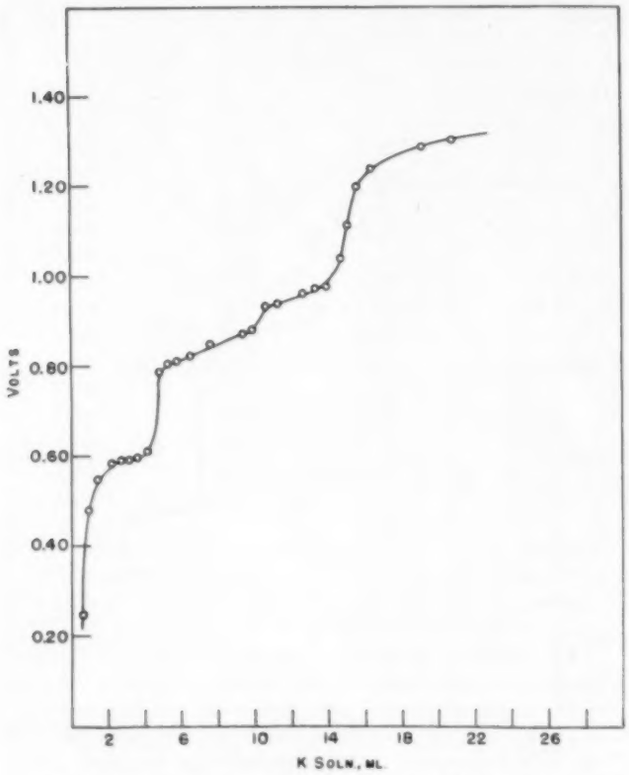

FIG. 5. Potentiometric titration: cobalt(II) nitrate with potassium.

Cobalt(II) nitrate.—An ammonate (0.0602 gram) corresponding to the composition $Co(NO_3)_2 \cdot 5.4NH_3$ dissolved in 46 ml of liquid ammonia was titrated with 0.0868*N* potassium solution. The initially pink solution became green in color and a black precipitate formed concurrently. A total of 21 ml of potassium solution was added over a period of 13 hr; the final reaction mixture consisted of a black precipitate and a greenish-yellow supernatant solution. Data are given in Fig. 5.

DISCUSSION

Titrations involving bismuth(III) iodide and potassium were carried out for the twofold purpose of attempting to detect the formation of Bi^{2+} and/or Bi^{+} and to clear up uncertainties in the results reported by Zintl and coworkers (9). In the reaction corresponding to Fig. 1, changes in potential occurred only upon addition of 12.0 and 16.5 ml of potassium solution; these values are to be compared with 12.0 and 16.0 ml calculated on the assumption of formation of Bi^0 and K_3Bi_3, respectively. Thus, the first reaction observed is the three-electron change resulting in precipitation of elemental bismuth, and there is no indication of intermediation of the +2 and +1 oxidation states of bismuth. Fig. 1 shows clearly the formation of the polybismuthide K_3Bi_3, but not the intermediate species K_3Bi_5. In contrast, data of Fig. 2 show formation of Bi^0 and K_3Bi_5 upon addition of 20.4 and 24.6 ml of potassium solution. The corresponding calculated values are 20.4 and 24.5 ml. Zintl and coworkers (9) titrated bismuth(III) iodide with sodium solutions at −60° and reported evidence for the formation of Na_3Bi, Na_3Bi_3, and Na_3Bi_5, although their evidence for the latter was admittedly inconclusive. While results of the present study are in reasonable agreement with those of Zintl and coworkers, it has been demonstrated that K_3Bi_3 may be formed without intermediation of K_3Bi_5 which exhibits an intense brown color in liquid ammonia solution; this color was not observed during the course of titration represented by Fig. 1. While the present work provides much more conclusive evidence for the existence of bismuthides of the type M_3Bi_5 (where M is an alkali metal), it is still not clear why these species are not formed in all cases. Zintl and coworkers suggested that the course of these reactions may be strongly dependent upon concentration, but the range of concentrations employed in the present work appears to rule out this explanation.

When potassium in liquid ammonia was titrated with saturated bismuth(III) iodide solution, the results obtained were in good agreement with comparable data for corresponding reactions with sodium (9). Marked changes in potential occurred after addition of 17.8, 28.2, and 34.0 ml of bismuth(III) iodide solution as compared with calculated values of 17.8, 26.7, and 35.6 ml corresponding to the formation of K_3Bi, K_3Bi_3, and Bi^0, respectively. For reasons indicated previously, the latter values were calculated on the basis of the volume of iodide solution required for formation of K_3Bi; this end point is visually detectable. Titrations of this type gave no evidence for the formation of K_3Bi_5.

Study of the reduction of iron(II) bromide was prompted by the desire to obtain evidence for the existence of Fe^{+} in liquid ammonia solution. It has been shown previously (10) that principal products of this reaction are elemental iron and iron(I) nitride. The latter may arise from the following sequence of reactions.

$$FeBr_2 + K \rightarrow FeBr + KBr \quad [1]$$

$$FeBr + K \rightarrow Fe + KBr \quad [2]$$

$$FeBr + NH_3 \rightarrow FeNH_2 + NH_4Br \quad [3a]$$

$$K + NH_3 \rightarrow KNH_2 + \tfrac{1}{2}H_2 \quad [3b]$$

$$FeBr + KNH_2 \rightarrow FeNH_2 + KBr \quad [3c]$$

$$3FeNH_2 \rightarrow Fe_3N + 2NH_3 \quad [4]$$

Iron(I) nitride most probably is formed by the deammonation of iron(I) amide which as indicated above may result from either ammonolysis of iron(I) bromide or from reaction between iron(I) bromide and potassium amide. In either case, the reduction of Fe^{+2} to Fe^{+1} must be postulated, and it was therefore considered worthwhile to attempt to obtain evidence for the existence of Fe^{+1} under these conditions.

In view of the immediate precipitation of elemental iron and the concurrent evolution of hydrogen (10), it follows that if iron(I) amide arises via reactions [1], [2], and [3*a*], competitive reactions with subsequently added potassium would involve reactions [1], [2], [3*b*], and the interaction of potassium with the ammonium bromide formed in [3*a*]. Of these, the latter and [3*b*] would probably proceed at the greatest rate. It is not surprising, therefore, that erratic potentials were observed in the early states of the titration. Although Fe^0 may, of course, result from the direct two-electron reaction with Fe^{+2}, there is an alternative mechanism that provides for both the precipitation of Fe^0 and at least the transitory existence of Fe^{+1}, i.e., reaction [1] followed by disproportionation,

$$2FeBr \rightarrow FeBr_2 + Fe^0 \qquad [5]$$

Thus, after formation of sufficient Fe^0 to catalyze [3*b*], the latter reaction would compete with the probably slow reaction [5].

Reduction of both alkali metal nitrates and nitrites to "hydronitrites" of the type M_2NO_2 has been observed previously (11–13) but only in terms of the identity of the initial and final substances. Formation of K_2NO_2 from KNO_3, for example, may follow the course,

$$KNO_3 + K \rightarrow K_2NO_3 \qquad [6]$$

$$K_2NO_3 + K + NH_3 \rightarrow KNO_2 + KOH + KNH_2 \qquad [7]$$

$$KNO_2 + K \rightarrow K_2NO_2 \qquad [7a]$$

or,

$$K_2NO_3 + 2K + NH_3 \rightarrow K_2NO_2 + KOH + KNH_2 \qquad [8]$$

As shown in Fig. 4, however, changes in potential corresponding only to two- and three-electron changes were observed, i.e., upon addition of 7.4 and 10.9 ml of potassium solution, as compared with calculated values of 7.5 and 11.2 ml. Hence, it appears that the formation of K_2NO_3 as an intermediate does not occur and that the only reactions that take place are,

$$KNO_3 + 2K + NH_3 \rightarrow KNO_2 + KNH_2 + KOH \qquad [9]$$

$$KNO_2 + K \rightarrow K_2NO_2 \qquad [10]$$

Watt and Keenan (14) suggested that reduction of cobalt(II) nitrate with potassium in ammonia may follow the course,

$$Co(NO_3)_2 + 2K \rightarrow Co(NO_2)(NO_3) + K_2O \qquad [11]$$

$$K_2O + NH_3 \rightarrow KOH + KNH_2 \qquad [12]$$

$$Co(NO_2)(NO_3) + KNH_2 \rightarrow Co(NO_2)(NH_2) + KNO_3 \qquad [13]$$

$$Co(NO_2)(NH_2) + KOH + NH_3 \rightarrow Co(NH_2)_2 + KNO_2 + H_2O \qquad [14]$$

$$KNO_3 + 2K \rightarrow KNO_2 + K_2O \qquad [15]$$

or alternatively,

$$Co(NO_3)_2 + 4K \rightarrow Co(NO_2)_2 + 2K_2O \qquad [16]$$

$$2K_2O + 2NH_3 \rightarrow 2KOH + 2KNH_2 \qquad [17]$$

$$Co(NO_2)_2 + 2KNH_2 \rightarrow Co(NH_2)_2 + 2KNO_2 \qquad [18]$$

Both mechanisms were compatible with their experimental data, but the methods employed did not lead to data that would permit a choice between the two.

From the data of Fig. 5 it is evident that significant changes in potential occur after addition of volumes of potassium solution corresponding to 2, 4, and 6 gram-atoms of potassium/mole of cobalt(II) nitrate. That the reaction must follow the path suggested by equations [11] to [15] rather than [16] is strongly indicated by the occurrence of a marked change in potential after addition of two equivalents of potassium. Further evidence in favor of the first mechanism is found in the fact that the plateau at 0.8 volt (Fig. 5) is in agreement with that for the reduction of nitrate ion to nitrite ion found in the reduction of potassium nitrate (Fig. 4). The last of the three observed changes in potential [i.e., that which corresponds to 6 gram-atoms of potassium/mole of cobalt(II) nitrate] is attributable to the previously observed (14) and relatively slow reduction of cobalt(II) amide to elemental cobalt.

Any discussion of this paper will appear in a Discussion Section, to be published in the December 1954 issue of the JOURNAL.

REFERENCES

1. G. W. WATT AND J. B. OTTO, JR., *This Journal*, **98**, 1 (1951).

2. G. W. Watt, J. L. Hall, and G. R. Choppin, *J. Am. Chem. Soc.*, **73,** 5920 (1951).
3. G. W. Watt, J. L. Hall, and G. R. Choppin, *J. Phys. Chem.*, **57,** 567 (1953).
4. G. W. Watt and J. L. Hall, Unpublished work.
5. G. W. Watt, W. W. Hakki, and G. R. Choppin, "Inorganic Syntheses," Vol. IV, McGraw-Hill Book Co., Inc., New York, In press.
6. V. Caglioti, *Gazz. chim. ital.*, **60,** 935 (1930).
7. G. W. Watt and W. A. Jenkins, Jr., "Inorganic Syntheses," Vol. IV, McGraw-Hill Book Co., Inc., New York, In press.
8. V. A. Pleskov and A. M. Monossohn, *Acta Physicochim. U.R.S.S.*, **1,** 871 (1935).
9. E. Zintl, J. Goubeau, and W. Dullenkopf, *Z. physik. Chem.*, **A154,** 1 (1931).
10. G. W. Watt and W. A. Jenkins, Jr., *J. Am. Chem. Soc.*, **73,** 3275 (1951).
11. E. B. Maxted, *J. Chem. Soc.*, **111,** 1016 (1917).
12. E. Zintl and O. Kohn, *Ber.*, **61B,** 189, 2063 (1928).
13. W. M. Burgess and F. R. Holden, *J. Am. Chem. Soc.*, **59,** 459 (1937).
14. G. W. Watt and C. W. Keenan, *ibid.*, **74,** 2048 (1952).

Potentiometric Titration of Ammines of Rhodium, Iridium, and Platinum with Solutions of Potassium and Potassium Amide in Liquid Ammonia[1,2]

GEORGE W. WATT, GREGORY R. CHOPPIN,[3] AND JAMES L. HALL[4]

Department of Chemistry, The University of Texas, Austin, Texas

ABSTRACT

Potentiometric titration of tetrammineplatinum(II) bromide with potassium in liquid ammonia at −38°C shows that reduction of this salt to an ammine of platinum(0) is exactly a two-electron change and that the +1 oxidation state of platinum is not an intermediate. Similar reduction of bromopentammineiridium(III) bromide is apparently more complex and leads to observed changes in potential that do not correspond to any reasonable or probable reactions. Titration of this same iridium salt with potassium amide solution, however, provides evidence for stepwise replacement of bromine by amido groups followed by conversion of the resultant iridium(III) amide to (probably) a potassium amidoiridate(III). Bromopentamminerhodium(III) bromide and potassium amide react similarly, but only to and including the formation of rhodium(III) amide.

INTRODUCTION

In previous papers from this laboratory, development of a method for carrying out potentiometric titrations in liquid ammonia and use of this method in the study of unusual oxidation states and reduction reaction mechanisms have been described (1). This paper is concerned with similar studies involving reduction of ammines of certain transitional metal bromides with solutions of potassium in ammonia. In addition, two reactions in which liquid ammonia solutions of potassium amide were used as titrant are described; the course of reactions of this type has not previously been followed potentiometrically.

EXPERIMENTAL

Experimental details were in all respects analogous to those described earlier (1). In all cases reported in this paper, anhydrous liquid ammonia solutions that were titrated with either standard potassium or standard potassium amide solutions contained not only the ammine bromide of interest but also a suitable supporting electrolyte. The two electrodes consisted of a platinum reference electrode and a differential electrode of the type used previously (1, 5). The differential electrode, which was connected to the positive terminal of the potentiometer, consisted of a platinum wire immersed in a solution having a composition the same as that of the solution to be titrated, and was connected to the main body of the latter solution via a fine capillary tube.

Appropriate ammine bromides of rhodium (2), iridium (3), and platinum (4) were prepared and characterized by methods described elsewhere.

Titration of tetrammineplatinum(II) bromide with potassium.—Preliminary experiments showed that adequately sensitive potentiometer readings could be obtained only through use of a supporting electrolyte. Accordingly, 0.1217 gram of $[Pt(NH_3)_4]Br_2$ and 0.10 gram of potassium bromide, both dissolved in 40 ml of liquid ammonia, were titrated with 0.0506*N* potassium solution over a period of 9 hr. The initially clear solution became progressively darker in color until near the end of titration, whereupon intensity of the color decreased relatively rapidly and the presence of a pale yellow precipitate was observed. Addition of a considerable excess of potassium failed to produce either the blue color characteristic of solutions of alkali metals in ammonia or the potential anticipated for an ammonia solution of potassium amide. The data are shown in Fig. 1.

Titration of trans-diammineplatinum(II) bromide with potassium.—Potentiometric titrations involving these two reactants gave results substantially identical with those in Fig. 1.

Titration of bromopentammineiridium(III) bromide with potassium.—In a typical case, 0.1114 gram of $[Ir(NH_3)_5Br]Br_2$ and 0.15 gram of potassium bromide in 70 ml of liquid ammonia was titrated with

[1] Manuscript received July 8, 1953.

[2] This work was supported in part by the Office of Naval Research, Contract N6onr-26610.

[3] E. I. du Pont de Nemours and Company Fellow, 1952–53; present address: Radiation Laboratory, University of California, Berkeley, California.

[4] Magnolia Petroleum Company Fellow, 1952–53; present address: Department of Chemistry, Michigan State College, East Lansing, Michigan.

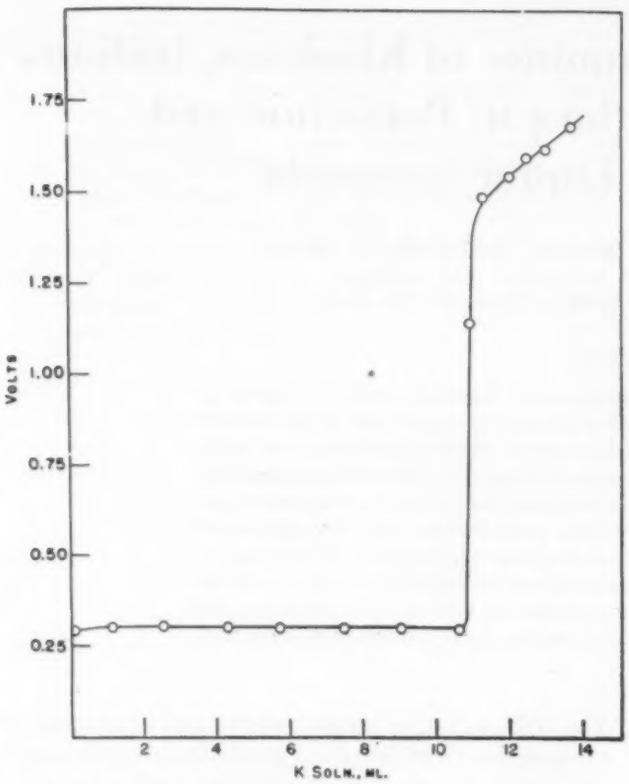

FIG. 1. Potentiometric titration: tetrammineplatinum (II) bromide with potassium.

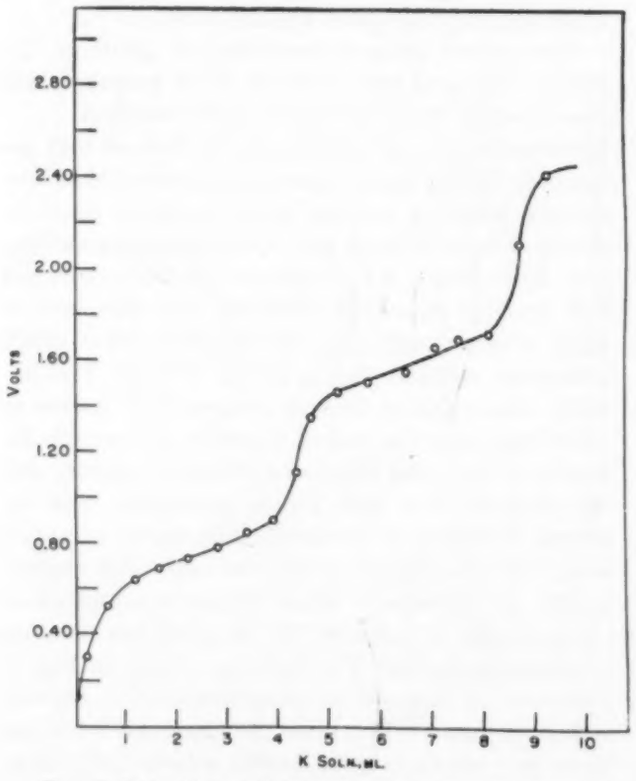

FIG. 2. Potentiometric titration: bromopentammineiridium(III) bromide with potassium.

0.0663*N* potassium solution (time, 14 hr). A precipitate formed slowly, and the blue color of the potassium solution was discharged rapidly during approximately the first half of the titration. Thereafter, rate

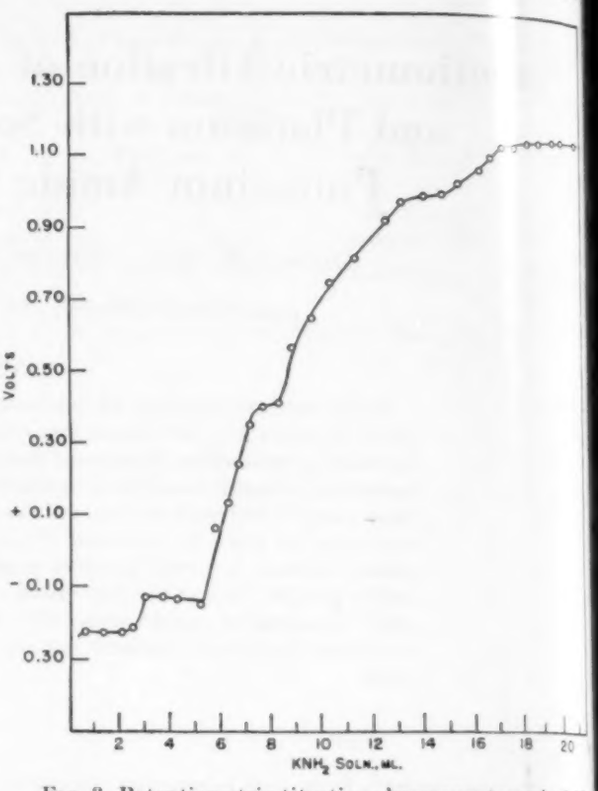

FIG. 3. Potentiometric titration: bromopentammineiridium(III) bromide with potassium amide.

of reaction decreased markedly, the presence of a cream colored precipitate was observed, and equilibrium was re-established relatively slowly after each addition of potassium solution. The blue color of the potassium solution persisted after addition of a total of 9.4 ml. The data are shown in Fig. 2.

Titration of bromopentammineiridium(III) bromide with potassium amide.—A solution of 0.125 gram of potassium bromide and 0.0931 gram of $[Ir(NH_3)_5Br]Br_2$ in 50 ml of liquid ammonia was titrated with 0.0605*N* potassium amide solution over a period of 20 hr (Fig. 3). The amide solution was prepared by interaction of potassium and liquid ammonia in the presence of an iron wire catalyst in the vessel ordinarily used for preparation of standard alkali metal solutions (5). A white finely divided precipitate was observed after addition of 4.2 ml of potassium amide solution, and the following solution colors were observed upon addition of the indicated volumes of titrant: 0, colorless; 7.0, yellow; 14, orange; 16.7, bronze.

Titration of bromopentamminerhodium(III) bromide with potassium amide.—In an experiment of the type described above, a solution of 0.91 gram of potassium bromide and 0.0433 gram of $[Rh(NH_3)_5Br]Br_2$ in 70 ml of liquid ammonia was titrated with 0.0266*N* potassium amide solution (time, 8 hr). Resulting data are given in Fig. 4. The intensity of color of the initially pale yellow solution decreased during addition of 6.5 ml of the amide solution, whereupon there appeared a turbidity that persisted until 10.0 ml had

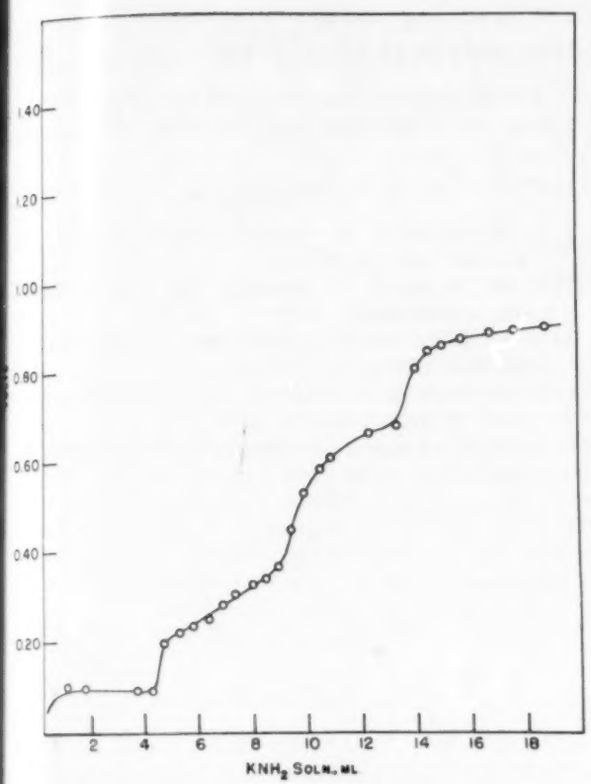

FIG. 4. Potentiometric titration: bromopentamminerhodium(III) bromide with potassium amide.

been added. Thereafter, the solution became progressively more intensely green in color until 14 ml had been added and the solution color began to change from green to yellow-green.

DISCUSSION

In studies leading to the conclusion that reduction of tetrammineplatinum(II) bromide with potassium in ammonia produces an ammine of platinum in the zero oxidation state (4), it became necessary to establish exactly the reaction ratio involved. Titrations of the type shown in Fig. 1 were carried out for this purpose and also with a view to determining whether this reaction proceeds via a single two-electron reaction or two consecutive one-electron changes. It is evident from Fig. 1 that intermediation of the +1 oxidation state is not involved and that reduction of one mole of the bromide requires exactly two gram-atoms of potassium. An increase in potential of the order of 1.3 volts occurred sharply upon addition of 11.0 ml of potassium solution; the volume calculated on the assumption of a two-electron change is 11.3 ml. That substantially identical results were obtained in titrations involving trans-diammineplatinum(II) bromide is consistent with the fact that the trans-isomer is slowly converted to the tetrammine in liquid ammonia at its boiling temperature (4).

In several titrations of bromopentammineiridium(III) bromide with potassium, changes in potential that apparently may not be correlated with any anticipated stoichiometry were observed. With reference to Fig. 2, for example, the increases in potential that occurred upon addition of 4.5 and 8.5 ml of potassium solution are to be compared with 6.5 and 9.7 ml calculated on the assumption of reduction of Ir^{+3} to Ir^{+1} and its subsequent reduction to Ir^0. Similarly, change in potential (and appearance of a permanent blue color) corresponding to complete reduction of Ir^{+3} to Ir^0 was also premature in all cases, and since different and authentic samples of the bromide were employed, these results cannot be attributed to impure starting materials. It is possible to postulate a mechanism in which it is assumed that Ir^{+3} is reduced to Ir^{+1} which in turn reduces Ir^{+3} to Ir^{+2} and the latter is reduced to Ir^0 upon further addition of potassium solution. If it is further assumed that (owing to competitive rates that may be involved) one-third of the Ir^{+1} is ammonolyzed to iridium(I) amide, then it may be shown that the observed changes in potential are almost exactly those to be anticipated under such conditions. This requires, however, that iridium(I) amide be stable in the presence of subsequently added potassium solution and that it constitute one of the final products. This is clearly incompatible with other data relative to the identification of pentammineiridium-(0) as the end product (3).

Changes in potential that are shown in Fig. 3 and that result from addition of 2.8, 5.8, 8.6, and 17.2 ml of potassium amide solution (calculated: 3.0, 6.0, 8.9, and 17.8 ml) apparently correspond to the reactions (coordinated ammonia omitted),

$$IrBr_3 + KNH_2 \rightarrow Ir(NH_2)Br_2 + KBr \quad [1]$$

$$Ir(NH_2)Br_2 + KNH_2 \rightarrow Ir(NH_2)_2Br + KBr \quad [2]$$

$$Ir(NH_2)_2Br + KNH_2 \rightarrow Ir(NH_2)_3 + KBr \quad [3]$$

$$Ir(NH_2)_3 + 3KNH_2 \rightarrow K_3Ir(NH_2)_6 \quad [4]$$

or,

$$Ir(NH_2)_3 + 3KNH_2 \rightarrow Ir(NHK)_3 + 3NH_3 \quad [4a]$$

This interpretation is further supported by the fact that iridium(III) amide has been isolated (in the form of the 1-ammonate) as the only ammonia-insoluble product of the interaction of the bromide and potassium amide in a $\frac{1}{3}$ mole ratio (3). Neither the present nor previous work (3) permits a choice between alternatives suggested by equations [4] and [4*a*].

From data shown in Fig. 4, it is apparent that reactions between bromopentamminerhodium(III) bromide and potassium amide are strictly analogous to those with the corresponding iridium compound,

i.e., equations [1] to [3], inclusive, except for the fact that rhodium(III) amide is not converted to a soluble species by action of excess potassium amide, i.e., rhodium(III) amide is less amphoteric than iridium(III) amide. Rhodium(III) amide has been independently isolated and characterized (2). Attention should be called to the fact that the volumes of potassium amide solution corresponding to the changes in potential shown in Fig. 4, i.e., 4.6, 9.5, and 14.0 ml, are higher than calculated volumes based on concentration of the potassium amide solution used, i.e., 3.8, 7.6, and 11.4 ml. However, if the final increase in potential is taken as evidence for the formation of rhodium(III) amide, which is reasonable in the light of other available evidence (2), then the two preceding changes in potential should occur upon addition of 4.7 and 9.3 ml.

Any discussion of this paper will appear in a Discussion Section, to be published in the December 1954 issue of the JOURNAL.

REFERENCES

1. G. W. WATT, G. R. CHOPPIN, AND J. L. HALL, *This Journal*, **101**, 229 (1954).
2. G. W. WATT, W. A. JENKINS, JR., AND A. BROOD To be published.
3. G. W. WATT AND P. I. MAYFIELD, *J. Am. Chem. Soc.*, **75**, 6178 (1953).
4. G. W. WATT, M. T. WALLING, JR., AND P. I. MAYFIELD *ibid.*, **75**, 6175 (1953).
5. G. W. WATT AND J. B. OTTO, JR., *This Journal*, **98**, (1951).

Adherence of Electrodeposited Zinc to Aluminum Cathodes[1]

F. H. C. Kelly

University of Tasmania, Hobart, Tasmania, Australia

ABSTRACT

An apparatus for measuring the adherence of zinc electrodeposited from acid zinc sulfate solutions on aluminum cathodes is described. Adherence was recognized as "sheet" or "spot" behavior. Chloride favored increase in sheet adherence and fluoride ion favored spot adherence. Mechanical, thermal, and electrolytic treatments of cathode surface as well as chemical composition of electrolyte were investigated. There was no correlation between surface roughness and adherence. Smaller aluminum crystals in the cathode surface favored stronger adherence.

The first stage of deposition was development of ovoid particles 8 x 5 microns, increasing in number until a complete sheet was obtained. Such particles preferred to develop at sharp points and crystal boundaries. Rupture of interface was observed microscopically in the aluminum surface. Zinc diffused into cathode with time, but aluminum on the surface of the zinc electrodeposit was attributed to fracture in aluminum during stripping. Mechanism of adherence was explained as an attachment at a varying number of active spots rather than by mechanical anchoring.

Introduction

In the commercial production of zinc by electrolysis, low adherence to an aluminum cathode is desirable. Separation of the zinc sheet from the cathode is effected manually, and the process of plating and stripping may be repeated up to 1000 times or more on a single cathode sheet before the aluminum is rejected from service, usually for reasons other than a damaged surface. Whereas electroplaters for ornamental or protective work require adherence values of probably 1000 or more kg/cm², production of electrolytic zinc commercially is best served if the adherence is between one and two kg/cm². In this paper, the measurement of adherence of zinc electrodeposits is described, and the mechanism of adherence is discussed by considering these results in relation to information obtained from the following investigations: (*a*) an examination of the microroughness of surfaces with "Talysurf" instrument (see later); (*b*) metallographic examination; (*c*) microscopic examination of first stages of electrodeposition; (*d*) examination of interface between cathode and electrodeposit; (*e*) chemical analysis of thin layers from the surface of metals at the interface after separation of the electrodeposit.

Experimental

Measurement of Adherence

The apparatus used for this purpose is illustrated in Fig. 1. It is a modification of the "Burgess" method described by Schlötter (1) giving results in absolute values, i.e., kg/cm². Schlötter soldered a metallic loop to the surface before pulling off the electrodeposit, but as this is undesirable for zinc electrodeposited on aluminum, a glue bond between the electrodeposit and the pulling bar was used.

For these measurements, cathodes 5 cm x 5 cm x 0.6 cm (thick) were cut from rolled aluminum sheet of a high grade of commercial purity. A single cathode was plated at a time in a beaker carrying electrolyte of the required composition. Anodes cut from pure lead sheet were used, one on each side of the cathode. Zinc was plated for three hours to a thickness of approximately 0.15 mm. These deposits were strong enough to be pulled off without breaking. A suitable area for the adherence test was 2.5 cm x 1.25 cm and this was outlined by grooving the face of the cathode sheet with a sharp pointed tool. The plated zinc sheet was cut along these lines with a very sharp knife and stripped from areas other than those required. For adherence values up to approximately 7 kg/cm² this proved satisfactory, but for greater adherence a smaller area of zinc was used.

Two test rectangles were marked on one face of the cathode sheet. One end of a steel bar 18 cm long and 2.5 cm x 1.25 cm cross section was glued to the back of one of the rectangles of zinc. The most satisfactory method for attaching the bar to the zinc sheet was to insert a piece of linen between the two metal surfaces and glue to each with a liquid glue, the whole being dried at 18°C for 15 hr.

A current density of 32 ma/cm² was used as a standard procedure in plating. The cell temperature was maintained at 35°C. The electrolyte was a solution of zinc sulfate (70 g/l zinc) in dilute

[1] Manuscript received May 4, 1953.

sulfuric acid (100 g/l of H_2SO_4). To this electrolyte was added one or more of the common impurities experienced in commercial zinc electrolysis. With only zinc sulfate-sulfuric acid solutions, no "addition" agent was necessary, but when additional ions were added, 24 mg/l of glue was used. When arsenic and/or antimony was present, then 10 mg/l of beta-napthol was also added. The addition agent was put in before electrolysis and the initial amount was sufficient for the three-hour plating period. Before each plate was deposited, the test cathode was immersed in the particular electrolyte for 16 hr at 18°C. Some exceptions to these standard procedures were also investigated.

Adherence values were difficult to reproduce with a high degree of accuracy, but it was possible to arrange results in groups according to certain ranges of adherence. The standard deviation of a determination from a single test area was ±50%. It was

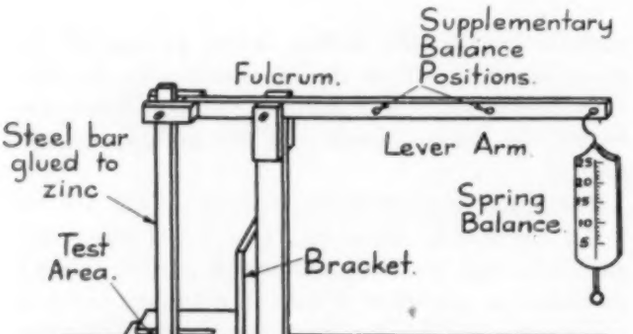

FIG. 1. Laboratory adherence tester

found that results from one side of the rolled aluminum sheet differed from those on the reverse side, so that for comparative purposes only one side of the sheet was used. The difference was related to crystal structure in the surface. Higher adherence was obtained on the surfaces with smaller crystals of aluminum.

Values for adherence from less than 0.1 to as high as 57 kg/cm² were observed. For this investigation, the important range of values was 1 to 2.5 kg/cm² and there was not much point in attempting to measure adherence in excess of 7 kg/cm². This was related to the requirements for manually stripping a zinc sheet from the aluminum cathode during the course of the commercial manufacture of electrolytic zinc. Sheets deposited under conditions giving adherence values in excess of this figure were far too difficult to remove.

In commercial plant practice it had been observed that on some occasions the electrodeposit adhered with reasonable uniformity over the whole cathode surface, whereas, in other cases, adherence was experienced in smaller patches. Two types of adherence conditions were therefore specified and referred to descriptively as "sheet" adherence and "spot" adherence. In order to differentiate between these conditions in the test cathodes the following method was adopted for interpretation of results. A quantitative estimate of adherence was determined, using values from two adjacent test areas of the experimental cathodes. Spot adherence was identified from the ratio of the higher value to the lower value of adherence from two adjacent areas. On the other hand, the average value from adjacent test areas has been used as a measure of sheet adherence.

Values for spot adherence estimations varied over the range 1 to 13, whereas for sheet adherence values from 0.1 to 57 kg/cm² were recorded, as has already been indicated.

Tests giving spot adherence ratio values lower than 3 were considered satisfactory, whereas values in excess of 6 were considered to be high, and those in excess of 9 to be very high and unsatisfactory.

Tests were conducted under 53 sets of conditions and the most significant of these are given in Table I.

From these tests it was concluded that mechanical roughening of the aluminum surface did not necessarily result in increased adherence of the zinc deposit. Of the chemical factors tested in the electrolyte only chloride ion showed increase in sheet adherence of statistical significance. Spot

TABLE I

Test No.	Electrolyte composition (rolled surface of Al as cathode)	Adherence—kg/cm²		Ratio of adherence of adjacent areas
		Individual values	Average values	
1	Pure $ZnSO_4$ at 70 g/l Zn and 100 g/l H_2SO_4	1.1 & 1.3	1.2	1.2
2	Same as above, with addition of 16 g/l Mn as $MnSO_4$	1.9 & 1.8	1.85	1.1
3	Same as for test 2, plus 80 mg/l Cl as HCl	3.2 & 3.9	3.55	1.2
4	Same as for test 2, plus 200 mg/l Cl as HCl	6.0 & 5.3	5.65	1.1
5	Same as for test 2, plus 40 mg/l F as HF	0.85 & 0.85	0.85	1.0
6	Same as for test 2, plus 80 mg/l Cl as HCl and 100 mg/l F as HF	2.25 & 1.4	1.82	1.6
7	Same as for test 2, plus 80 mg/l Cl as HCl and 40 mg/l F as HF	2.25 & 2.55	2.4	1.1
8	Same as for test 7, but with 64-hr pickle	5.3 & 0.4	2.8	13.0
9	Same as for test 7, plus 0.5 mg/l Cu as $CuSO_4$	1.3 & 0.85	1.08	1.5
10	Same as for test 7, plus 10 mg/l Cu as $CuSO_4$	1.0 & 0.4	0.7	2.5

adherence was experienced when electrolysis was conducted in an electrolyte containing fluoride ion. This type of adherence was also experienced if the cathode had been pickled in acid electrolyte for a long period before electrodepositing. The effect after long pickling was the same, whether fluoride ion was present or not.

Surface Roughness Measurements

Through the services of the Defence Research Laboratories (one time Munitions Supply Laboratories), Maribyrnong, Victoria, Australia, measurements were obtained of the surface roughness of 31 specimens of aluminum and 6 of zinc using a "Talysurf" indicator-recorder. The description and use of this instrument has been published elsewhere by the D.R.L. (then called M.S.L.) (2).

Some of these results are given in Table II. No correlation was found between surface roughness so measured and the degree of adherence.

Metallographic Examination of Crystal Structure

Metallographic examination had limitations because the observation of crystal structure involved destruction of the surface used for electrodeposition.

For microscopic examination, specimens of aluminum were prepared by polishing selected areas of a cathode surface with fine abrasive cloth, followed by a buffing with alunite powder. The final finish was obtained by polishing with "Brasso,"[2] and using freshly prepared etchant of the following composition: 50% hydrochloric acid; 47% fuming nitric acid; and 3% pure hydrofluoric acid.

With a 30-sec etch, the orientation and size of crystals were clearly seen at a magnification of 900×. Surface scratches were widely enough spaced to enable clear fields to be observed at this magnification.

In all cases examined, the crystals were smaller in the specimens which had given higher values for the adherence of the electrodeposit (other factors remaining unchanged).

Microscopic Observation of Electrodeposition

Specimens of aluminum were examined microscopically after deposition of zinc had proceeded for periods such as 30, 60, 90, and 120 sec.

Zinc did not deposit as a uniform sheet but as small ovoid particles, each with its long axis normal to the plane of the aluminum surface. Size of these particles was remarkably uniform and with axis lengths of approximately 8 and 5μ. The number of particles rather than the size of individual particles

[2] "Brasso" is a product of Reckett and Colman Ltd., Hull, England, and is recommended for polishing soft metals.

TABLE II

Specimen examined	Talysurf meter readings		Adherence kg/cm²
	Max. & min.	Mean of six readings	
New aluminum, pickled 16 hr at 18°C; plated and stripped (electrolyte = pure zinc sulfate, 70 g/l Zn & 100 g/l H_2SO_4)	0.38–0.51 0.38–0.51 0.43–0.66 0.46–1.08	0.46 0.43 0.53 0.66	1.27 1.15
Specimen as above, but electrolyte contained 16 g/l Mn and 200 mg/l Cl in addition	0.38–0.46 0.43–0.81	0.41 0.53	5.28 6.05
Specimen as above, but electrolyte contained 16 g/l Mn and 4 mg/l F in addition to $ZnSO_4$ and H_2SO_4	0.41–0.53 0.48–0.71	0.51 0.53	0.84 0.84
Specimen as above, but pickled 64 hr at 18°C in electrolyte with 40 mg/l F	0.81–1.02 0.58–0.74	0.91 0.63	7.75 1.27
Specimen brushed by hand with steel wire brush. Pickled, plated, and stripped, electrolyte from commercial plant cells	1.78–2.59 1.35–1.58	2.16 1.50	1.69 2.32
New aluminum, different sheet	0.28–0.30 0.36–0.41	0.28 0.38	— —
Same as above, but brushed by hand with steel wire brush	0.70–1.98 1.60–2.29	1.86 2.03	— —

increased as plating progressed. Also, by changing the surface treatment or electrolyte characteristics the rate at which these particles appeared could be varied. It would appear that these primary particles deposit at points where the aluminum oxide film is cracked or particularly thin. Where surface irregularities were conspicuous it was noted that particles developed preferentially at sharp peaks or ridges or at the lips of surface depressions. These, no doubt, were points of higher current density.

On a specimen prepared for examination of crystal structure, it was noted that particles preferred to form at crystal boundaries. This was in agreement with work reported by Kyropoulos (3) who studied the manner in which electrodeposits form on aluminum crystals.

Conditions which favored rapid development of primary zinc particles also favored strong adherence of the zinc electrodeposit, and vice versa. Conditions for strong adherence showed 20 to 30 times as many primary particles in 90 sec of plating as conditions for weak adherence.

It was found possible to obtain an estimate of the relative adherence of primary zinc particles by

manipulating a thin steel wire under the objective of the microscope when examining prepared specimens. Adherence of these particles was found to vary appreciably; those which were earliest to appear were generally more firmly attached than those appearing after a longer plating period.

Dependence of points of deposition on the oxide film was demonstrated by anodizing an aluminum cathode in a chromic acid bath. Using this as a cathode in acid zinc sulfate electrolyte, a continuous sheet of zinc was obtained, but it was attached to the cathode at only a very few points.

A film type of deposit was obtained following the technique of Bullough and Gardam (4), designed to remove the oxide film completely and limit its reappearance before deposition commences. The aluminum surface was prepared in a nitric-hydrofluoric acid bath, and then transferred to a sodium zincate bath, through water washes, without allowing the face to dry. A thin, but continuous, immersion deposit of zinc, very firmly adherent to the aluminum, was obtained in this manner. Attachment was virtually at an infinite number of points and adherence values of the order of the tensile strength of aluminum were recorded by Bullough and Gardam (4).

Film type deposits were also obtained in the current experiments when copper and lead were used as cathodes instead of aluminum.

Microscopic Examination of the Interface

Plated specimens, cut on the taper using the technique described by Nelson (5), were prepared but were not suitable for microscopic examination owing to the softness of the aluminum. A specimen cut normal to the plane of plating allowed zinc or aluminum to be etched individually, but at magnifications high enough to reveal the structure of the interface it was not possible to obtain both surfaces in focus simultaneously.

Specimens of smooth rolled aluminum which had been plated and stripped were examined microscopically. Small craters appeared in the surface after removal of the electrodeposit. In subsequent short periods of plating, primary particles of zinc preferred to form at the lips of these craters rather than in the depressions. These crater-like pits apparently had been foci of attachment for the original zinc deposit, and rupture had taken place in the aluminum surface. These craters were of the order of 1.5μ deep and several microns across; frequently several craters were joined to give trough-like indentations.

Bullough and Gardam (4) when examining the adherence of nickel deposits to aluminum and its alloys, using zinc as an intermediate layer, also observed fracturing in the aluminum.

A Brinell indenter was used to examine the hardness of specimens of aluminum and zinc. Nothing unusual was noted in specimens of aluminum for which values of the order of 40 were obtained. Values for the zinc were, however, appreciably higher. Over the surface of stripped zinc electrodeposited sheets, values varying between 150 and 225 were obtained, the average being approximately 200. On the other hand, with sections cut through the zinc sheet, normal to the face, values of the order of 70 were obtained. While all these values for zinc may have been unexpectedly high, nevertheless they are consistent with the microscopic observation of fracture in the aluminum surface, indicating greater softness of this metal.

Hanley and Clayton (6) investigated the adherence of zinc electrodeposits to aluminum cathodes. These authors explain the mechanism of adherence in terms of physical anchorage. Generally results obtained by the present author were in line with the findings of Hanley and Clayton, but it is not possible to agree on the mechanism of adherence. On the other hand, there are no results quoted by Hanley and Clayton which could not be explained by a theory of attachment at electrochemically active points.

Analysis of Interfacial Layers

Some tests were made in which a thin layer of aluminum was scraped from the surface of a cathode after having been in service for some time in the commercial zinc plating plant. These scrapings were analyzed for copper and zinc. Of ten cathodes tested, five had been associated with a zinc electrodeposit which stripped easily, and five had been difficult to strip.

The thickness of the layer scraped averaged between 40 and 50μ. The analysis of the easily stripped cathodes averaged 0.071% copper and 3.44% zinc. Zinc content was remarkably uniform, but copper varied widely from sample to sample, from a maxi-

TABLE III

Depth of layer examined, microns	% Aluminum	Remarks
8.3	0.15	Commercial plant cathode, stripped easily
4.35	0.035	Commercial plant cathode, stripped with difficulty
4.2	0.015	Commercial plant cathode, stripped with difficulty
Not determined	0.0026	Pilot plant cathode, stripped easily

mum of 0.191% to a minimum of 0.023%. In the case of the cathodes which were difficult to strip, both copper and zinc concentrations were reasonably uniform, averaging 0.022% and 2.43%, respectively.

Hanley and Clayton (6) drew attention to the influence of copper in the electrolyte increasing the adherence of the electrodeposit, but this effect was not obtained in the present series of tests (see tests 9 and 10 in Table I). It is believed that the initial distribution of copper in the aluminum sheet exercises a controlling influence on the adherence, but the tests were not carried far enough to produce conclusive evidence on this point. The solid solubility of copper in aluminum is usually reported as 0.25–0.30% at room temperature. Some workers, however, consider that the solubility is nearer 0.08–0.12%. Copper concentration of the aluminum sheet used for cathodes covers this range, and presence of $CuAl_2$ as a solid phase may have some bearing on the problem.

The effect of pickling in spent electrolyte on the removal of zinc from the aluminum surface was examined. Large lumps of zinc left after stripping were removed quite effectively in this manner. Whether they fell off as the result of aluminum in the immediate vicinity being dissolved, or whether they dissolved preferentially in spite of the relative positions of zinc and aluminum in the electrochemical series was not examined critically. There was, however, obvious liberation of hydrogen from large lumps of zinc still attached to the cathode surface. The zinc of more particular interest for this investigation was that which had apparently diffused into the surface of the aluminum. It was observed that during the pickling process zinc was certainly not removed any faster than aluminum, but tests were not extended to determine whether the converse may have been the case, although such was not conspicuous.

Full sections of aluminum sheets were also analyzed for copper, and the following results were obtained from nine sheets of aluminum: 0.051, 0.27, 0.04, 0.05, 0.07, 0.153, 0.04, 0.04, and 0.006% Cu. The heterogeneity with respect to copper was thus a property of the sheet as a whole, not confined to the surface, and not a result of electrolysis. The new aluminum sheet was free from zinc. There was no evidence that the zinc referred to in these analyses had been left in the aluminum as the result of fracturing of a bond during the stripping process, but it seemed quite logical to conclude that, with long periods of interfacial contact, diffusion could take place.

Four surfaces of zinc electrodeposit were scraped on the adhering side and analyzed for aluminum. Results are summarized in Table III.

While commercial plant cathodes appeared to leave more aluminum on the zinc face when stripping was relatively easy, this was not confirmed by pilot plant tests. It is believed that the presence of aluminum on the surface of the zinc can be attributed to the fracture of the bond in the aluminum sheet as observed in microscopic examinations reported above. It is unlikely that very much diffusion would have taken place during the plating period which was 72 hr in the case of sheets sampled for analysis of surface. More extensive sampling and analysis is required to provide a rational explanation on the basis of chemical analysis.

Conclusion

The mechanism of adherence of a zinc electrodeposit to an aluminum cathode is more plausibly explained in terms of attachment at a varying number of electrochemically active spots than by a concept of mechanical anchoring under ledges and crevices.

Acknowledgment

Acknowledgment is gratefully made to the Electrolytic Zinc Company of Australasia Limited, Risdon, Tasmania, where the author was employed as an investigator in the research department when these experiments were conducted.

Any discussion of this paper will appear in a Discussion Section to be published in the December 1954 issue of the Journal.

REFERENCES

1. F. Schlötter, *Z. Metallkunde*, **10,** 242 (1910).
2. *Commonwealth Engineer*, **34,** 130 (1946).
3. S. Kyropoulos, *Z. anorg. allgem. Chem.*, **119,** 299 (1922).
4. W. Bullough and G. E. Gardam, *J. Electrodepositors' Tech. Soc.*, **22,** 169 (1947).
5. H. R. Nelson, Special Summer Conf., Proc. Mass. Inst. Tech., 217 (1940).
6. H. R. Hanley and C. Y. Clayton, *Am. Inst. Mining Met. Engrs.*, **159,** 210 (1944).

Luminescence of the System β $Zn_3(PO_4)_2$-$Cd_3(PO_4)_2$:Mn[1]

A. L. Smith

Tube Department, Radio Corporation of America, Lancaster, Pennsylvania

AND

A. D. Power

Tube Department, Radio Corporation of America, Harrison, New Jersey

ABSTRACT

When zinc orthophosphate and cadmium orthophosphate mixtures are activated by manganese and fired at 850°C, phosphors are obtained whose luminescence is not a linear function of the mole proportions of the initial ingredients. The peak emission vs. composition curve shows several abrupt breaks which correspond to abrupt phase changes as determined by x-ray diffraction analysis.

Introduction

Luminescence of end members of the system β $Zn_3(PO_4)_2$-$Cd_3(PO_4)_2$ has been described by Smith (1), Andrews (2), and Kroeger (3). Color of the luminescence of zinc orthophosphate:manganese may vary from green to red, depending on manganese content and firing temperature (1). Cadmium orthophosphate:manganese was erroneously reported by Andrews (2) to have a red emission, but Kroeger (3) correctly described its emission as yellow. Although double activation of the cadmium salt by lead and manganese causes greater phosphorescence than that obtained by simple manganese activation, the yellow emission remains unaltered (4). McKeag (5) and McKeag and Randall (6) found that when halides in almost any form are added to cadmium orthophosphate, new compound formation occurs and structures of the type $Cd_3(PO_4)_2$:MX_2 result; halide fluxes cannot be used, therefore, without altering internal composition to some extent.

Andrews (2) prepared a zinc-cadmium orthophosphate containing equal weights of zinc and cadmium orthophosphates. If the possible use of hydrates is neglected, this mixture corresponds to approximately 40 mole % zinc orthophosphate. The mixture was fused "at full red heat for 15–20 min and poured onto a cold soapstone. The fluorescence under the iron spark is a light pink, and its phosphorescence is a deep red, resembling hot coals, and fairly persistent" (2).

Preparation

Zinc orthophosphate dihydrate was prepared as previously described (1). Cadmium orthophosphate was prepared in a similar manner: disodium hydrogen phosphate was added to a cadmium sulfate solution; the precipitate was filtered, then dried at 160°C. The material thus obtained was a tetrahydrate, $Cd_3(PO_4)_2 \cdot 4H_2O$, the x-ray diffraction pattern of which agreed with the A.S.T.M. card index labeled "$Cd_3(PO_4)_2$" (7). Firing the hydrate at 650°C converts it to the anhydrous form, the x-ray diffraction pattern of which is given in Table I. A step-by-step dehydration occurs and some intermediate hydrate is formed; composition and stability range of this hydrate, however, were not determined.

In preparation of the phosphors, a water slurry of individual phosphates in proper molar ratio was ball-milled together with the requisite proportion of manganous sulfate for about 14 hr, then evaporated to dryness at 160°C. Equivalent results were obtained by coprecipitation of zinc-cadmium-manganese phosphates, but preparation of various zinc-to-cadmium ratios by ball-milling techniques was more convenient. After evaporation, samples were placed in quartz vessels and fired either at 650° or 875°C in air for two 1-hr periods. Samples were lightly ground between firings to promote homogeneity.

Testing of Phosphors

X-ray diffraction analyses were made with nickel-filtered radiation from a copper target tube operated at 40 kv and 15 ma. Samples were rotated within a circular camera 14.32 cm in diameter.

Cathodoluminescent efficiencies and emission spectra were determined by use of a defocused electron beam having a current density of 1.5μa/cm^2 and an accelerating potential of 8000 volts. Peak efficiencies and spectral distributions of energy were measured by means of the spectroradiometer and the method described by Hardy (8).

[1] Manuscript received July 6, 1953. This paper was prepared for delivery before the New York Meeting, April 12 to 16, 1953.

TABLE I. *Diffraction data for anhydrous* $Cd_3(PO_4)_2$

Lattice spacing (*d*-) Å	Estimated relative intensity
4.3	0.80
4.0	0.40
3.8	0.40
3.42	1.00
3.35	0.80
3.29	1.00
3.15	0.30
3.06	0.35
2.95	1.00
2.89	0.20
2.82	0.30
2.65	0.90
2.59	0.70
2.50	0.30
2.43	0.90
2.30	0.10
2.15	0.20
2.10	0.20
2.02	0.20
1.97	0.35
1.92	0.35
1.87	0.20
1.84	0.20
1.77	0.20
1.70	0.25
1.65	0.15
1.59	0.25
1.57	0.15
1.54	0.10
1.51	0.20
1.47	0.10
1.435	0.30
1.402	0.10
1.390	0.20
1.360	0.20
1.265	0.20
1.235	0.20
1.220	0.20
1.210	0.20
1.140	0.30
0.990	0.30

Results and Discussion

A number of binary phosphor systems are known in which the peak wave length of emission shifts in a regular manner with change in composition. Before this study was undertaken, it was assumed that the zinc-cadmium orthophosphate:manganese system would also exhibit a simple shift of color from the light red of zinc orthophosphate to the deep yellow of cadmium orthophosphate. Such a simple shift does not occur, however, as can be seen in Fig. 1, in which the peak wave length of emission is plotted vs. the mole per cent concentration of cadmium phosphate. Each rectangular box shown on the graph indicates relative variance obtained from a particular composition. Included within the rectangles are values obtained from manganese-concentration tests, firing-temperature studies, and repetitive runs. Variances between repetitive runs were as great as those from processing variables, hence all values are grouped as a single unit.

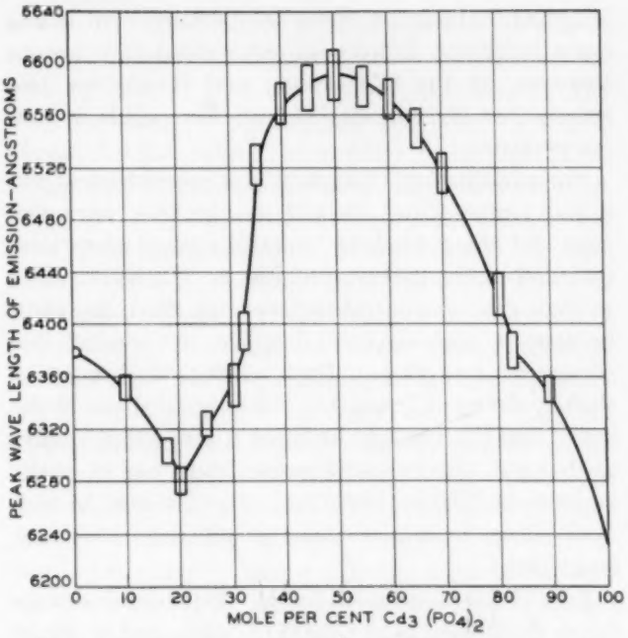

FIG. 1. Peak wave length, in Å, of emission as a function of composition in the system β $Zn_3(PO_4)_2$-$Cd_3(PO_4)_2$:Mn.

Effect of manganese concentration.—As in zinc orthophosphate (1), concentrations of manganese between 2 and 5% did not change the position of the peak of emission. Since this investigation was concerned primarily with β $Zn_3(PO_4)_2$, concentrations below 2 mole % manganese were not tested systematically. This procedure was followed to insure the presence of only β $Zn_3(PO_4)_2$, for it has been established that lower manganese content gives rise to α $Zn_3(PO_4)_2$ (1). Only one spot check of 0.5 mole % manganese was made at the 50–50 composition. Although the efficiency of this sample was low, all other properties were similar to those of samples of higher manganese content. It was also found that x-ray diffraction patterns of pure cadmium orthophosphate containing as much as 5 mole % manganese were identical with those without added manganese. This result indicates that cadmium orthophosphate does not display a phase change upon addition of manganese as does the zinc analogue.

Effect of firing temperature.—Although the majority of tests were conducted at 875°C, several runs were made at 650°C to determine whether phase changes due to temperature would occur. Except in the 100 to 90 mole % zinc region, where the expected α to β shift occurred, no other phase change was found which was due solely to temperature. A possible trend toward shorter wave lengths was found at the 650° firing temperature and toward longer wave

lengths for the 875°C firing temperature, but it was quite indefinite. Efficiencies were about 20% better, however, at the 875° value, and it was for this reason that the majority of tests were made at that temperature.

Since results involving activator concentration and firing temperature showed no greater variances than did those between repetitive runs, they were included in the make-up of Fig. 1. The 650° values at high zinc concentrations were omitted, however, because it was obvious that the α form of zinc phosphate was present. Each series tended to give a slightly different curve, but the over-all shape of the curve and position of the breaks were substantially unchanged, the only difference being one of slight magnitude. The plot is a very sensitive one, so that small errors in measurement or preparation appear magnified.

Fig. 2 shows spectral energy distribution curves for β $Zn_3(PO_4)_2$:Mn, $Cd_3(PO_4)_2$:Mn, and a 50–50 mole ratio of the two substances. The curve of the 50–50 composition is symmetrical, without the hint of a double peak. This symmetry is evident in all other ratios as well. As the cadmium content is increased, the curve remains relatively narrow until a content of 20 mole % is reached. The curve broadens rather abruptly at about the same concentration at which emission starts to shift toward deep red, and remains relatively unchanged for all concentrations up to pure $Cd_3(PO_4)_2$. This fact is

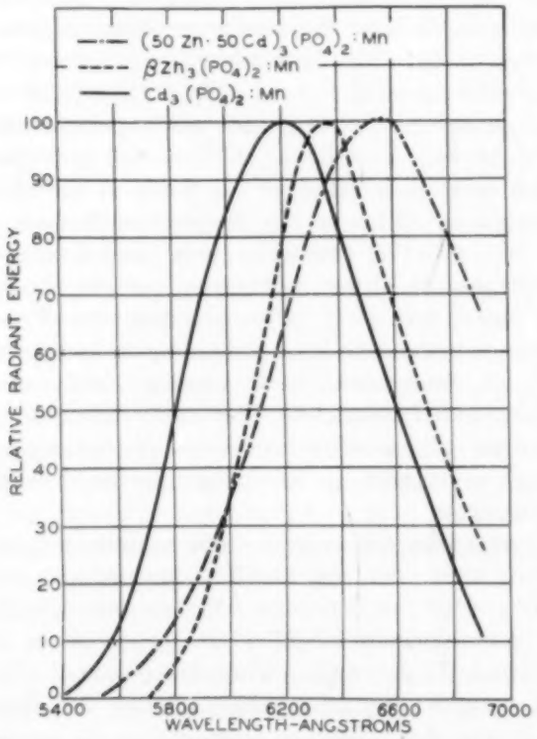

FIG. 2. Spectral energy distribution curves of the phosphors [$Zn_3(PO_4)_2$:$Cd_3(PO_4)_2$]:0.05 Mn, β $Zn_3(PO_4)_2$:Mn, and $Cd_3(PO_4)_2$:Mn.

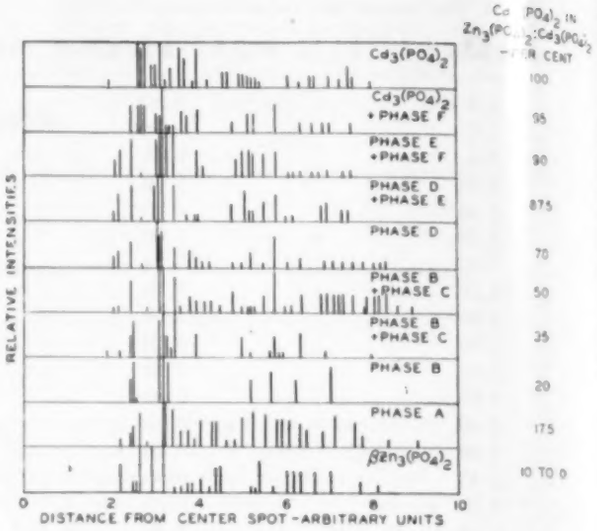

FIG. 3. Schematic representation of typical x-ray diffraction patterns obtained for various compositions in the β $Zn_3(PO_4)_2$-$Cd_3(PO_4)_2$:Mn system.

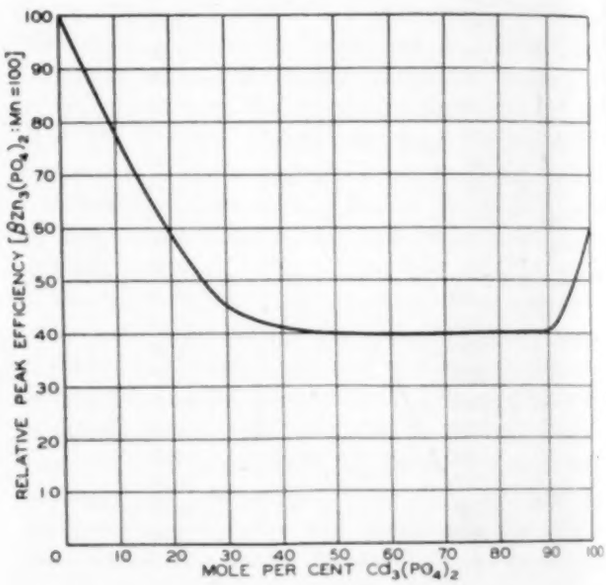

FIG. 4. Plot showing the variation in efficiency as a function of composition for the system β $Zn_3(PO_4)_2$-$Cd_3(PO_4)_2$: Mn fired at 875°C.

especially interesting because x-ray diffraction patterns indicate that pure phases are present at only a few points, all other points showing mixed phases (see Fig. 3). It might be assumed that each phase would have its own peak of emission and, with two phases present, either a double peak would be seen or the curve would be quite broad. Why this does not occur is not known.

Fig. 4 shows rather rapid decrease in peak efficiency as cadmium content is increased (preparation at 875°). At concentrations of about 40 or 50 mole % cadmium orthophosphate, the efficiency curve flattens to a value of about 40% of that of β $Zn_3(PO_4)_2$. The efficiency remains at that value until

90% $Cd_3(PO_4)_2$ is reached, at which point it rises to 60% of $Cd_3(PO_4)_2$ itself.

From pure zinc orthophosphate to compositions with up to 17.5 mole % cadmium orthophosphate, the structure is essentially that of β $Zn_3(PO_4)_2$:Mn (see Fig. 3). At about the latter value a very abrupt phase change occurs which corresponds quite closely to the abrupt shift in peak of the emission curve (Fig. 1). The first phase, *A*, is of very narrow composition. At concentrations of 20 mole % cadmium orthophosphate another apparently pure phase, *B*, appears; this phase persists through concentrations having 50 mole % cadmium orthophosphate. Somewhere in the 50 mole % region a *C* phase is also found, but it could not be isolated. The *D* phase begins at concentrations of about 70 mole % cadmium orthophosphate and continues to concentrations of about 90 mole %; the *D* phase is contaminated in small portion by the *E* phase at concentrations of about 85 mole %. The *D* phase disappears at concentrations of 90 mole %, but another phase, *F*, is then found with the *E* phase. The *E* form could not be isolated; the appearance of the *E* form is coincident with another sharp break in the peak of the emission curve. At concentrations of 95 mole % cadmium orthophosphate, the *F* form is found together with normal cadium orthophosphate. No pure cadmium orthophosphate phase is present in the composition made with as much as 90 mole % cadmium phosphate.

Chloro-complexes of some of these phases are of interest. At and above 87.5 mole % cadmium composition, chloro-complexes were formed having emission and x-ray diffraction patterns essentially identical with those published by McKeag and Randall (6). At and below 20 mole % cadmium composition, emissions and patterns were distorted γ $Zn_3(PO_4)_2$ (1). Between these limits, however, no complexes were formed; the added chloride acted only as a "mineralizer" promoting crystal growth and did not affect emission or x-ray diffraction patterns.

Conclusions

When β zinc orthophosphate and cadmium orthophosphate mixtures are activated by manganese and fired at 875°C, phosphors are obtained whose luminescence is not a linear function of the mole proportions of the initial ingredients. The peak emission vs. composition curve shows several abrupt breaks, which correspond to abrupt phase changes as determined by x-ray diffraction analysis. There are probably six phases present in the β zinc orthophosphate-cadmium orthophosphate system, some of which are partially intersoluble. Three of these phases could be isolated, but the other three could not, even though only fractional percentage changes were made in regions where these compositions were thought to lie. Only two of the abrupt phase changes manifested themselves as abrupt changes in luminescence; the other variations showed only what would be expected from simple solid solutions. The unusual feature of these mixtures is that more abrupt changes in emission were not observed in the light of complex phase changes indicated by x-ray analyses. Lack of abrupt emission changes implies that the activator center was not altered radically by these phase changes, but rather was influenced in a very gradual manner.

Acknowledgments

Thanks are due to L. E. Whitmer for preparation of most of the samples, and to A. E. Hardy and R. F. Jefferies for optical measurements.

Any discussion of this paper will appear in a Discussion Section, to be published in the December 1954 issue of the Journal.

References

1. A. L. Smith, *This Journal*, **98**, 363 (1951).
2. W. S. Andrews, *Am. Mineral.*, **7**, 19 (1922).
3. F. A. Kroeger, "Some Aspects of the Luminescence of Solids," Elsevier Publishing Co., New York (1948).
4. A. H. McKeag and P. W. Ranby, U. S. Pat. 2,476,676, July 19, 1949.
5. A. H. McKeag, U. S. Pat. 2,201,698, May 21, 1940; 2,214,643, Sept. 10, 1940; 2,226,407, Dec. 24, 1940.
6. A. H. McKeag and J. T. Randall, U. S. Pat. 2,191,351, Feb. 20, 1940.
7. "Alphabetical and Grouped Numerical Index of X-ray Diffraction Data," Special Technical Publication 48-B, American Society for Testing Materials, Philadelphia (1950).
8. A. E. Hardy, *Trans. Electrochem. Soc.*, **91**, 127 (1947).

Sensitized Luminescence of CaF_2:(Ce + Mn)[1]

R. J. Ginther

Chemistry Branch, Metallurgy Division, Naval Research Laboratory, Washington, D. C.

ABSTRACT

Calcium fluoride activated by cerium and manganese is shown to be a sensitized phosphor of high quantum efficiency. Studies of its reflection and excitation spectrum reveal that both cerium singlets and aggregates of cerium ions serve as sensitizers for manganese. The range of interaction (K) over which energy may be transferred from sensitizer to activator was found to be from 30 to 80 lattice sites. Variation in K with increasing sensitizer and constant manganese concentration is interpreted as being due to the competition of two types of sensitizing centers rather than to an energy transfer between sensitizer ions.

Introduction

The sensitized luminescence of manganese-activated phosphors has been the subject of numerous investigations. While a number of sensitized systems of simple structure, principally alkali halides (1) and calcite (2), are known, the most recent investigations have been concerned with compounds of more complicated structure such as $CaSiO_3$:(Pb + Mn) (3), $Sr_3(PO_4)_2$:(Sn + Mn), $Ca_3(PO_4)_2$:(Ce + Mn) (4), and $3Ca_3(PO_4)2CaFCl$:(Sb + Mn) (5). Although the interest in the more complicated systems originated largely in their practical application, it is from these phosphors that the most recent information concerning the mechanism of energy transfer and the range of sensitizer-activator interaction has been derived (6, 7, 8). Alkali halides and calcite, either for reasons of low activator or sensitizer solubility or because of poor luminescence efficiency, are not well adapted to the detailed investigation of the transfer mechanism and range.

Calcium fluoride is a compound of simple structure which has high solubility for both sensitizer and activator permitting preparation of efficient phosphor samples over a wide range of concentrations. It therefore appears to be ideally suited for the investigation of sensitized luminescence.

Experimental Methods and Results

Preparation and Identification of Samples

No commercially available raw materials were found satisfactory for preparation of the phosphors studied. Although calcium and manganous fluorides sufficiently free of heavy metals were available, all samples of these materials were partially hydrolyzed, leading to oxidation of the manganese activator upon firing. Some samples of calcium fluoride contained sufficient calcium hydroxide to produce a separate manganese-activated calcium oxide phase upon firing phosphor samples prepared from them.

A satisfactory calcium fluoride raw material can be prepared from calcium carbonate and hydrofluoric acid. When 25.0 grams of $CaCO_3$ are added to a solution of 25.0 ml of 48% HF in 250 ml of water, the calcium fluoride produced settles rapidly and may be washed by decantation. When dried at low temperature, preferably *in vacuo*, it suffers little or no hydrolysis, and samples will nearly completely disappear in a liquid of refractive index 1.434. The effect of using more concentrated acid is to produce finer particles of calcium fluoride which do not settle well, are more difficult to wash, and apparently are more susceptible to hydrolysis. Samples prepared from concentrated acid will not disappear in the refractive index medium mentioned above presumably because of the presence of an extra hydrolyzed phase. Of commercially available calcium fluoride, only optical quality crystals, either natural or synthetic, would meet the above described immersion test.

Cerous fluoride was prepared by a rather complicated procedure. Cerous nitrate solution was purified first with H_2S, then with ammonium sulfide in an alkaline solution of ammonium tartrate. Next, cerous oxalate was precipitated and washed. The oxalate was then dissolved in nitric acid; the solution was reduced with hydrogen peroxide, then the fluoride was precipitated with hydrofluoric acid. No attempt was made to separate other rare earths from cerium.

The most satisfactory source of manganese proved to be an ammonium manganous fluoride which is easily precipitated from manganous chloride solution with ammonium fluoride. The manganese content of this complex fluoride is somewhat variable; samples

[1] Manuscript received October 2, 1953. This paper was prepared for delivery before the New York Meeting, April 12 to 16, 1953.

of it prepared in this laboratory averaged about 70.0% MnF_2.

While luminescent preparations can be made simply by coprecipitation of the mixed fluorides and drying under an infrared lamp, the most efficient phosphors were prepared by dry mixing the component fluorides and firing at 1000°–1200°C in an inert atmosphere. Most of the samples prepared in this investigation were fired in platinum containers in helium or nitrogen at 1100°C. Inert gas was purified by passage over hot copper and calcium hydride. This firing technique produced samples with as much as 20% Mn which were perfectly white by reflected light and free of any observable effects of manganese oxidation. No "skinning" of any sample was necessary.

Representative samples were examined by x-ray diffraction. All samples had the fluorite structure. Manganese produced a contraction, and cerium an expansion of the crystal lattice, as one would expect. Only in samples containing 20% cerium was an extra unidentified line observed in the x-ray pattern. This line could not be correlated with any of the reported lines of any fluoride or oxide of calcium, cerium, or manganese.

Calcium Manganous Fluoride Phosphors

Many references to natural luminescent fluorite containing manganese have been made. Emission colors are variously reported as green to yellow. Synthetic manganese-activated fluorite was prepared by Wick (9), but no details of its emission spectrum were reported. Fig. 1 shows the cathode ray excited emission spectra of typical members of a series prepared in this laboratory and containing from 0.05 to 10.0 mole % Mn. Samples of from 0.05% to 1.0% Mn have an emission peak at 4900 Å.[2] With increasing manganese concentration, the emission peak shifts to longer wave lengths. At 5.0% Mn the peak is at 5000 Å, while the peak of a 10.0% Mn sample is at 5100 Å. A sample containing 20.0% Mn was luminescent only at low temperature under cathode rays. None of the above described samples was appreciably excited by ultraviolet in the wave length range from 2200–4000, although a weak excitation band at 4000 Å exists in these phosphors as will be shown in a later section.

CaF_2(Ce) *Phosphors*

Kroger and Bakker (10) have briefly investigated calcium fluoride activated by cerium. They report

[2] In concurrent work, Dr. Arthur L. Smith, of Radio Corporation of America, located the emission peak of synthetic fluorite contining 1.0% Mn at 4950 Å. The reason for the minor discrepancy between his and the present work is not known, but may possibly be due to differences in either raw materials or preparation technique employed.

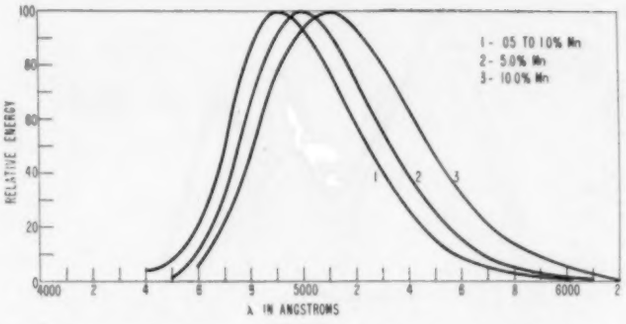

FIG. 1. Emission spectra of CaF_2:(Mn) under cathode ray excitation.

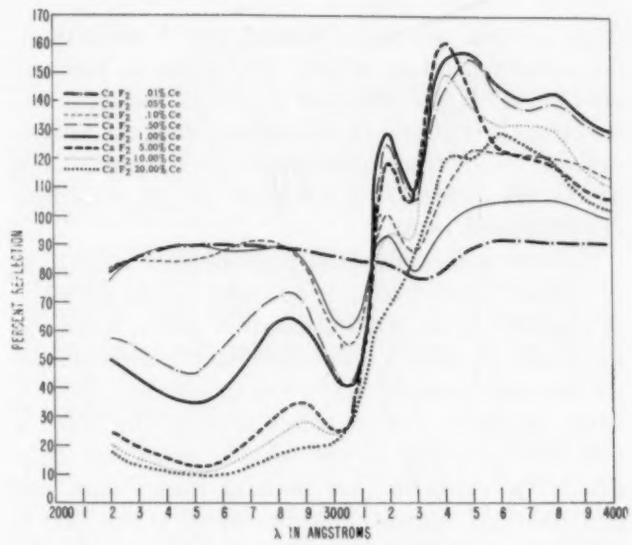

FIG. 2. Reflection spectra of CaF_2:(Ce)

an absorption edge at 3000 Å and an emission consisting of two peaks at 3100 Å and 3300 Å in a sample containing 1.0% Ce. In a sample containing 10% Ce, a third emission peak between 3500 Å and 4000 Å was observed.

In the present work, samples of from 0.01 to 20.0 mole % cerium were prepared. Absorption spectra of this series, as shown by the reflection curves of Fig. 2, are much more complicated than the simple edge described by Kroger and Bakker. At a concentration of only 0.01% Ce, a single reflection minimum corresponding to an absorption band at 3300 Å is observed. With concentrations of from 0.05% to 0.10%, only one additional minimum at 3050 Å is obtained. With concentrations of 0.50% Ce and higher, a band at about 2500 Å appears. While the absorption band at 3050 Å grows continuously with increasing cerium content, the band at 2500 Å grows much more rapidly at the higher cerium concentrations. At 1.0% Ce the 2500 Å and 3050 Å reflection minima are about equal, while the 2500 Å minimum is predominant at all higher cerium concentrations.

Reflections of more than 100% are obtained at

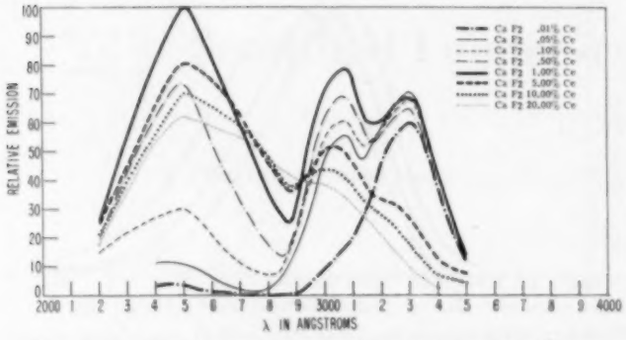

FIG. 3. Excitation spectra of CaF_2:(Ce) for 3850 Å emission band.

3200 Å and in two peaks between 3400 Å and 4000 Å. Apparent reflections of over 100%, due to luminescent emission, are obtained whenever the reflection spectrum of a phosphor is measured with the sample exposed to the total spectrum of the hydrogen lamp at the monochromator entrance slit, as was done in the present work.

Growth of the 3300 absorption band as a function of cerium concentration is obscured by the presence of the 3200 Å and 3400 Å emission peaks, while the growth of the 3050 Å absorption band is accentuated by its superposition upon the tail of the 2500 Å band. However, the presence of both the 3050 Å and 3300 Å bands in the sample containing only 0.05% Ce indicates that both of these bands are due to cerium singlets. The appearance of the 2500 Å band at only high concentrations of cerium and the rapid growth of this band relative to the singlet bands as a function of cerium concentration demonstrates that the shortest wave length absorption is due to cerium aggregates. For the present purpose, a cerium aggregate may be defined as consisting of at least two cerium ions whose proximity provides sufficient interaction to modify the absorption properties of the cerium center. The question of actual maximum separation of ions of an aggregate is left open.

Excitation spectra of CaF_2:(Ce) phosphors cannot be completely determined by the usual excitation measurement. The close proximity of the 3050 Å absorption and the 3200 Å emission bands as well as the proximity of the 3300 Å absorption to the emission at about 3400 Å prohibits the measurement of the excitation of the two short-wave emission bands by conventional methods. The technique of interposing filters between the phosphor sample and the phototube detector in order to separate the phosphor emission from light of the exciting wave length reflected from the sample surface could not be applied, since no filters could be found to effect the separation. The excitation spectrum for the 3800 Å emission was obtained in the usual manner by employing a Corning #5113 filter.

Fig. 3 represents the excitation spectra for the 3800 Å emission band. At the lowest cerium concentration a single sharp excitation peak at 3300 Å is obtained. As the cerium concentration is increased, a second excitation peak at about 3070 Å is observed. This latter peak grows relative to the 3300 Å peak with increasing cerium concentration. At a concentration of 0.10% Ce, an excitation peak at 2500 Å is well defined, and this peak is the most prominent at all higher concentrations. The latter excitation peak grows relative to the longer wave length excitation peaks with increasing cerium concentration, and its rapid growth at high cerium content is consistent with the interpretation that this peak is due to cerium aggregates. The growth of the 3070 Å peak relative to the 3300 Å peak is not obviously in agreement with the assumption that both these absorption bands are due to cerium singlets. However, it will be shown in the next section that the emission produced upon excitation in these two bands is not identical. Therefore, an identical behavior in the growth of the two excitation bands for only the 3800 Å emission should not necessarily be expected. It may be observed that the 2500 Å and 3070 Å excitation bands overlap considerably for all cerium concentrations except the lowest three, and that the amount of overlap increases with increasing cerium content.

Correction to equal energy of excitation was made only in the wave length range 2500–4000 Å; consequently, decrease in excitation shown at wave lengths shorter than 2500 Å is an exaggeration of the true decrease. However, since the excitation peak at 2500 Å coincides exactly with the absorption peak at this wave length, there can be little doubt that the peak is correctly located.

In the behavior of aggregate cerium ions as absorbers for 2500 Å radiation may lie the explanation why relatively high cerium concentrations are necessary for efficient excitation of other cerium-activated phosphors by 2537 Å radiation.

Since excitation spectra for all three emission bands could not be determined, information concerning the emission associated with the individual absorption bands was obtained by measuring the emission spectra of the phosphors with monochromatic exciting radiation in each of the three absorption bands. Exciting light was rendered monochromatic by passage through two quartz monochromators in series. Emission spectra were then recorded with a spectroradiometer in the conventional manner. For excitation in the 2500 Å band, 2537 Å radiation was employed, while for excitation in the 3070 Å band, the 2967 Å mercury line was used. The source of these mercury lines was an H-4 type mercury burner enclosed in a quartz envelope. For

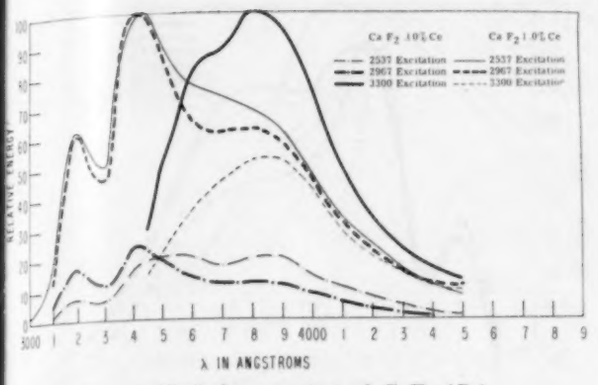

FIG. 4. Emission spectra of CaF_2:(Ce)

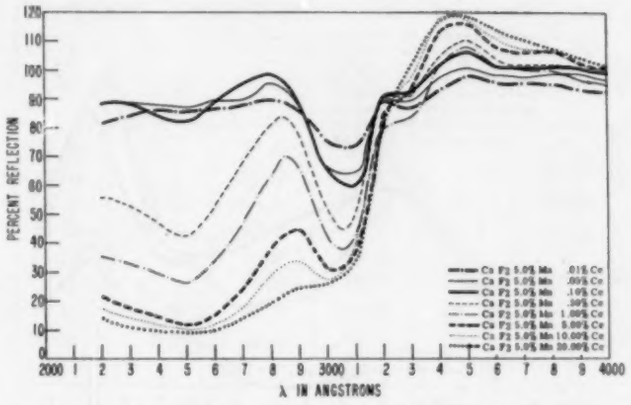

FIG. 5. Reflection spectra of CaF_2:(5.0% Mn, varying Ce).

3300 Å excitation, a band about 100 Å wide centered at the desired wave length was selected from the spectrum of either an AH-6 water-cooled mercury lamp or from a Xenon arc lamp. Emission spectra of all samples of the series were similar under any particular type of excitation. The emission of samples containing 0.10% Ce and 1.0% Ce are shown in Fig. 4. Under 3300 Å excitation, an emission consisting of a single peak at 3850 Å is obtained from the 1.0% Ce sample, while the emission of the 0.10% Ce sample shows resolution with a second peak at about 3650 Å. With both 2537 Å and 2967 Å excitation, emission peaks at 3200 Å and 3450 Å, as well as the 3850 Å peak, are observed. Minor variations in both peak positions and in their relative intensities were obtained as a function of cerium concentration, but emission spectra shown are typical for all members of the series. It can be observed with reference to Fig. 3 that excitation with 2967 Å radiation will result in absorption in both singlet and in aggregate cerium centers because of the overlap of the absorption bands of these centers at high cerium concentration. However, for cerium concentrations of 0.50% and lower, the overlap at 2967 Å is insignificant so that it can be stated with certainty that absorption in both the 3050 Å and 2500 Å bands produces all three emission peaks.

CaF_2:(Ce + Mn) *Phosphors*

While calcium fluoride activated separately by cerium and by manganese has been previously prepared, no sensitized combination of these two activators in fluorite seems to have been reported. In the present investigation, sensitized luminescence was observed in samples containing from 0.01% to 20.0% Ce and 0.05% to 20.0% Mn. Optimum concentration for 2537 Å excitation was found to be in the region of 1.0% to 10.0% of both cerium and manganese.

Reflection Spectra

Reflection spectra of sensitized phosphors are similar to those of phosphors containing only cerium. Fig. 5 shows the reflection spectra of a series of samples of 5.0% Mn and of varying cerium concentration. The three absorption bands found are located at the same wave lengths as in phosphors activated by cerium alone. The only distinguishing difference between the data of Fig. 5 and the reflection spectra of CaF_2:(Ce) phosphors is the smaller amount of ultraviolet emission obtained from phosphors containing manganese. Ultraviolet emission of these phosphors is depressed by transfer of energy to manganese, resulting in visible emission.

Reflection spectra of another series of phosphors of the same cerium contents but of 0.50% Mn were found to be identical with those of the 5.0% Mn phosphors except for the magnitude of the ultraviolet emission. The reflection spectra of two series of samples of constant cerium concentration but of varying manganese content from 0.05% to 20.0% were also determined. For samples of both 0.10% Ce and 1.0% Ce, reflection spectra were independent of manganese concentration, except in regard to the magnitude of the ultraviolet emission. It may, therefore, be concuded that no new absorption bands are introduceld by the presence of cerium + manganese pairs. In this respect, the sensitized calcium fluoride phosphor resembles most sensitized phosphors whose absorption spectra have been investigated. Notably, it differs from $CaSiO_3$:(Pb + Mn) in which Pb + Mn pairs appear to have a discrete absorption (7).

Excitation of Ce *Emission*

Excitation spectra for the 3850 Å-peaked ultraviolet emission of the CaF_2:5% Mn, Ce phosphors are shown in Fig. 6. Again, correction to equal energy of excitation was made only to 2500 Å. For all samples, the excitation peak in the region of 3300 Å is predominant. Poor sensitization of manganese should, therefore, be obtained at this wave length. The rapid growth of a 2500 Å excitation band due to cerium aggregates is not demon-

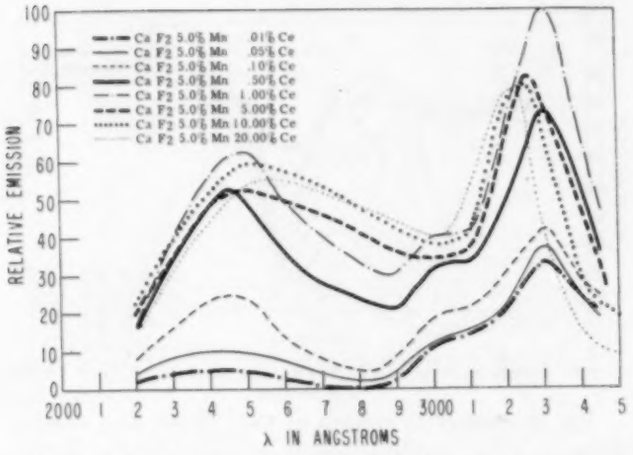

FIG. 6. Excitation spectra for 3850 Å emission band of CaF_2:(5.0% Mn, varying Ce).

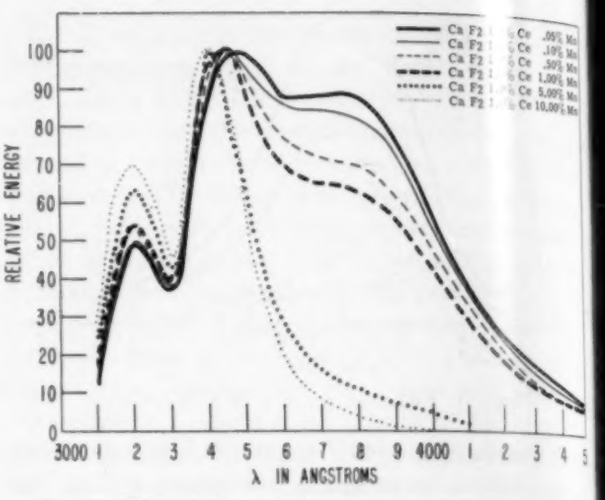

FIG. 7. Ultraviolet emission spectra of CaF_2:(1.0% Ce, varying Mn).

strated in these curves. This growth should not be expected if good sensitization of manganese occurs in this band. In none of the samples is the 3050 Å excitation band well resolved, indicating that good sensitization should occur at this wave length.

Excitation spectra for ultraviolet emission obtained with other phosphor series were in agreement with the data for the series illustrated. A series containing constant 0.50% Mn and varying cerium concentrations showed the 2500 Å and 3050 Å bands in greater intensity relative to the 3000 Å band than was obtained with the 5.0% Mn series. Since at lower manganese concentration the opportunity for energy transfer and emission from manganese is lower than in the phosphors of 5.0% Mn, excitation spectra should more nearly resemble the data obtained for CaF_2:(Ce) phosphors. Measurements on phosphors of constant cerium but of varying manganese concentrations gave results also in agreement with data reported above. With 0.10% Ce and low manganese concentration, strong ultraviolet excitation peaks at 3050 Å and 3300 Å are obtained. As manganese is increased, the 3050 Å peak is suppressed. With 1.0% Ce present, excitation peaks at 2500 Å, 3050 Å, and 3300 Å are obtained with low manganese content. As the manganese concentration of this series is increased, the two short wave length peaks are reduced relative to the 3300 Å peak, indicating efficient sensitization of manganese in both the short wave length absorption bands.

Ultraviolet Emission Spectra

Ultraviolet emission spectra of Mn-activated CaF_2:Ce phosphors varied very little as a function of cerium concentration. As in the case of the phosphors activated with cerium alone, three emission peaks were obtained with either 2537 Å or 2967 Å excitation, but only a single peak at about 3800 Å was obtained with excitation at 3300 Å. Minor differences occurred in the relative heights of the three emission bands of some samples, but no regular variation of peak intensities was found as a function of cerium concentration.

A more significant variation of ultraviolet emission spectra of phosphors of constant cerium but varying manganese concentration was obtained. As shown in Fig. 7 the 3800 Å emission of samples of 1.0% Ce is depressed relative to two short-wave emission bands with increasing manganese concentration. At a concentration of 5.0% Mn, the 3800 Å band is no longer distinguishable. Emission spectra shown were obtained with 2967 Å excitation. Results with 2537 Å excitation were similar.

Excitation Spectra of Manganese Emission

Excitation spectra of the manganese emission of a series of samples with 5.0% Mn are shown in Fig. 8. As expected, poor excitation occurs in the 3300 Å band. All samples have a strong excitation at 3050 Å, while the 2500 Å band grows relative to the 3050 Å band with increasing cerium content in agreement with the assumption that it is due to aggregated cerium ions. While aggregates of activators are recognized as luminescent centers in

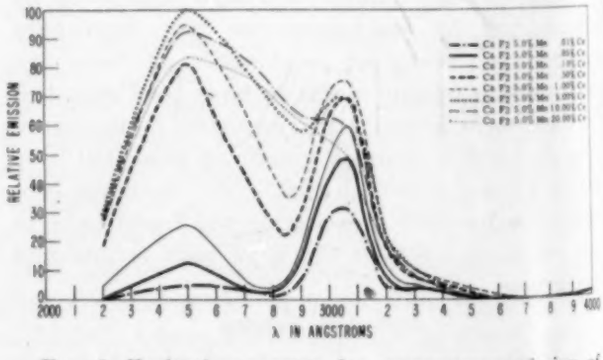

FIG. 8. Excitation spectra for manganese emission of CaF_2:(5.0% Mn, varying Ce).

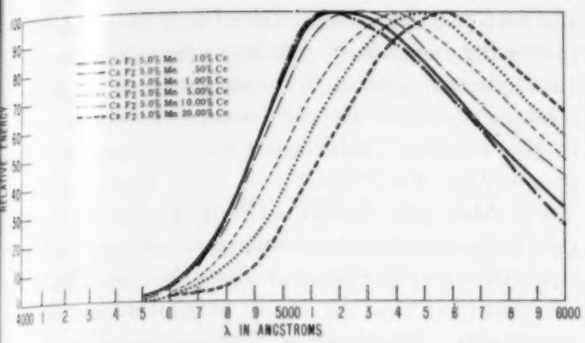

FIG. 9. Manganese emission spectra of CaF_2:(5.0% Mn, varying Ce) under monochromatic 2537 Å excitation.

many systems, no previous evidence for the behavior of aggregated ions as sensitizers for manganese appears to have been reported. The very slight rise in excitation at 4000 Å is real. From measurements on samples of varying manganese content it was found that this band peaks at about 4000 Å and is dependent on manganese, not upon cerium, concentration. It is apparently due to a weak manganese absorption band.

Manganese Emission Spectra

Manganese emission spectra under optical excitation were obtained with monochromatic excitation from the double monochromator arrangement mentioned earlier. Since the excitation energy available at 2537 Å is very low with this arrangement, a 1P21 photomultiplier tube was used as the detector in the spectroradiometer. Use of this tube prevented reliable calibration of the system at wave lengths longer than 6000 Å.

Emission spectra of a series of samples of 5.0% Mn and of varying Ce concentration obtained with 2537 Å excitation is shown in Fig. 9. Increasing cerium content shifts the emission to longer wave lengths. A shift from 5150 Å to 5550 Å in the emission peak is obtained upon a cerium concentration increase from 0.10% to 20.0%. Emission spectra of samples containing less than 0.10% Ce could not be obtained with 2537 Å excitation because of the low concentration of cerium aggregates in these samples.

TABLE I. CaF_2:5.0% Mn—*2537 Å excitation*

1 % Ce	2 QE Ce	3 QE Mn	4 Total QE	5 $B = \frac{QEMn}{QECe}$	6 K
0.01	0.44	5.1	5.5	11.6	49.3
0.05	1.8	20.9	22.7	11.6	49.3
0.10	3.0	32.7	35.7	10.9	48.2
0.50	7.5	87.7	95.2	11.7	49.5
1.0	7.4	75.9	83.3	10.2	47.0
5.0	6.8	82.6	89.4	12.1	50.1
10.0	7.0	87.7	94.7	12.5	50.7
20.0	7.1	76.7	83.8	10.8	48.1

TABLE II. CaF_2:5.0% Mn—*2967 Å excitation*

1 % Ce	2 QE Ce	3 QE Mn	4 Total QE	5 $B = \frac{QEMn}{QECe}$	6 K
0.01	9.0	39.6	48.6	4.4	32.8
0.05	12.5	58.8	71.3	4.7	33.9
0.10	14.5	68.3	82.8	4.7	33.9
0.50	10.4	62.0	72.4	6.0	
1.0	9.2	60.7	69.9	6.6	
5.0	7.0	66.6	73.6	9.4	
10.0	7.1	72.8	79.9	10.2	
20.0	6.3	62.2	68.5	9.8	

Only manganese ions coupled to aggregated cerium absorbing centers are excited by 2537 Å. Different emission spectra were obtained upon excitation in the 3050 Å absorption band of cerium singlets and upon excitation with cathode rays. Further details of the emission spectra of these phosphors will be reported in a separate publication.

Quantum Efficiency

Quantum efficiencies of two series of phosphors were measured by a method similar to that described by Kroger (11). Separation of the cerium and manganese emissions was made with filters. Corning #5970 was employed for the ultraviolet measurement and Corning #3387 was used for the visible emission. Details of the method of measurement will be reported separately.

Quantum efficiencies of samples containing either 5.0% Mn or 0.50% Mn and 0.01% to 20.0% Ce are shown in columns 2, 3, and 4 of Tables I, II, III, and IV. Samples of lower manganese content could not be measured with any accuracy. Total quantum efficiencies as high as 95% were obtained with some samples of 5.0% Mn, while the maximum total quantum efficiency obtained with samples of 0.50% Mn was about 82%. The tables indicate that high transfer efficiency, evidenced by high quantum efficiency for manganese emission, is obtained when the 5.0% Mn phosphors are excited in either the absorption band of cerium singlets or in the aggregated cerium absorption band.

TABLE III. CaF_2:0.50% Mn—*2537 Å excitation*

1 % Ce	2 QE Ce	3 QE Mn	4 Total QE	5 $B = \frac{QEMn}{QECe}$	6 K
0.05	1.8	0.63	2.4	0.35	59.2
0.10	8.6	3.6	12.2	0.42	69.2
0.50	58.0	19.5	77.5	0.34	57.8
1.0	62.8	19.6	82.4	0.31	53.3
5.0	41.4	18.7	60.1	0.45	73.4
10.0	38.2	20.0	58.2	0.52	82.6
20.0	47.8	19.0	66.8	0.40	66.4

TABLE IV. CaF_2:0.50% Mn—*2967 Å excitation*

(1) % Ce	(2) QE Ce	(3) QE Mn	(4) Total QE	(5) $B = \frac{QEMn}{QECe}$	(6) K
0.05	40.2	6.8	47.0	0.17	31.0
0.10	59.5	11.9	71.4	0.20	36.0
0.50	61.7	15.8	77.5	0.26	
1.0	61.9	18.1	80.0	0.29	
5.0	38.2	18.2	56.4	0.48	
10.0	36.0	16.4	52.4	0.46	
20.0	41.8	15.0	56.8	0.36	

Discussion

Several explanations of the phenomenon of sensitized luminescence have been proposed. These explanations have been reviewed by Botden (8). Since some of the mechanisms had been disproved on the basis of experimental evidence, Botden was concerned with the evaluation of three theories.

The first theory attributes transport of energy from sensitizer to activator to a so-called long wave exciton of the base lattice. The optical absorption of this exciton is assumed to be forbidden so that its existence is not normally recognized. This mechanism was suggested but not indorsed by Botden and Kroger (6).

A second theory proposed by Botden and Kroger ascribes excitation of the manganese activator to a direct transfer of energy between neighboring sensitizer and activator. Transfer between only nearest neighbor "pairs" of activators and sensitizers is assumed possible. To account for the high transfer efficiency existing in efficient phosphors, Botden and Kroger assumed that there is a preferential production of activator-sensitizer pairs in the phosphor synthesis. These authors also suggest that an excited sensitizer ion may transfer its energy to a neighboring sensitizer ion and hence to an activator, in order to account for the high transfer efficiency observed.

The third theory is that of Schulman (7) who proposed that energy is transferred from sensitizer to activator over distances greater than those separating only nearest neighbor pairs. From measurements of the absorption spectra of $CaSiO_3$:(Pb + Mn), Schulman concluded that transfer from an excited lead ion could take place to about the nearest 28 manganese ions.

Botden's critical evaluation of the three theories was based upon their predictions of the dependence of the ratio

$$B = \frac{\text{quantum efficiency of manganese emission}}{\text{quantum efficiency of sensitizer emission}}$$

upon the sensitizer concentration at constant manganese concentration. He demonstrated that the first two theories predicted a decrease in B with increasing sensitizer concentration, whereas the third theory predicted no dependence of B upon sensitizer content. Botden found experimentally that in the systems $Ca_3(PO_4)_2$:(Ce + Mn), $Sr_3(PO_4)_2$:(Sn + Mn), $Ca_2P_2O_7$:(Sn + Mn), $Mg_2P_2O_7$:(Ce + Th + Mn) (12), and $3Ca_3(PO_4)_2 \cdot CaF_2$:(Sb + Mn) that B increased with increasing sensitizer concentration in disagreement with all three theories. Therefore, he concluded that all three were either incorrect or incomplete. He further demonstrated that an extension of Schulman's explanation which included the transfer of energy from sensitizer to activator via other sensitizer ions would account for the dependence of B upon sensitizer concentration. His calculation of K (the number of cation sites surrounding an excited sensitizer to any one of which energy may be transferred if it is occupied by an activator) gave values from 26 to 50 in agreement with the value obtained by Schulman.

Values of B, the ratio of manganese to cerium quantum efficiencies, for both 2537 Å and 2967 Å excitation are shown in column 5, Tables I, II, III, and IV. Under 2537 Å excitation, there is no increase of B with increasing cerium concentration. This is obviously apparent from data of the series of samples containing 5.0% Mn. While data of the samples containing 0.50% Mn show some scatter because of poorer precision in the measurement of these less efficient samples, nothing resembling a real increase in B with cerium content can be observed. With 2967 Å excitation, a constant B is obtained up to a concentration of 0.10% Ce in the 5.0% Mn phosphors. Less data at low cerium concentration are available for the 0.50% Mn concentration, but, for this manganese concentration as well, B can be interpreted as constant up to 0.10% Ce. At concentrations of 0.50% Ce and greater, B increases with increasing Ce concentration under 2967 Å in agreement with the results of Botden.

The behavior of CaF_2:(Ce + Mn) suggests an explanation of the dependence of B upon cerium concentration which does not involve transfer of energy between sensitizers.

A dependence of B upon sensitizer concentration in the absence of any sensitizer to sensitizer transfer can be expected in a system in which: (*a*) two species of sensitizers with different transfer ranges (K) exist; (*b*) the species of sensitizer with the greater transfer range is favored by an increase in sensitizer concentration; (*c*) the excitation energy is shared by the two sensitizer species. As the sensitizer concentration is increased, more of the excitation energy is absorbed by sensitizing centers with the greater transfer range. The increased transfer range of the system makes manganese emission more probable

with respect to sensitizer emission since the excited sensitizers have an opportunity to transfer energy to activator centers situated at greater distances from the sensitizer. Therefore, the ratio B will increase with increasing sensitizer content.

Sensitized System

In order to conclude that the foregoing mechanism takes place in a sensitized system it is necessary to demonstrate that:

1. Two species of sensitizer centers exist in the system with one type favored at higher sensitizer concentrations.

2. No sensitizer-to-sensitizer transfer takes place when each type of center is excited separately. Evidence for this must be no dependence of B upon sensitizer concentration when the centers are separately excited.

3. The sensitizer species favored at high sensitizer concentration must have a greater transfer range (K).

4. An increase of B is obtained with increasing sensitizer content when the excitation energy is shared by the two types of absorbing centers.

An examination of the data obtained from CaF_2:(Ce + Mn) reveals that this system meets all four specifications listed.

1. Both reflection and excitation data demonstrate that two types of sensitizer species exist with different absorption and excitation bands. The 3050 Å and 3300 Å bands appear at low cerium concentrations, while the 2500 Å band is created only at higher cerium contents and grows relative to the long wave length bands with increasing cerium concentration. The assignment of the long wave length bands to cerium singlets and the 2500 Å bands to aggregated cerium ions is an obvious designation.

2. No increase in B is observed from the data of Tables I and III under 2537 Å. This indicates that no sensitizer-to-sensitizer transfer occurs upon excitation in the aggregated cerium absorption band. B increases with cerium content under 2967 Å only in samples containing more than 0.10% Ce. From the excitation spectra of Fig. 6 and 8 it may be seen that considerable overlap of the singlet and aggregate cerium excitation bands exists at 2967 A in samples with concentrations of cerium higher than 0.10%. It is therefore only in the samples of 0.10% and lower cerium concentration that 2967 Å radiation excites only singlet cerium absorbers. Within this concentration range no dependence of B upon cerium content is observed under 2967 Å as well. It can therefore be concluded that no evidence for a transfer of energy from sensitizer to sensitizer exists.

3. The transfer range of aggregated cerium ions is greater than the range of cerium singlets. The transfer range K may be determined from the ratio B according to the relationship

$$B = \frac{1 - (1 - X\mathrm{Mn})^K}{(1 - X\mathrm{Mn})^K} \qquad \text{(I)}$$

in which X Mn is the mole fraction of manganese. The formula represents the ratio of the number of sensitizers having at least one manganous ion within the nearest K cation sites to the number of sensitizers not having a manganous ion within this range of lattice positions. No specification to denote either the presence or absence of sensitizer aggregates is needed in the formula since this specification would appear in both the numerator and denominator of the expression. In this relationship, radiationless transitions are neglected. The derivation of this ratio was made by Schulman (7) who related it to the ratio of Pb + Mn pair absorption to Pb singlet absorption in $CaSiO_3$:(Pb + Mn). The relation of the same expression to B, the ratio of the quantum efficiencies of activator to sensitizer emission, was made by Botden (8), who concluded that its use is not justified for systems in which an energy transfer between sensitizers takes place. However, the demonstration that no sensitizer-to-sensitizer energy transfer takes place in calcium fluoride justifies the use of the formula with this system. Values of K calculated from the above formula are tabulated in column 6 of Tables I, II, III, and IV. The transfer range of singlet cerium sensitizers is found to be about 35, and good agreement is found in the data for both manganese concentrations. The value of K found for aggregate cerium sensitizers in the case of the 5.0% Mn samples is about 50, whereas in the case of 0.50% Mn the average value of K was found to be 66.

4. An increase of B as a function of cerium concentration is obtained when both the aggregate and singlet cerium sensitizers are simultaneously excited. It may be observed with reference to Fig. 6 and 8 that because of the overlap of the aggregate and singlet cerium excitation bands at 2967 Å, excitation energy of this wave length is shared by the two species of sensitizer ions. As the cerium concentration is increased, an increased number of sensitizer aggregates are formed, and the ratio of aggregates to singlets increases. Since aggregates have a greater transfer range than singlets, an increase in B is observed as a function of cerium concentration under 2967 Å excitation. From excitation data, it appears that significant overlap of excitation bands occurs only at concentration of 0.50% Ce and greater. An increase in B as a function of cerium should be observed, therefore, only within this concentration range. The latter con-

clusion is corroborated by the data of Tables II and IV.

No variation in K as a function of either manganese or cerium content is predicted by the derivation of equation (I). No variation of K for singlet cerium sensitizers is obtained, nor is any variation of K for aggregate cerium sensitizers observed in the 5.0% Mn series. In the samples of 0.50% Mn, the value of K for cerium aggregates shows a spread from 53.3 to 82.6. Since this spread is simply a scatter, not a regular function of the cerium content, it must be within the limits of experimental error for these samples. Better precision in the determination of K at higher manganese concentrations is to be expected. Not only are samples of higher manganese concentration more easily reproducible since small errors in manganese content are less significant, but the value of K is a less sensitive function of B at the higher manganese content. At a value of $K = 50$, the slope of the curve of K vs. B has a value of about 150 for 0.50% Mn, whereas the slope of the curve for 5.0% Mn at the same value of K is only about 1.5. The values of the slope were calculated from

$$\frac{dK}{dB} = \frac{-(1 - X\mathrm{Mn})^{K}}{\ln(1 - X\mathrm{Mn})}$$

Therefore, although it appears more desirable to calculate K from data obtained at high manganese content in order to obtain better precision, it is necessary to demonstrate that no sensitizer-to-sensitizer transfer exists at low manganese contents as well, for at high manganese contents, sensitizer-to-sensitizer transfer should not be expected since the probability that at least one of the K sites around a sensitizer ion is occupied by an activator is so great that energy transfer between sensitizers is improbable. The probability that at least one of the K sites is occupied by an activator in a sample containing 5.0% Mn with $K = 50$ is 0.92. However, at a concentration of 0.50% Mn with the same values of K, the probability is only 0.22. Therefore, if sensitizer-to-sensitizer transfer existed in the calcium fluoride system, it would have appeared at the lower manganese concentration.

From the determination of K it may be concluded that the transfer range of aggregate cerium sensitizers is about 50% greater than that of cerium singlet centers. This is based on the value of K for cerium aggregates obtained at high manganese concentration, where the determination is made with better precision.

Interpretations of Difference in K

The simplest explanation of the higher value of K for cerium aggregates might be based on the geometry of the phosphor system. A cerium aggregate could be considered as consisting of a pair of sing et ceri sensitizers whose fields of possible transfer sites overlap. Sensitization of a manganous ion situat at any lattice site included in the overlapping fie could occur following absorption in either of t cerium ions of the aggregate. Transfer from t more remote sensitizer to the activator could to place via the intermediate sensitizer. This proc would involve a limited type of sensitizer-s sensitizer transfer which is restricted to cerium io constituting an aggregate. While this explanati cannot be completely excluded, it is not particula attractive. In regarding a cerium aggregate as a p of singlet sensitizers, absorption and excitati properties which distinguish the aggregate cen from the singlet center are overlooked. Moreov further evidence against this explanation may b derived from manganese emission spectra. Excit tion of cerium singlets produces a manganese em sion situated at shorter wave lengths than th manganese emission observed upon excitation cerium aggregates. According to the intermedia transfer scheme, the manganese emission spectru should be affected only by the cerium ion from whi it receives the transferred energy directly. Thi would be particularly true if the separation betwee cerium ions constituting an aggregate is greate than the distance between nearest cation neighbor

A second interpretation of the difference in K for singlet and aggregate sensitizers is more plausible. From the excitation data of Fig. 2 and 6, it may be observed that the 3050 Å and 3300 Å excitation bands overlap at all cerium concentrations. It has been demonstrated that poor excitation of manganese occurs upon excitation in the 3300 Å band while efficient excitation takes place upon irradiation at 3050 Å. Obviously at all cerium contents the excitation energy is shared by the two excited states of the cerium singlet ion upon excitation at 2967 Å while it is only from the higher of these two states that efficient transfer can proceed. In the determination of B it is assumed that energy transfer is governed only by the consideration that a manganese ion is situated sufficiently near to a sensitizer ion. The probability that a sensitizer ion is in an excited state from which transfer can proceed is assumed to be unity. In the case of 2967 Å excitation, this probability is less than unity since the absorbed quantum can produce excitation of the sensitizer to either of two states. If an expression which incorporates this probability could be used to define B, a higher value of K than that reported here for cerium singlets would be necessary in order to account for the measured value of B. Since no way of approximating a value of this probability is at hand, the determination of K for cerium singlets cannot be further refined at the present time.

Although this interpretation invalidates the value K obtained for cerium singlets, it does not affect value determined for cerium aggregates. It does concern the demonstration that no sensitizer-to-sitizer transfer occurs in this system and that the erved variation in B under 2967 Å excitation at h sensitizer concentrations is due to the com-ition of two types of sensitizing centers.

Although the absence of sensitizer-to-sensitizer nsfer has been shown in the CaF_2:(Ce + Mn) tem, its existence in other systems as proposed by tden may be quite correct. However, it should be nted out that in the systems discussed by Botden existence of two types of sensitizer species with ferent transfer ranges was not considered, although gregates of sensitizers existed in the concentration ge he studied. For none of these systems is ficient absorption and excitation data available to termine whether aggregated sensitizers constitute distinct species of sensitizer center.

Acknowledgments

The author wishes to express his indebtedness to . David L. Dexter, who has made a general oretical analysis of the sensitized luminescence of rganic solids (13), and to Dr. C. C. Klick for ny discussions and to Mrs. E. W. Claffy for the ay diffraction data and for the preparation of some the samples.

Any discussion of this paper will appear in a Discussion Section to be published in the December 1954 issue of the JOURNAL.

REFERENCES

1. K. J. MURATA AND R. L. SMITH, *Am. Mineral.*, **31,** 527 (1946); J. H. SCHULMAN, E. BURSTEIN, L. W. EVANS, R. J. GINTHER, AND M. WHITE, *Bull. Am. Phys. Soc.*, **24,** 25 (1949); R. J. GINTHER, *This Journal*, **98,** 874 (1951).
2. J. H. SCHULMAN, L. W. EVANS, R. J. GINTHER, AND K. J. MURATA, *J. Applied Phys.*, **18,** 732 (1947).
3. J. B. MERRILL AND J. H. SCHULMAN, *J. Optical Soc. Am.*, **38,** 471 (1948); H. C. FROELICH, *This Journal*, **93,** 101 (1948).
4. M. HUNIGER AND H. PANKE, U. S. Pat. 2,241,950 and 2,241,951 (1941).
5. H. G. JENKINS, A. H. MCKEAG, AND P. W. RANBY, *This Journal*, **96,** 1 (1949); R. NAGY, R. W. WOLLENTIN, AND C. K. LUI, *ibid.*, **95,** 183 (1949).
6. TH. P. J. BOTDEN AND F. A. KROGER, *Physica*, **14,** 553 (1948).
7. J. H. SCHULMAN, R. J. GINTHER, AND C. C. KLICK, *This Journal*, **97,** 123 (1950).
8. TH. P. J. BOTDEN, *Philips Research Repts.* 7, 197 (1952).
9. F. WICK, *J. Optical Soc. Am.*, **27,** 275 (1937).
10. F. A. KROGER AND J. BAKKER, *Physica*, **8,** 628 (1941).
11. F. A. KROGER, "Some Aspects of The Luminescence of Solids," p. 257, Elsevier Publishing Co., Inc., Houston (1948).
12. H. C. FROELICH, *This Journal*, **95,** 254 (1949).
13. D. L. DEXTER, *J. Chem. Phys.*, **21,** 836 (1953).

Effect of Solvents and Electrolytes on Polarograms of Carbon Tetrachloride[1]

JOHAN J. LOTHE[2] AND L. B. ROGERS

Department of Chemistry and Laboratory for Nuclear Science, Massachusetts Institute of Technology, Cambridge, Massachusetts

ABSTRACT

Polarographic reduction of carbon tetrachloride has been studied in different mixtures of organic solvents with water, using a number of alkali halides and tetraalkylammonium halides as supporting electrolytes. On the positive side of the electrocapillary maximum of mercury, a marked effect of the nature of the anion of the supporting electrolyte on the half-wave potential was observed. On the negative side of the electrocapillary maximum, the cation effected a similar change. It was further observed that reduction became more difficult with increasing concentration of organic solvent. The last can be interpreted in terms of a change in activation energy of the electron transfer process. An equation has been derived which gives the effect of drop-time on the observed half-wave potential for irreversible reactions where the rate of the electron transfer process is the limiting factor. This has been verified experimentally with carbon tetrachloride. Finally, factors governing the occurrence of maxima on the polarographic wave in predominantly aqueous solutions have been investigated.

INTRODUCTION

During recent years a steadily increasing amount of work has been done on the polarographic reduction of organic halides (1–6). Von Stackelberg and Stracke (2) found that the half-wave potentials of halogenated hydrocarbons are independent of the *p*H of the medium, and that iodides are reduced more easily than bromides, and these, in turn, more easily than chlorides. By controlled-potential, large-scale electrolysis of some halogenated hydrocarbons showed that in most cases waves represented conversion of a carbon-halogen bond to a carbon-hydrogen bond according to the following all-over scheme:

$$RX + 2e + H_2O \rightarrow RH + X^- + OH^-$$

For halogenated organic acids, the polarographic wave is *p*H-dependent and is shifted to more negative values with increasing *p*H (3–5). Elving and coworkers (5), studying the polarographic wave of α-bromo-*n*-butyric acid, found that an increase in ionic strength in the alkaline region displaced the half-wave potential to more positive values, whereas the effect was opposite in the low *p*H region and much less pronounced. In some cases, they observed that the half-wave potential, at constant *p*H and ionic strength, depended on the kind of buffer used.

Shreve and Markham (7) reported on the effect of organic solvent on the polarographic reduction of *p*-nitroaniline. A marked shift of the half-wave potential to more negative values occurred with increasing ethanol concentration.

Only scattered remarks can be found in the literature about the effect of organic solvents on polarographic reduction of organic halogen compounds. It has been reported that half-wave potentials for halogenated acetones are shifted to more negative values by the addition of alcohol (8). Von Stackelberg and Stracke (2), working in a 90% butanol-water solution, found half-wave potentials up to 0.10 volt more negative than corresponding potentials in a 75% dioxane-water solution. Gergely and Iredale (6) mentioned, without data, that the half-wave potential for some aromatic iodo compounds was a function of the ionic strength, the alcohol content of the solution, and the nature of the cation of the supporting electrolyte. Rosenthal, Albright, and Elving (9) found that increasing ethanol concentration in the alkaline region shifted the half-wave potential of 2-bromo-*n*-alkanoic acids to more negative values, whereas, in the acid region, evidence of a shift was inconclusive

A stepwise removal of the halogen atoms has been reported for carbon tetrachloride (2, 10). In 75% dioxane and 0.05*M* tetraethylammonium bromide, two waves were observed (2) with half-wave potentials of −0.78 volt and −1.71 volts. The latter corresponds well to the wave at −1.67 volts for the reduction of chloroform. In a (2:1) methanol-water mixture containing 0.10*M* tetramethylammonium bromide (10), waves for carbon tetrachloride were found at −0.75 volt and −1.70 volts and, for chloroform, at −1.70 volts. In this laboratory (11)

[1] Manuscript received July 9, 1953.

[2] Visiting Fellow. Present address: Central Institute for Industrial Research, Blindern, Oslo, Norway.